

Copyright
by
Alexander Douglas Brand
2013

The Dissertation Committee for Alexander Douglas Brand certifies
that this is the approved version of the following dissertation:

**DEVELOPMENT OF THERMAL HYDRAULIC
CORRELATIONS FOR THE UNIVERSITY OF TEXAS AT
AUSTIN TRIGA REACTOR USING COMPUTATIONAL FLUID
DYNAMICS AND IN-CORE MEASUREMENTS**

Committee:

Erich Schneider, Supervisor

Steven Biegalski

Sheldon Landsberger

Greg Sitz

John Howell

Mark Deinert

**DEVELOPMENT OF THERMAL HYDRAULIC
CORRELATIONS FOR THE UNIVERSITY OF TEXAS AT
AUSTIN TRIGA REACTOR USING COMPUTATIONAL FLUID
DYNAMICS AND IN-CORE MEASUREMENTS**

by

Alexander Douglas Brand, B.S.Phys.; M.S.E;

Dissertation

Presented to the Faculty of the Graduate School of

The University of Texas at Austin

in Partial Fulfillment

of the Requirements

for the Degree of

Doctor of Philosophy

The University of Texas at Austin

August 2013

Acknowledgments

I would first like to thank my advisor Dr. Erich Schneider for his endless support and guidance throughout this process. I would also like to thank Paul Whaley for his assistance with getting this project started, Larry Welch for his electronics expertise, Mike Krause for his mechanical and design help, and the rest of the NETL staff for their assistance. Last but not least, I'd like to thank my family for helping and supporting me through this challenging and time consuming procedure.

**DEVELOPMENT OF THERMAL HYDRAULIC
CORRELATIONS FOR THE UNIVERSITY OF TEXAS AT
AUSTIN TRIGA REACTOR USING COMPUTATIONAL FLUID
DYNAMICS AND IN-CORE MEASUREMENTS**

Alexander Douglas Brand, Ph.D.

The University of Texas at Austin, 2013

Supervisor: Erich Schneider

Safety is a paramount concern in the operation of training and test reactors. A major component of a reactor is the maintenance of safe thermal hydraulic operating conditions. If the temperature of the water coolant exceeds the boiling point, the heat transfer out of the fuel rods into the coolant will greatly decrease and will need to rely upon other safety feedbacks and systems to avoid an accident condition.

TRIGA thermal hydraulic systems are currently modeled using a finite differencing code, TRACE/SNAP, developed by the Nuclear Regulatory Commission. While the code is currently certified, it has shortcomings that this work improves upon, notably the simplification of the more complex flow geometries by using circular pipes and a heat transfer correlation that is valid across all flow regimes observed during operation of the TRIGA.

A computational fluid dynamics code, FLUENT, along with real-time thermocouple probe measurements of the channel were used to solve both of these major issues. A high resolution model of four adjacent flow channels was

created to provide a numerical experimental data set for enhancing the correlations used in the TRACE model. The hot flow channel is connected to three surrounding channels where crossflow occurs causing a more complex flow pattern than the isolated single channel system used in TRACE/SNAP. To calibrate the FLUENT model, a thermocouple probe was designed and placed in the TRIGA core in the center of the flow channel. The reactor was operated over the full range of licensed power levels to obtain a fully encompassing data set of coolant temperatures. The FLUENT model was then adjusted so that the temperatures at the location of the probe in the model matched those from the experimental measurements.

Based on the results from the FLUENT testing, data was extracted to develop a new heat transfer coefficient correlation and loss factor coefficient correlation due to the non-circular geometry and fuel rod end fittings for use in the TRACE/SNAP code. These adjustments were then implemented into TRACE/SNAP to improve the code for future users performing safety analysis on TRIGA reactors.

Contents

List of Tables	xi
List of Figures	xiii
1 Introduction	1
2 Literature Review	6
2.1 Computer Codes Developed for Thermal Hydraulic Modeling for Nuclear Reactors	6
2.2 Previous TRIGA Models	11
2.3 Navier-Stokes Solvers	13
3 Single Channel Nodal Models	17
3.1 TRACE	17
3.1.1 Geometry	17
3.1.2 Results	24
3.1.3 Sensitivity Analysis of the TRACE Model	26
3.2 MATLAB	29
3.2.1 MATLAB Formulation	29
3.2.2 Results of MATLAB model	43
3.2.3 Prandtl Number, Reynolds Number and Nusselt Number	46
4 Computational Fluid Dynamic Model and Model Comparison	49
4.1 FLUENT	49
4.1.1 Geometry	49

4.1.2	Mesh	50
4.1.3	Single Channel Nodalization	54
4.1.4	Solution	58
4.1.5	Multi Channel FLUENT Model	62
4.2	Fuel rod power profiles	68
4.3	Comparison of all 3 models	76
4.3.1	Convergence Test	76
4.3.2	TRACE and MATLAB	81
4.3.3	All 3 Models	83
5	TRIGA Data Collection and Scale Modeling	86
5.1	Data Collection and Simulation	86
5.1.1	TRIGA Reactor	86
5.1.2	FLUENT Testing and Adjustment	90
5.1.3	Using Measured Data to Determine Heat Transfer Coefficient and Minor Loss Coefficient	92
5.1.4	Scaled Model	97
5.2	Measurement of coolant temperature in a TRIGA flow channel	100
5.2.1	Design of apparatus to lower probe into the core	100
5.2.2	Procedure of probe use during reactor operation	103
5.2.3	Results from probe measurements	109
5.2.4	Proposed new probe	111
5.2.5	FLUENT Model Adjustment Based on TRIGA Probe Measurements	112
5.3	Development of a scaled hot channel model	113

5.3.1	Scaling factors and similitude	114
5.3.2	Parts required to build the model	122
5.3.3	Measurements of flow and temperature profiles	128
5.3.4	Extra additions/Values for Scaled System	130
5.3.5	Safety Analysis Report	131
5.3.6	Scaled Model Validation using FLUENT	131
6	Results	132
6.1	Fitting FLUENT Results to HTC Correlations	132
6.1.1	Validity of the 4 Fitting Equations	134
6.2	Loss Factor Determination for Non-Heated Sections	148
6.3	TRACE Results Based on New Correlations	154
6.3.1	K Factor Implementation	154
6.3.2	Results from HTC Correlation Implementation into TRACE model	155
6.4	Sources of Error and Uncertainties	156
6.4.1	Error due to TRIGA and Scaled Model Measurements	156
6.4.2	Thermocouples and RTDs	156
6.4.3	Power Fluctuations	157
6.4.4	Error due to FLUENT Measurements	158
7	Conclusion	159
A	MATLAB Solver code	161
References		164

List of Tables

1	Inlet flow areas[13]	21
2	Turns in the flow channel and their effect on K[13]	21
3	Outlet flow areas[13]	21
4	Dimensions of individual heated section	22
5	Heat applied to individual cells in the heated element	23
6	Sensitivity Analysis of TRACE Model	27
7	Initial conditions for the inlet of the MATLAB solver	36
8	Constants used in the MATLAB solver and their values	38
9	Single Channel Nodalization Study Nodal Mesh Quantities . .	54
10	Region Boundaries	71
11	KENO-VI results 200kW (fissions are e-4)	72
12	KENO-VI results 400kW (fissions are e-4)	73
13	KENO-VI results 600kW (fissions are e-4)	74
14	KENO-VI results 800kW (fissions are e-4)	75
15	KENO-VI results 950kW (fissions are e-4)	76
16	KENO-VI Power Ratios	76
17	Allowed operating conditions for the TRIGA core	87
18	Testing conditions for TRIGA core	87
19	Allowed operating conditions for the scaled TRIGA core . .	98
20	Testing conditions for scaled TRIGA core	99
21	FLUENT Adjustment based on TRIGA Probe Results	113

22	Variables for scaled model	116
23	Values for 0.2 scaled model	130
24	Data taken from both scaled models	132
25	Results from 830,000 node, 4 channel model run, 950 kW . . .	135
26	Nusselt number determined from 4 different HTC correlation fits from 830,000 node, 4 channel model run, 950 kW	136
27	Valid ranges for Heat Transfer Coefficent Correlations	136
28	Coefficients for the 4 functional forms used for Nusselt number fitting, 950 kW	138
29	Results from 830,000 node, 4 channel model run, 200 kW . . .	140
30	Results from 830,000 node, 4 channel model run, 400 kW . . .	141
31	Results from 830,000 node, 4 channel model run, 600 kW . . .	141
32	Results from 830,000 node, 4 channel model run, 800 kW . . .	142
33	Heat Transfer Coefficient Fits for All Power Levels	147
34	Input values for K factor determination of lower unheated section	151
35	Input values for K factor determination of upper unheated section	152
36	K factors for Lower Section from FLUENT Testing	152
37	K factors for Upper Section from FLUENT Testing	153
38	Results from K Factor Implementation into TRACE Model . .	154
39	Results from HTC Correlation Implementation into TRACE Model	155
40	Sources of error	156

List of Figures

1	Flow Cross Section of the Hot Channel	17
2	Dimensions of fuel rod	19
3	Close-up of side angle of end fitting	20
4	Model used in TRACE	24
5	Temperature of Water in the channel versus Position	26
6	Pressure in flow channel versus Position	27
7	Velocity of Water in the channel versus Position	28
8	Pipe model used in MATLAB solver with cell divisions	30
9	Temperature of Water in the channel versus Position	43
10	Pressure in flow channel versus Position	43
11	Velocity of Water in the channel versus Position	44
12	Heat transfer coefficient along the channel versus Position	44
13	Reynolds Number of the flow channel versus Position	45
14	Pipe used in original FLUENT testing developed in SolidWorks	50
15	Mesh of pipe used in original FLUENT	51
16	Error in Wall to Bulk Temperature Difference Across 15 Cells	56
17	FLUENT Temperature of Water in the channel versus Position	58
18	FLUENT Pressure in flow channel versus Position	59
19	FLUENT Velocity of Water in the channel versus Position	59
20	FLUENT Heat transfer coefficient along the channel versus Position	60

21	Geometry for the Multi Channel Model	63
22	FLUENT Comparison to Probe Data for Multi Channel FLUENT Model	65
23	Temperature in K of Multi Channel FLUENT Model at 950 kW - X and Y Axis Cut	66
24	Temperature in K in Center Channel of Multi Channel FLUENT Model at 950 kW - Z Axis Cut	67
25	Crossflow in m/s from Multi Channel FLUENT Model at 950 kW	68
26	Z Velocity of Flow in m/s from Multi Channel FLUENT Model at 950 kW	69
27	Centerline temperature values for single channel, multi channel with and without probe to determine significance of models . .	70
28	Configuration for SCALE runs	70
29	6 rods involved in the four channel model	74
30	Heat flux distribution in the 6 rods associated with the multi channel model	77
31	Relative Error in Temperature vs. Number of Cells	78
32	Relative Error in Velocity vs. Number of Cells	79
33	Relative Error in Pressure vs. Number of Cells	80
34	Absolute Temperature (K) vs. Z-location in the pipe (m) . . .	81
35	Velocity of fluid (m/s) vs. Z-location in the pipe (m)	82
36	Absolute Pressure (Pa) vs. Z-location in the pipe (m)	82
37	FLUENT Temperature of Water in the channel versus Position	83

38	FLUENT Pressure in flow channel versus Position	84
39	FLUENT Velocity of Water in the channel versus Position . .	84
40	Location of hot channel in the TRIGA core	88
41	Probe length and thermocouple locations along fuel element .	89
42	Bare thermocouple probe for water measurements in TRIGA flow channels	101
43	8 channel thermocouple input device	102
44	90 degree turn in aluminum pipe system to protect thermocou- ple wires	103
45	Full pipe system with fittings disconnected	104
46	Connections between thermocouple probe and lengths of wire	105
47	Probe just above reactor core with pipe system attached . . .	106
48	Camera output to check if probe fully inserted in flow channel	107
49	Turn in pipe after full insertion in flow channel	108
50	Pipe secured above water during TRIGA operation	109
51	Results of initial probe measurements at 5 reactor power levels	110
52	Results from thermocouple probe during 30 minute run at 950 kW	111
53	Moody diagram for the Darcy friction factor	118
54	Temperature profile in fuel rod using two dimensional heat trans- fer equation	121
55	Overall Setup	123
56	Dimensions of fuel rod	125
57	Radial view of model design	126

58	HTC Fit for 950kW FLUENT Data	139
59	HTC Fit for 200kW FLUENT Data	143
60	HTC Fit for 400kW FLUENT Data	144
61	HTC Fit for 600kW FLUENT Data	145
62	HTC Fit for 800kW FLUENT Data	146
63	Geometry of upper unheated section	150
64	Geometry of lower unheated section	151
65	Error due to mesh size in FLUENT for single channel model .	158

1 Introduction

A major component in the safety of reactor operation is the temperature of the coolant and cladding of the fuel. To determine safe operating levels for the reactor, computer code packages have been written that model thermal hydraulic phenomena by using multiple balance equations that conserve mass, momentum, and energy to determine the time dependent state of the system. This type of code package can be used to model the behavior of the coolant traveling through the core in the presence of a heat source. By inputting material properties and geometric attributes, the codes return the temperatures, pressures, and velocities of the fluid in the core. Different power levels can be tested to determine the maximum power of a reactor design and set a power limit based on that analysis. The NRC certifies certain code packages that it believes does an adequate job in approximating the conditions in the core.

The scenario that is of the greatest concern in the safety of the reactor initiates as follows. A combination of liquid water and steam bubbles at the fuel cladding help to remove heat from the fuel rods. Small steam bubbles form in a typical reactor which help to increase heat transfer into the water because of the flow patterns that are created due to these bubbles. This is known as nucleate boiling. However, if enough of the coolant exceeds the boiling point of water at the pressure in the core, a steam blanket begins to form around the fuel rod. These significantly reduces the heat transfer into the coolant and the void fraction in the core section will exceed the level required to maintain nucleate boiling and a departure from nucleate boiling will occur in the core. The heat flux at which this event occurs is known as the critical heat

flux and it is an important value to calculate for a specific reactor for safety and certification purposes. This will lead to detrimental effects in the reactor requiring that other safety systems become involved to prevent a catastrophic event in the core.

However, NRC certified code packages for performing hot channel analysis for TRIGA power certification could be improved in a few key areas that require addressing. Current solvers are nodal solvers that use bulk conditions in cells of user defined size to simulate the flow channel. This approach can be valid if high fidelity correlations for the heat transfer coefficient and loss factor coefficient obtained from computational fluid dynamic modeling and experimental testing are used in the nodal solver. For the TRIGA flow channels, the nodal solver can be improved since the Nusselt number correlation used is shown to not be ideal for multiple reasons. Those reasons are the hexagonal geometry of the TRIGA core, the flow and temperature conditions in the core, and the loss coefficients due to the bends, constrictions, and expansions that the flow experiences through the core. Finally, the simplified nodal approach does not take into account the crossflow that occurs between neighboring channels.

Another area where the current code packages lack sophistication is in the geometry used in the solver. Non-cylindrical pipe geometries are not accurately accounted for since pipes without a circular cross sectional area are estimated as circular by measuring the wetted perimeter and hydraulic diameter of the flow channel. This simplification can cause results that deviate significantly from the actual system in geometries where the cross sectional area is much

different from a circle (as in our case).

Finally, the current packages assume straight pipes and simulate any turns or other losses due to changing geometry by using loss factors. Those loss factors are experimentally determined or empirically calculated for a system and input as a set of initial conditions. There are no loss factors measured for the exact flow channels of our TRIGA therefore, the hydraulic diameter is used to estimate the loss created by these turns. This increases the error in the modeling since the non-circular cross section experiences multiple 45 degree turns.

This research has seven major components:

- model the TRIGA hot channel using current nodal finite difference codes;
- build a nodal solver in MATLAB to validate the results from the finite differencing codes;
- take experimental measurements of a coolant channel over the entire licensed range of operating powers of the TRIGA ;
- develop computational fluid dynamic models of the hot channel, adjacent channels, and inlet and outlet constrictions;
- create a new heat transfer correlation and loss coefficients using the computational fluid dynamics and experimental results;
- adjust the nodal model to reflect these improvements for future users;
- propose a scale model design for further validation and data generation of the models.

Currently, no correlations specific to TRIGA reactor have been developed by combining both a computational fluid dynamic code to simulate the system and a probe to take real time temperature measurements of the channel. This is the first method of its kind to determine heat transfer coefficient and loss factor coefficient correlations specific to the TRIGA reactor. The computational fluid dynamics code yields a finer resolution of the channel operating conditions since the model geometry can be adjusted so that the probe lies in the flow channel. Therefore, the probe data can be matched to the same location in the computational fluid dynamics model because of intricacy of the model. The new heat transfer correlation and loss factors are a new development in the field and will improve the results of the finite differencing model for not only the University of Texas TRIGA reactor but all TRIGA reactors with similar geometries. This improved model will also allow for a potential uprate of the maximum operating power for the University of Texas TRIGA.

This dissertation first includes a background and literature review on the history of this field. Next, the finite element models (NRC and MATLAB models) are presented and their results are supplied. Then, the computational fluid dynamics model is introduced and the design improvements over the finite element models are listed. The experimental testing with the thermocouple probe is then addressed and the temperature results are given for the entire range of TRIGA operating conditions. The results are then given for the adjustment of the computational fluid dynamics code based on the probe results as well as the new heat transfer correlation and loss factors. Finally, the new nodal results from TRACE are presented along with proposals for

further development of the work.

2 Literature Review

The following is an introduction into the different computer codes developed for use in modeling these flow channels and their disadvantages followed by a discussion of current work on utilizing these codes to model TRIGA components. Finally, prospects for using a Navier-Stokes solver to augment the capabilities of the nodal solvers will be assessed.

2.1 Computer Codes Developed for Thermal Hydraulic Modeling for Nuclear Reactors

Modeling of the TRIGA and its coolant channels has been ongoing since the inception of the design. Originally, flow calculations were done without the aid of computers but since their inception into the engineering workplace, computer codes have evolved to increase the accuracy of those calculations. This subsection will provide a high level review of thermal hydraulic simulation and modeling approaches. An early approach, pursued at Sandia National Lab [1] in the 1970s, developed an iterative numerical scheme to solve the balance equations involved in the thermal hydraulic modeling of the ACRR. This model involved equations that accounted for

- entrance pressure losses,
- exit pressure losses,
- friction pressure losses in both the fuel and non fuel sections,
- acceleration pressure losses due to changing density,

- pressure gain due to buoyancy.

The group attained results within 10% of the measured values in their ACRR core.

Also during the 1970s, Lawrence Livermore National Lab developed the first computer code available from the Radiation Safety Information Computational Center (RSICC) that treated transient and steady state temperature distributions in multi-dimensional systems, TRUMP [2]. TRUMP was written in FORTRAN and solved systems of parabolic partial differential equations to describe the flow in various fields such as electricity and magnetism, temperature, pressure and fluid flow. Initial conditions were defined based on the spatial position, time or dependent variables such as temperature. This code was not directly developed for the hot coolant channel but it was used to solve the system. Because of the development of newer code packages that better handle reactor components and conditions, TRUMP is no longer used for TRIGA modeling.

The first RSICC code package available for the thermal hydraulic analysis for a light water reactor was TRACE (first named TRAC-P1A) [2]. TRACE was first distributed in 1979 as a loss of coolant accident code. The code was further expanded to be used in a wide range of thermal hydraulic experiments including hot channel analysis. This code was written in FORTRAN 77 and developed at Los Alamos National Lab. It takes into account multi-dimension two-phase flow, non-equilibrium thermodynamics, generalized heat transfer and reactor kinetics. Partial differential equations that describe the two phase flow and heat transfer are solved using a finite difference method. The equa-

tions governing the fluid dynamics and heat transfer for the three dimensional model use semi implicit differencing. A semi implicit difference scheme is one where by limiting the number of iterations used to solve the scheme, the scheme can be converted into an explicit scheme which can be solved more easily. This creates an approximate discrete answer to a much more complicated problem. This method uses a first order integrator so the error is based on the number of iterations performed. To solve this system of coupled, nonlinear equations, the Newton-Raphson iteration was used. TRACE serves as the basis for other RS-ICC codes published in later years as well as the code package used to initially model the hot channel due to the current version's reactor components and its various features for simulating the turns and non-circular cross sectional area. Its disadvantages lie in the fact that it is still a nodal solver that averages the behavior of the fluid over a cell as well as not being able to handle the actual geometry.

RELAP3b became available from RSICC beginning in 1980 [2]. RELAP uses FORTRAN IV as its language to model the behavior of water cooled reactors during accident scenarios or large power transients. RELAP also models pump failures and other component mishaps. The program calculates the mass and energy inventories of the system, and the flow, pressure and temperature of the water coolant. RELAP can handle a system as small as a single coolant channel to a full reactor design. The solution is obtained by integrating a set of differential equations that describes the time-dependent thermal and hydraulic parameters of the system. RELAP was paired with TRAC in the final version of SNAP (discussed below) as a combined code

package which was used for the initial hot channel modeling.

COBRA-EN was developed in the 1980s as a FORTRAN based code that starts from a steady-state condition for a full LWR core or a single fuel element and calculates the effect of changes in total power, pressure and mass flow rate [2]. These changes can be enacted by the user to observe the effects of those changes on the entire system. Three daughter codes resulted from COBRA: NORMA, QUARK and NORMA-FP which all deal with thermal hydraulic scenarios in light water reactors. The method for solution in COBRA deals with creating three conservation equations: mass, energy and momentum, to describe the system. A later enhancement included an equation for void fraction that made the solver a four equation system. Two different solution schemes were used. First, an iterative algorithm was used, similar to the ACRR work from Sandia, that solved for the pressure gradient in the system. The second was an implicit solution based on the Newton-Raphson method which adjusts the axial flows at different mesh points to force the continuity of the mass of the coolant mixture. COBRA-EN was not used since it focused on a steady state reactor that dealt with accident scenarios as opposed to our model where the reactor performs a cold startup.

TRISTAN-EJP was developed in the early 1990s to calculate the steady state axial temperature distribution and flow velocity in a coolant channel of a TRIGA reactor with its corresponding geometry [2]. This code package is only valid at low power levels (below 2 MW) in a TRIGA assembly. TRISTAN is based in FORTRAN and runs by iterating the Bernoulli equation to find a stable operating point for the reactor. TRISTAN was not used since it has

few variables that the user can adjust and the system can only be a single flow channel. Our modeling expands to handle more than one flow channel flowing at the same time so TRISTAN was not feasible for our system.

SNAP was developed by the NRC as a graphical interface for ease of use in developing thermal hydraulic models [3]. SNAP is not a thermal hydraulic code alone, it instead requires plug-ins that allow the user to create a visual model as opposed to one in a text file, that runs the corresponding code package provided by RSICC. The code packages supported by SNAP are:

- TRACE - TRAC/RELAP Advanced Computational Engine
- RELAP5 - Reactor Excursion Leak Analysis Program
- PARCS - Purdue Advanced Reactor Core Simulator (an NRC regulated code that is based on TRACE and RELAP) [4]
- MELCOR - Severe Accident Analysis Code (a code developed in 1986 by Sandia National Lab to handle a wide variety of nuclear related tests including thermal hydraulics) [4]
- COBRA-IE - Coolant Boiling in Rod Arrays Code

By evaluating the strengths and weaknesses of each of the codes provided by the SNAP plug-ins, the TRAC/RELAP (TRACE) code package was selected since it had the tools that would best model our base system.

2.2 Previous TRIGA Models

Several groups have done work in modeling the TRIGA coolant channels. A research team from Oregon State [5] in 2008 used RELAP5-3D (an updated version of RELAP5) to model the hot channel in the Oregon State Test Reactor (OSTR). Their geometry was circular as opposed to the hexagonal array that exists at NETL. Measurements were taken of their hot channel using a thermocouple and the OSTR model was benchmarked against those values. No other computer codes were used to benchmark the results from the RELAP-3D output. Their work assumed a circular cross section of the flow channel and was expanded to handle the hot channel in conjunction with the average flow channel from each ring to simulate the full core.

A group from Algeria with a circular geometry used RELAP5, ATHLET and CATHENA (LWR Systems Analysis from GRS and AECL respectively) to model their research reactor with a proposed new core configuration [6]. They used the code packages to determine if they could more effectively use the reactor time by optimizing the reactor utilization. By using the natural convection operating mode, they validated the new core configuration against allowed safety parameters. Two accident scenarios were also looked at: an unprotected fast reactivity insertion and a flow blockage of a flapper valve. Output temperatures of the coolant were monitored to ensure the water remained subcooled.

A Moroccan group modeled their TRIGA Mark II research reactor to show that, under all operating ranges currently allowed, that the coolant parameters fell within allowed guidelines [7]. A new code package named SACATRI (Sub-

channel Analysis Code for Application to TRIGA reactors) was developed to return results ideal for use in other numerical simulation codes. Their code uses four partial differential balance equations (mass, energy, axial momentum and transverse momentum) and an iterative solver to determine the coolant flow parameters. Benchmark cases were used to determine the accuracy of their solver which were supplemented with a code to code comparison. Finally, an evaluation of the order of accuracy test (a test where the discretization error is reduced at the expected rate due to changes in the scheme) was done to better determine the accuracy of their solver.

Umar et al. used the STAT code package to perform the safety evaluation of the upgrade from 1 MW to 2 MW of the TRIGA reactor at the Institute of Technology Bandung in Indonesia [8]. STAT calculates the natural convection through the water coolant which is bounded by heat sources that simulate the fuel rods. After theoretical analysis, the actual temperature in the modeled channel was measured using a probe consisting of eight thermocouples. The purpose of this test was to verify the STAT results so that they could be used in the increase of the licensed power of their reactor.

Fiantini and Umar used a computational fluid dynamics code to assess whether it was feasible to use a CFD code to model fluid flow in a full reactor system [9]. By modeling the entire core, they defined the natural convection in both the original TRIGA design and the modifications to the original design that exist in the TRIGA 2000 design. It was determined that the computational fluid dynamics code package was adequate in calculating the fluid flow pattern in and around the TRIGA core. It was also determined that forced

convection plays a small role in the overall flow in the flow channels during reactor operation.

Mesquita et al. carried out extensive measurements of the coolant temperature in their TRIGA Mark I reactor (100 kW) located at the Nuclear Technology Development Center in Brazil [10]. They used thermocouples in multiple flow channels simultaneously to determine the temperature of different locations in the coolant at various power levels. Since multiple channels were evaluated at once, the group determined that there is a significant amount of cross-flow between neighboring channels. Also, measurements of other parameters such as the heat transfer coefficient were done to best describe the behavior of their reactor.

Buke and Yavuz used the TRISTAN code package to calculate theoretical average flow parameters of the coolant in their TRIGA core and compare those numbers to previously determined actual values [11]. A mathematical model was developed to also model their core which was benchmarked against the TRISTAN code. Through their measurements, their code was seen to agree well with TRISTAN at lower reactor powers but as the reactor power increases, their code is less accurate due to the temperature dependence of the water properties at their effect as the power increases.

2.3 Navier-Stokes Solvers

FLUENT is a computational fluid dynamics code that uses a discrete grid to handle a model with a continuous domain. A mesh of grid points is created for the geometry of the pipe so that the relevant variables to the flow are calculated

at each point. Therefore, FLUENT solves a set of coupled algebraic equations at each grid point.

The FLUENT code uses the finite-volume method to determine the flow characteristics of the channel. The grid points are known as nodes in the meshing software where quadrilaterals are formed between four nodal points which are known as cells. For 3D versions of the solver, the cells can be hexahedral, tetrahedral or prisms. In this case, tetrahedrals were used since they best characterized the geometry. For this approach, each volume defined by a cell satisfies the integral form of the conservation equations as opposed to the differential equations used in the finite difference method. Fundamental to this approach are balance equations. For instance the net volume flow into the each individual volume must be 0:

$$\int_S V \cdot n dS = 0 \quad (1)$$

Therefore, the mass entering and leaving the cell must also be conserved so the following equation is also true (for a tetrahedral cell).

$$-u_1\Delta y - v_2\Delta x + u_3\Delta y + v_4\Delta x = 0 \quad (2)$$

Where:

- v is the velocity in the x direction

- u is the velocity in the y direction
- each number denotes the side of the cell that the liquid crosses

This changes the continuous equation in eq. (1) to the discrete form needed for the solver. The velocities are found by interpolating between the bulk values of surrounding cells. The equations for the momentum and energy are determined in the same way. For grid locations on a surface or near a boundary of the pipe, the discrete equations are coupled with boundary conditions that are set by the user such as the properties of the pipe inlet, outlet and walls. Various parameters can be initialized such as the velocity, pressure, temperature and other fluid factors.

FLUENT inverts the discrete equations to solve the system where the smaller the cells, the more accurate the characterization of the parameters. FLUENT uses a matrix inversion across the number of cells in the model to execute a solution. Much of the matrix is filled with zeros since the equations for each cell only depend on the neighboring cells. The code then iterates to find the a solution to the matrix equations associated with each balance.

However, not all of these balance equations are linear which complicates the solver. The equations for the momentum conservation and turbulence in the pipe give rise to nonlinear terms. Therefore, FLUENT iterates by guessing the values at all of the grid points and then uses the guess from the previous iteration when it runs again. As the number of cells used in the model increases, so does the run time so a balance must be struck between error in the measurements and overall run time. This balance is typically achieved through a convergence study for the model.

If these sets of equations were set up in a large matrix, solving this system may take too long. Each grid point is expressed in terms of the values of the neighboring cells. Since each point is defined as a relationship between the neighboring points, the solver can use an initial guess for the system at the inlet and obtain an approximate solution for the entire matrix. This greatly reduces the runtime and memory storage for the solver. Once the matrix converges to a steady set of values, the system is solved and the values at each grid point are their final values. The convergence depends on a user set value of difference between iterations for the system to be declared converged. There are 7 equations checked: energy, x-velocity, y-velocity, z-velocity, k, epsilon, and continuity. The solver is complete when the differences between iterations are below the required level.

3 Single Channel Nodal Models

3.1 TRACE

The TRACE model was based on previous work done at the University of Texas at Austin. The model used for this work was adapted from that model with adjustments to the geometry, heat profile, initial conditions and K-factors.

3.1.1 Geometry

Adjustments were needed to convert the flow channel into a cylinder so that it met the requirements of the TRAC/RELAP code. The flow area in the hexagonal array of the channel is far from cylindrical as seen in figure 1.

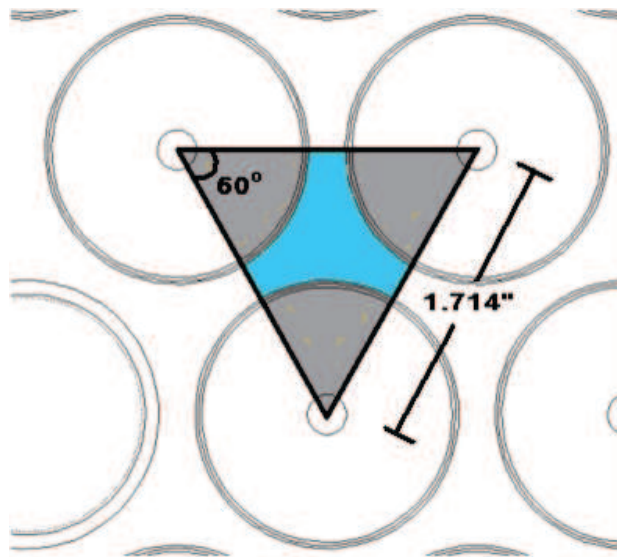


Figure 1: Flow Cross Section of the Hot Channel

The wetted perimeter was used to determine the hydraulic diameter of an equivalent circular cross section flow channel since the TRIGA channel is not circular. While the flow will not behave in an identical manner as the TRIGA channel, it will be simplified for the TRACE program and be an estimate of the actual channel.

The wetted perimeter is the cross sectional length of the pipe that is in contact with the fluid. Since the flow channel is simulated using a pipe filled with water, the wetted perimeter of the pipe is equivalent to the actual perimeter of the flow channel. The hydraulic diameter converts pipes that are not circular into circular pipes that have approximately the same effective diameter. The hydraulic diameter is then used to find other quantities relevant to the pipe such as the Reynolds number of the flow and the pressure loss.

The wetted perimeter for the heated section of the flow channel was calculated by taking the technical drawings of the fuel elements by General Atomics and placing them in a program to determine the pixels that encompass the flow channel. By knowing the number of pixels, the flow channel perimeter was measured. The dimensions for the fuel rods are defined and given however, the dimensions for the flow channel are not published by General Atomics. For the hydraulic diameter of the flow channel, a relation between the flow cross sectional area and the wetted perimeter is used:

$$HydraulicDiameter = \frac{4 \cdot FlowArea}{WettedPerimeter} \quad (3)$$

While this method works well for a pipe with a constant radius, the flow

area significantly changes at the ends of the flow channel, so that a different approach to is needed to approximate those sections given the constraints imposed by the TRACE platform.

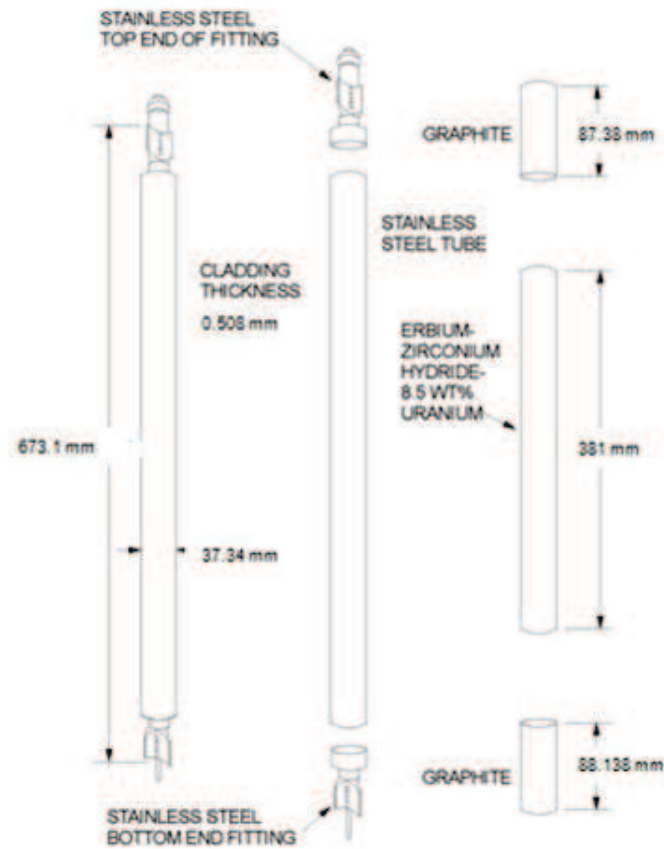


Figure 2: Dimensions of fuel rod

The stainless steel ends of the fittings which help hold the rods in place in the upper and lower grid plates have fins that change the flow properties of the water through the coolant channel as seen in figures 2 and 3.

These fins along with the entrance/exit through the grid plate cause losses

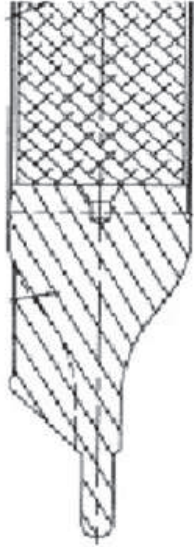


Figure 3: Close-up of side angle of end fitting

to occur in the flow channel. To account for these losses, a loss coefficient or K-factor is used. The loss coefficient is an experimentally determined value that depends on geometries at the inlet, outlet, and turns in the pipe. Tables 1,2 and 3 were used to determine the individual loss coefficients for each component. These were summed to find the overall loss coefficient. The inlet loss coefficient was found using the ratio between the flow area at the lower grid plate to the flow area of the pipe exiting the grid plate. The outlet loss coefficient was found using the ratio between the flow area of the pipe exiting the grid plate and the flow area at the upper grid plate. Fig 8.17 from [13] was used in conjunction with the ratio to determine the loss coefficient due to the sudden expansion and contraction. This is an approximation of the turns that occur in the actual system and a more geometrically sensitive model is needed for better treatment of the bends the water makes around the fins of

the fuel rods.

Table 1: Inlet flow areas[13]

Inlet Location	Area in cm ²
Area of lower grid plate at entrance	1.2
Area in pipe at entrance at exit	3.9

Table 2: Turns in the flow channel and their effect on K[13]

Angle of turn	Contribution to the loss coefficient
45°	16*friction factor
90°	30*friction factor

Table 3: Outlet flow areas[13]

Outlet Location	Area in cm ²
Area in pipe at exit	3.9
Area of upper grid plate at exit	1.2

Using these 3 tables to perform the respective calculations, the K factor (unitless) for the entire pipe system was determined to be 2.188. The K factor was split into two sections, loss above and loss below the heated section. The inlet loss coefficient was 1.244 due to the 45° turn ($K=0.344$) and the sudden expansion at the grid plate ($K=0.9$). The outlet loss coefficient was 0.844 due to the 45° turn ($K=0.344$) and the sudden contraction at the grid plate ($K=0.43$). Those factors were applied to the single unheated section included above and below the heated section in the model.

Since all of the pipe properties are now accounted for, the pipe was built with 15 equally sized heated sections to simulate the heat generated from the fuel section and a section above and below the fuel to simulate the graphite reflector and fins. The measurements for an individual heated section are in table 4.

Table 4: Dimensions of individual heated section

Dimension	Value
Volume in cm ³	6.85
Length in cm	2.54
Flow Area in cm ²	2.70
Hydraulic Diameter in cm	1.8524

The graphite reflector sections at the ends of the heated sections are identical and have the same dimensions as the individual heated section cells except for the volume and length which are 87.8 cm³ and 16.55 cm respectively.

The heat applied to the flow channel was determined to be a total power of 13645 watts. This value was determined from a total reactor power of 0.95 MW divided equally across 110 flow channels and then multiplied by a peaking factor (power in a particular flow channel versus the average power in a flow channel) of 1.58 since it is the hot channel [12]. An axial power distribution was also applied to the model using results obtained from the same MCNP work that determined the peaking factor shown in table 5.

To simulate the flow of the water below, above and through the core, additional components were included in the model.

A larger pipe is connected to the inlet to simulate the amount of water in the pool below the flow channel that will travel through the flow channel. The size was determined by taking the entire pool size below the core and adjusting for the number of flow channels and peaking factor. The plenum (number 41) simulates the entire pool by using the dimensions of the TRIGA pool and setting it at a temperature of 322 K. The break (number 61) is connected to the outlet of the pipe and it keeps the pressure of the outlet constant at the

Table 5: Heat applied to individual cells in the heated element

Distance to center of cell from bottom of heated element (m)	Heat applied to cell (W/m ²)
0.0127	7.04e5
0.0381	7.92e5
0.0635	8.80e5
0.0889	9.69e5
0.114	1.06e6
0.139	1.09e6
0.165	1.13e6
0.19	1.17e6
0.216	1.13e6
0.241	1.09e6
0.2667	1.05e6
0.292	9.68e5
0.3175	8.80e5
0.343	7.92e5
0.368	7.04e5

pressure due to the atmosphere and water pressure (149000 Pascals) because the flow channel lies at 4.75 meters below the top of the pool (eq. 4). In this way, the flow will be driven by the heating of the water as well as the gravitational force in the pipe.

$$Total\ Pressure = Atmospheric\ Pressure + \rho gh \quad (4)$$

Where:

- ρ is the density of the pool water
- h is the depth in the pool

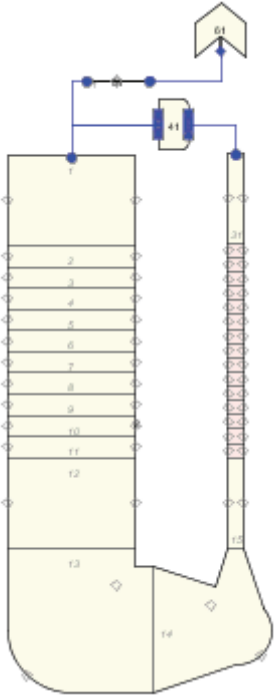


Figure 4: Model used in TRACE

3.1.2 Results

TRAC/RELAP was designed to start with a system at full power and a transient would be introduced to cause a problem in the system and the results of that insertion, such as a pipe break, could be analyzed. The solver was setup to run for 1000 seconds of real time so that the flow channel could reach a stable state. The heat was applied in 3 steps with the heat at time zero having a value of a fourth of the full power applied to the flow channel, half of the full power was applied at 250 seconds and full power was applied at 500 seconds. This ramping of the power was done to make sure the continuity equations across the cells did not change too quickly due to a large power insertion (no

power to full power) causing instability in the system. The solver operates at user defined timesteps that balance speed with accuracy. If the timesteps are too large, instability may arise in the solver due to significant changes between steps. If they are too small, the solver may take too long to find a solution. As the amount of power applied to the system increases, smaller timesteps are required to keep the system from becoming unstable.

The data was taken and graphed in MATLAB in figures 5 through 7. The temperature distribution shown in 5 shows a steady increase since the total heat added to the flow channel increases almost linearly with the axial position. The slight deviations from linearity are due to the axial temperature distribution that was applied to the heated section, which is not linear. The pressure decreases as the axial location increases since less water lies above that location in the flow channel. It is also linear due to eq. 4. The density of the water is constant in the TRACE program but since the density of the water actually decreases as heat is applied, an actual pressure measurement would yield a graph that would have less pressure change between two points at the top of the flow channel as opposed to the bottom. The velocity slowly increases in the flow channel due to the heating of the water in the flow channel and the buoyancy effects that result due to that heating.

The accuracy of the solver is in question based on the fact that loss factors are used to estimate the turns in the flow channel, the actual flow channel does not have a circular cross section and average values for each cell are measured which assumes radial trends that may not be true for the system. These trends are determined using the heat transfer and loss coefficients in the model.

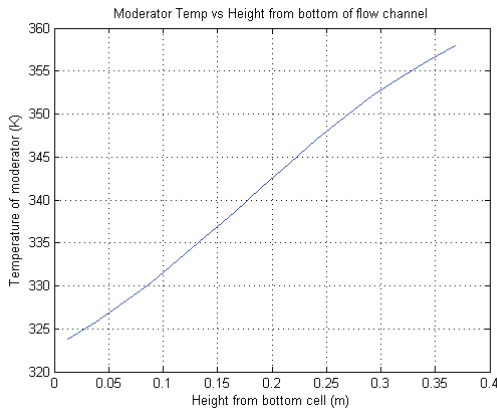


Figure 5: Temperature of Water in the channel versus Position

3.1.3 Sensitivity Analysis of the TRACE Model

Four parameters were varied in the TRACE model to determine their effect on the overall flow rate and outlet temperature in the hot channel. This is done to determine which parts parameters most strongly drive the outcome of the model. The parameters varied were:

- Inlet K-factor
- Outlet K-factor
- Hydraulic diameter
- Overall heat into hot channel using the same axial temperature profile

Shown in table 6 are sensitivity analyses of these variables on the total output flow rate and outlet temperature of the hot channel.

These results imply that the model is most sensitive to changes in the hydraulic diameter; therefore, the cross flow between channels could cause

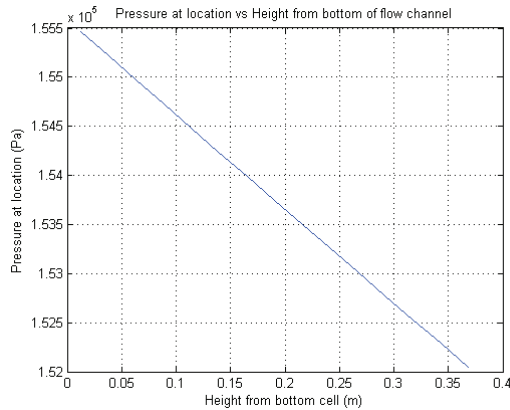


Figure 6: Pressure in flow channel versus Position

Table 6: Sensitivity Analysis of TRACE Model

Ratio	Range of denominator values	Change in denominator	Change of flow rate (%)	Change in temperature (%)
$\frac{d(\text{Change})}{d(K_{\text{input}})}$	0.766	- per 0.1	1.445 ±	0.411 ±
	1.766		0.184	0.052
$\frac{d(\text{Change})}{d(K_{\text{outlet}})}$	0.366	- per 0.1	1.593 ±	0.485 ±
	1.366		0.1929	0.056
$\frac{d(\text{Change})}{d(\text{Hyd. Diameter})}$	1.352	- per 1 mm	6.769 ±	1.782 ±
	2.352 cm		0.421	0.054
$\frac{d(\text{Change})}{d(\text{OverallHeat})}$	11.5 - 21.5 kW	per 1 kW	1.84 ±	0.4259 ± 0.01

the effective hydraulic diameter of the system to vary from the value implied by the geometry of an isolated channel. Since this parameter causes a large change in the overall behavior of the system, use of the FLUENT cross flow model to quantify an effective hydraulic diameter will be a key part of future work. The inlet and outlet K-factors are also significant, confirming the initial premise that the loss due to the turns and grid plate entrance and exit must

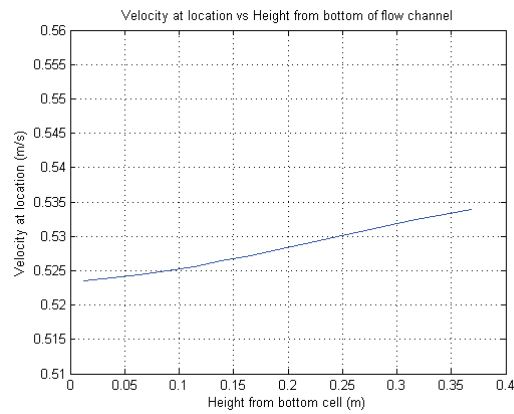


Figure 7: Velocity of Water in the channel versus Position

be looked at in greater detail to determine the actual loss coefficient.

3.2 MATLAB

3.2.1 MATLAB Formulation

A simplified model of the hot channel was made to demonstrate the sensitivity of the results to changes in parameters such as the pipe properties (e.g., diameter, length, friction factor) and channel properties (e.g., heat applied to the channel, density changes of the water).

The MATLAB model was used as an intermediary between the TRACE and FLUENT model. Hereafter, the flow channel has been more accurately modeled using the actual geometry and a more robust computational fluid dynamics code, and the MATLAB solver will be adjusted to achieve a result similar to the FLUENT results. This understanding of how the code needs to change to obtain better results for the MATLAB solver will assist in improving the execution of the TRACE code to achieve a more adequate result for the flow properties in the hot channel.

The goals of this model were to:

- determine how the following variables change with respect to changes in the geometry and heat applied to the system and determine the trends of these variables over the length of the channel:
 - velocity of the water through the channel,
 - temperature of the water in the channel,
 - pressure in the channel;

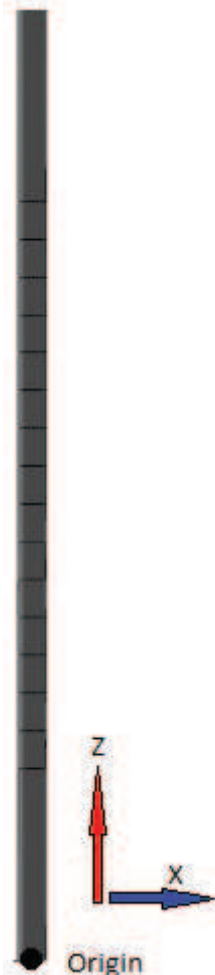


Figure 8: Pipe model used in MATLAB solver with cell divisions

- develop a model that approximates the work done in TRACE,
- compare the model with TRACE and achieve reasonable agreement between the two,
- provide as a check and a balance for the TRACE program at a basic level

To adequately model the flow channel while retaining simplicity and trans-

parency, the following simplifications were made:

- loss factors were included to account for the energy lost in the turns the flow makes in the actual system,
- an axially discretized nodal approach was used to model the bulk flow properties, as is done in TRACE.

However, the MATLAB model has limitations that render it useful only as a validation and sensitivity analysis tool. Both the MATLAB and TRACE models greatly simplify the geometry of the actual flow channel through the use of K-factors. These are estimations at best since the flow in these turns and contraction/expansion of the pipe cause turbulence in the pipe that is not well approximated with the loss factors. The total energy at any location along the flow channel is composed of potential energy and kinetic energy where frictional losses, change in internal energy of the fluid and energy supplied by the heating of the channel act to change the total energy at that location. When the static pressure (pressure at a certain point in the fluid) decreases, the velocity of the water increases since the force due to pressure is larger behind the fluid than in front of the fluid along the streamline. Since the heated water has a lower density than the unheated water above the channel, the heated water experiences a buoyant force that causes the water to rise. Therefore, as more heat is added to the system, the water becomes less dense and increases the flow rate in the channel. The Bernoulli Equation assumes an idealized system that:

- is frictionless,

- has no external energy sources such as heat,
- is incompressible.

Therefore, the equation is only a starting point in that just takes into account the pressure, kinetic energy and potential energy of the system. All other forms of energy that are existent in the actual system will be included by adding additional terms to this base equation. The Bernoulli Equation (in units of meters) for the system is[13]:

$$\frac{P_i}{\rho g} + \frac{0.5v_i^2}{g} + h_i = \frac{P_o}{\rho g} + \frac{0.5v_o^2}{g} + h_o \quad (5)$$

Where:

- i is the inlet location of a pipe,
- o is the outlet location of a pipe,
- P is the pressure at that location [Pa],
- ρ is the density of the material flowing at that location [g/cm³],
- v is the velocity of the flowing material at that location [m/s],
- g is the gravitational coefficient [9.8 m/s²],
- h is the height of that location above the origin along the z axis [m]

Solving this system where the entire pipe is treated as one cell severely limits the flexibility of the solver since it doesn't allow for changes in the properties of the flow channel along the pipe. By dividing the pipe into smaller

sections, changes in fluid properties can be resolved more finely and the axial dependence of the heat source treated more accurately than in a one cell model. Therefore, the index i and $i+1$ will now identify two consecutive cells where the $i+1$ cell is the cell adjacent to the cell denoted by i . The cell division used is shown in Figure 8.

There are two methods of energy loss through the pipe that are quite significant that are not included in Bernoulli's equation: major and minor losses. Major losses are due to the friction between the flowing material and the pipe wall that it comes into contact with. Major loss through a pipe section is given by[13]:

$$h_{major} = f \frac{LQ^2}{2gDA^2} \quad (6)$$

Where:

- h_{major} is the loss due to major losses [m],
- f is the friction factor [unitless],
- L is the straight length of the pipe [m],
- Q is the flow rate [m^3/s],
- D is the hydraulic diameter of the pipe [m],
- A is the flow area in the pipe [m^2]

Minor losses occur when the flow passes through fittings, bends, or abrupt changes in cross sectional area such as entrance or exit from a pipe to a significantly different flow area. They are denoted "minor" since if the pipe has a

long straight section, the loss in the aforementioned manner is minor compared to the loss due to friction in the pipe. Minor losses are given by[13]:

$$h_{minor} = \frac{KQ^2}{2gA^2} \quad (7)$$

Where:

- h_{minor} is the loss due to minor losses [m],
- K is the loss coefficient [unitless]

The flow receives an energy input via the heat in the fuel element section. To take this into account, a heat source term was added to the equation. This term describes the heat transferred into the water flowing through the heated section from the steel boundaries of the channel. The heat source contribution given in units of meters is[14]:

$$\frac{\dot{q}}{\rho g Q} \quad (8)$$

Where:

- \dot{q} is the power output of the heated section [W]

For the channel being modeled, the heat energy applied to the fuel section of the pipe was 21500 W.

This energy absorption causes the water particles to move faster because of the increase in internal energy causing the density to decrease while the temperature rises. To account for that internal energy change in the fluid in

the overall energy equation, the term below is used[14]:

$$\frac{\dot{m}c_p\Delta T}{\rho g Q} \quad (9)$$

Which reduces to:

$$\frac{c_p\Delta T}{g} \quad (10)$$

Where the following are true:

- \dot{m} is the flow rate [kg/s],
- c_p is the specific heat of the water [J/(kg K)],
- ΔT is the temperature difference between the two locations [K]

Therefore, the final equation describing the energy in the flow channel after combining (5) with all of the losses and energy inputs is:

$$\frac{P_i}{\rho g} + \frac{0.5v_i^2}{g} + h_i = \frac{P_{i+1}}{\rho g} + \frac{0.5v_{i+1}^2}{g} + h_{i+1} + f \frac{L_{i+1}Q^2}{2gD_{i+1}A_{i+1}^2} + \frac{K_{i+1}Q^2}{2gA_{i+1}^2} \quad (11)$$

$$- \frac{\dot{q}_{i+1}}{\rho_{i+1}gQ} + \frac{c_{p_{i+1}}\Delta T_{i+1}}{g} \quad (12)$$

Terms with positive signs on the right side of the equation remove energy from the system and negative signs add energy to the system. The major loss and minor loss have a positive sign since the loss draws from the energy available at the outlet of the pipe. The heat source contribution has a negative sign since it adds energy to the system and the energy absorption of the water has a positive sign since it adds internal energy to the particles in the water.

Mass and energy are continuous across the cell boundaries (11). For the mass balance, the following must hold true:

$$\rho_i A_i v_i = \rho_{i+1} A_{i+1} v_{i+1} \quad (13)$$

To solve this system, the equations for the mass balance (13) and energy balance (11) are used though terms in the equations are coupled so an arithmetic solver was used to solve the balance equations in the flow channel. The inlet conditions, pressure, bulk velocity, and temperature, were chosen to equal those of the TRACE model.

Table 7: Initial conditions for the inlet of the MATLAB solver

Variable	Value
Pressure	1.58×10^5 Pa
Temperature	322 K
Velocity	$0.52 \frac{m}{s}$

To determine the number of cells to divide the pipe, the TRACE model was used as a guide. The TRACE model was composed of 15 heated cells, each 1 inch in length, along the length of the flow channel plus 2 additional cells, one above and below the heated section, to model the graphite on the ends of the fuel rod. Therefore in our model, 17 cells were used that matched the dimensions of the cell sections of the ones used in the TRACE model. The two cells that surround the heated elements also served as an location to implement the loss factors for the turns in the pipe that were omitted from the geometry of the model. Refer to the convergence section of the TRACE chapter for discussion on why this many cells were used in the final model.

MATLAB was used to solve for the unknown variables (pressure, temperature and velocity) of locations further downstream as well as the flow rates. Included in Appendix A is the code used in the solver. The heat was distributed along the pipe in the same sinusoidal distribution that was done in the TRACE model which mimics the TRACE program. The boundary conditions for the cell interfaces are:

- conservation of mass,
- conservation of energy

Below is a description of the variables and constants in the MATLAB solver:

The known variables in the system are:

- Heights: Gives the boundaries of each of the cells. In this case, each cell is the same size with a size of $\frac{\text{lengthofheatedsection}}{\text{numberofnodes}}$,
- FlowAreas: The area that the flow travels through in the pipe,
- Majorloss: The value of the dimensionless variable that represents the major loss in the pipe due to friction,
- Minorloss: Simulates turns in the pipe without adding geometric turns to the model,
- Heat: Heat power applied to the cell,
- \dot{m} : Mass flow rate of coolant. It was initialized by multiplying the density, velocity and flow area through which the water travelled in the

pipe. Then it was set constant for the length of the pipe since mass flow must be conserved

The constants defined in the code are:

Table 8: Constants used in the MATLAB solver and their values

Constant	Value
Gravity	9.81 m/s ²
Diameter of the pipe	0.0205 m
Length of heated section of the pipe	0.371 m
Heat applied to the entire pipe	21500 W
Friction factor inside of the pipe	0.0215

The unknown variables in the system are:

- T_{surf} : The temperature of the surface of the pipe (K),
- Temps: The temperature of the coolant at the given location in the pipe (K),
- Pressures: The pressure at the given location in the pipe (Pa),
- Velocities: The velocity of the coolant at a given location in the pipe (m/s),
- h : The heat transfer coefficient in the cell ($\frac{W}{m^2 K}$),
- c_v : The specific heat of the water ($\frac{J}{kg K}$),
- k : The thermal conductivity of the water ($\frac{W}{m K}$),
- Nu: Nusselt number. Refer to section 3.2.3 for a detailed explanation (unitless),

- Pr: Prandtl number. Refer to section 3.2.3 for a detailed explanation (unitless),
- Q: Volumetric flow rate of the coolant ($\frac{m^3}{s}$),
- β : Expansion Coefficient of the coolant (K^{-1}),
- Re: Reynolds number (unitless),
- μ : Viscosity of the coolant (Pa*s),
- ρ : Density of the coolant (kg/m³)

The definition of heat capacity is used to find the temperature of the next cell using the equation:

$$Temps_{i+1} = \frac{Heat_i}{c_v \dot{m}_i} + Temps_i \quad (14)$$

To find the Prandtl number, thermal conductivity, expansion coefficient, specific heat, and viscosity, tabular values from table A.6 [14] were fit to a curve which was used to determine each variable. This was done by taking the values of the variables below at an interval of 5 Kelvin from 273 K to 420 K and performing a second order polynomial fit to the data except in the β case where it was a linear function. The equations for those 5 fits are below:

$$Pr_i = 0.0002685Temps_i^2 - 0.225Temps_i + 47.354 \quad (15)$$

$$k_i = -0.00000628Temps_i^2 + 0.00511Temps_i - 0.3529 \quad (16)$$

$$\beta_i = 0.000005621 \text{Temps}_i - 0.001348 \quad (17)$$

$$c_{pi} = 0.0109 \text{Temps}_i^2 - 6.8945 \text{Temps}_i + 5270.8 \quad (18)$$

$$\mu_i = 0.00000003695 \text{Temps}_i^2 - 0.00003097 \text{Temps}_i + 0.006687 \quad (19)$$

To find the density of the water of the next cell, a relation between the temperature difference of the initial and final cells and the expansion coefficient of the water was used:

$$\rho_{i+1} = \frac{\rho_i}{1 + \beta_{i+1}(\text{Temps}_{i+1} - \text{Temps}_i)} \quad (20)$$

To find the bulk Reynolds number of the cell, the following was used:

$$Re_{i+1} = \frac{\rho_{i+1} V_{i+1} D_{i+1}}{\mu_{i+1}} \quad (21)$$

For the Nusselt number, the Gnielinski correlation was used[14]. Refer to section 3.2.3 for a detailed explanation.

$$Nu = \frac{\frac{f}{8}(Re - 1000)Pr}{1 + (12.7(\frac{f}{8})^{0.5}(Pr^{\frac{2}{3}} - 1))} \quad (22)$$

Then the heat transfer coefficient follows from the definition of the Nusselt

number[14]:

$$h_i = \frac{k_i N u_i}{D_i} \quad (23)$$

To find the surface temperature of the flow channel, the following relation was used:

$$T_{surf} = \frac{Heat}{\pi D(h)L} + T_{water} \quad (24)$$

To find the velocity in the next cell, the mass balance equation (13) was rearranged:

$$v_{i+1} = \frac{\rho_i A_i v_i}{\rho_{i+1} A_{i+1}} \quad (25)$$

To find the volumetric flow rate, the mass flow rate was divided by the density of the water in the cell:

$$Q_i = \frac{\dot{m}_i}{\rho_i} \quad (26)$$

Finally, the energy balance equation (11) was shuffled to solve for P_2 to yield the equation:

$$P_{i+1} = \frac{\frac{P_i}{\rho g} + \frac{0.5v_i^2}{g} + h_i - \frac{0.5v_{i+1}^2}{g} - h_{i+1} - f \frac{LQ^2}{2gDA^2} - \frac{KQ^2}{2gA^2} + \frac{\dot{q}}{\rho g Q} - \frac{c_p \Delta T}{g}}{\rho g} \quad (27)$$

The velocity, temperature, pressure, heat transfer coefficient and Reynolds number were graphed and are shown below in Figures 9 - 13 with the first

three graphs compared to the TRACE output.

3.2.2 Results of MATLAB model

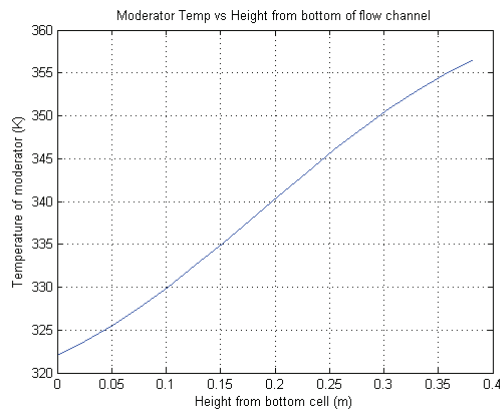


Figure 9: Temperature of Water in the channel versus Position

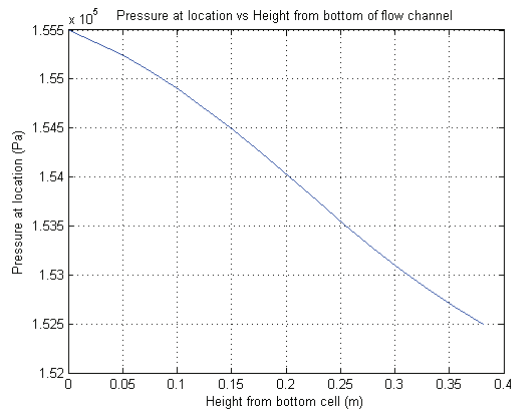


Figure 10: Pressure in flow channel versus Position

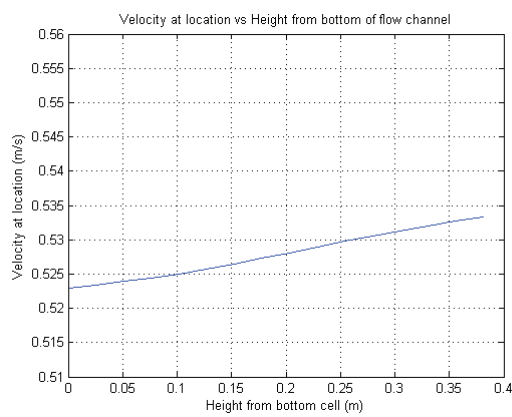


Figure 11: Velocity of Water in the channel versus Position

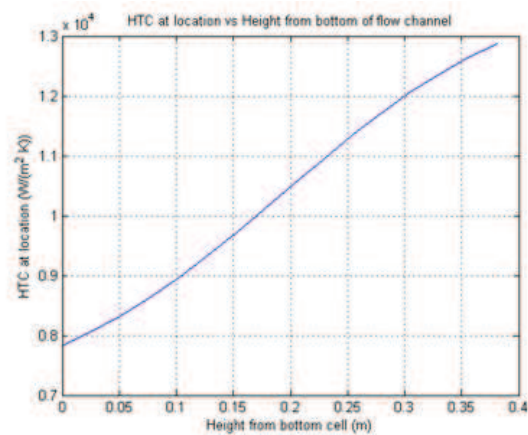


Figure 12: Heat transfer coefficient along the channel versus Position

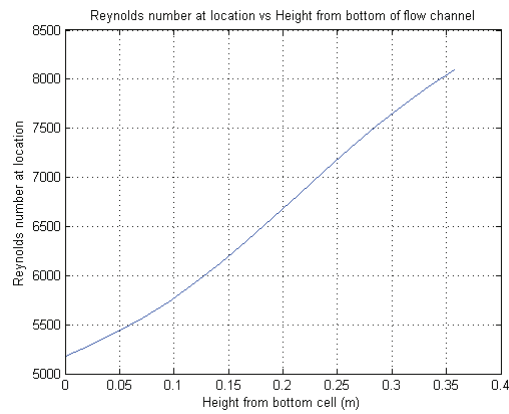


Figure 13: Reynolds Number of the flow channel versus Position

The results agree very well with the TRACE output. HTC is in the 8000-13000 range and the Reynolds number implies the flow is turbulent in the pipe. This gives a better understanding of what is occurring in the flow channel as well as providing a basic check to the TRACE model. A more in-depth check of the TRACE code was done using the computational fluid dynamics code "FLUENT"[15].

The input parameters of the channel were taken from the TRACE model (velocity, pressure, temperature, density, etc.) where those values (especially the velocity and mass flow rate) may not be the actual values of the parameters, as the MATLAB model served as a check to the TRACE model. However, that does not imply that since two models strongly agree that they are confirming those values of the variables to be the true values; it instead shows that the models are in agreement.

3.2.3 Prandtl Number, Reynolds Number and Nusselt Number

Three important quantities that describe the flow throughout the flow channel are Prandtl, Reynolds and Nusselt numbers.

The Prandtl number is the ratio of the kinematic viscosity to thermal diffusivity. When the Prandtl number is small, the heat diffuses through the material very quickly in comparison to the momentum diffusion of the fluid therefore, conduction is more effective than convection. As the Prandtl number rises, convection plays a larger role in the heat transfer in the material. Prandtl number falls as the temperature of water increases so convection plays a larger role in the heat transfer of the material as the water is heated.

The Reynolds number describes the type of flow in the channel. It is the ratio of the inertial forces to viscous forces. Unlike the Prandtl number, the Reynolds number depends on a characteristic length that is descriptive of the flow field of the channel. When inertial forces are small compared to viscous forces, the flow is considered laminar. That occurs in situations where the energy that the individual particles in the fluid have aren't enough to deform the flow of the material. As the energy of those particles increase, they increase the turbulence in the fluid since those particles are less bound to the streamline in the channel and cause the flow patterns to change. It can also be thought as a balance between the energy of fluid particles and the internal friction holding the fluid together along the flow path. As the energy of the particles increase, they overcome the internal friction in the fluid and break away, causing a turbulent flow. Values of the Reynolds number below 2000 are considered laminar while above 5000 are turbulent with the area in between referred to as the transition zone.

The Nusselt number depends on both the Prandtl and Reynolds numbers. It is a measure of the type of heat transfer occurring in the fluid; a ratio between the convective and conductive heat transfer coefficients. There are multiple ways to calculate this ratio depending on the Prandtl number and Reynolds number of the system. Since our system has a turbulent Reynolds number and a Prandtl number between 0.5 and 2000, the Gnielinski correlation was used since it is valid for turbulent Reynolds numbers which is true for our system and a Prandtl number between 0.7 and 5, also true for our system[14]. The last variable of the equation for the Nusselt number involves the Darcy

friction factor which is found by using the Moody chart. As the Prandtl number increases (convection plays a larger role in the heat transfer) then the Nusselt number increases as well. As flow in the pipe becomes more turbulent, the increase in fluid particle movement increases heat transfer due to convection as opposed to conduction which is more prominent in laminar flows.

4 Computational Fluid Dynamic Model and Model Comparison

4.1 FLUENT

No radial discretization of the variables was done in the MATLAB and TRACE solvers which limits the accuracy of measurements. MATLAB and TRACE solve nodal balances on bulk properties while FLUENT solves for local properties at each mesh cell. There is also a radial distribution for the velocity of the water (especially near the pipe wall) flowing through the channel that is not accounted for in the MATLAB or TRACE models that FLUENT is much better suited to handle.

4.1.1 Geometry

The pipe geometry was built to mimic the geometry used in the TRACE and MATLAB models so that the three models can be compared accurately. This model uses the same base assumptions such as the circular cross section of the pipe which is not true of the actual system. The model was developed using SolidWorks 2010 and imported into the ANSYS meshing program included with WorkBench.

To build the pipe, each change in the diameter of the pipe was individually drawn as a circle on a plane with the correct z dimension. Those circles were connected using the loft function so that the angle during the turns the flow



Figure 14: Pipe used in original FLUENT testing developed in SolidWorks

experiences would be preserved as well as the original shape of the turns. The heated section was split into 15 sections of one inch each in length in the z-direction. Heat was applied to the pipe using the same distribution as in the TRACE and MATLAB models.

4.1.2 Mesh

The mesh was created using the default settings except for the following (due to results of convergence test): Under the sizing tab

- Min size = 0.0004 m
- Max face size = 0.07 m
- Max size = 0.1 m
- Minimum Edge Length = 0.058 m

The mesh displayed shows the difference in nodal spacing depending on the section of pipe the mesh is mapped on. The turns have the densest nodal



Figure 15: Mesh of pipe used in original FLUENT

distribution since the Reynolds number is most turbulent and the velocity changes most rapidly there.

That model was imported into FLUENT where it was set up using the following settings (listed by tab):

- General
 - Gravity was set in the z direction with a value of 9.81 m/s^2 .
- Models
 - Energy balance was turned on.
 - Flow was made to be modeled by a k-epsilon model. The k-epsilon model was used since it was the simplest model with the lowest number of equations (minimizes run time) that addresses the turbulent flow in the pipe.
 - * The model is a two equation system where the first equation is an equation for k (turbulent energy of the system) and the second equation is (turbulent dissipation rate).

- * Equation for k :

$$k = \frac{3}{2}(U * I)^2 \quad (28)$$

- U is the mean bulk velocity (m/s)
- I is the turbulence intensity (dimensionless)

- * Equation for ϵ

$$\epsilon = C_\mu^{\frac{3}{4}} \frac{k^{\frac{3}{2}}}{l} \quad (29)$$

- C_μ is the turbulence model constant (dimensionless)
- l is the turbulent length (m)

- Materials

- The fluid was set to liquid water, a material present in the FLUENT database. The density, specific heat, thermal conductivity, and viscosity were changed from being constant (FLUENT default) to varying with the polynomials defined in the MATLAB section (eqs. (16) to (19)).

- Steel was used for the wall of the pipe

- Boundary Zone Conditions

- The inlet was set as a mass flow inlet where the mass flow was set to be 0.14 kg/s (taken from the TRACE model).

- No gauge pressure was used since the operating pressure of the inlet of the pipe was set to 158000 Pa.
 - Inlet temperature was set at 322 K.
 - An outflow condition was applied to the outlet.
 - The wall was split up into 16 sections, 15 heated sections and one section that included the rest of the walls which were unheated.
- Solution Initialization
 - The initialization was done using the pipe-inlet values to start the solver.

4.1.3 Single Channel Nodalization

To optimize run time while maintaining acceptable accuracy of the results, a nodalization convergence study was done on the single channel FLUENT model. The number of nodes was increased from the allowable minimum of 1,080 to a maximum of 380,006. The intervals were determined by doubling the previous interval until 100,000 nodes were reached and then variably increased between 1.25-1.5 times to increase the resolution in that section. The 16 tested nodal meshes are given in Table 9.

Table 9: Single Channel Nodalization Study Nodal Mesh Quantities

Test Case	Number of Nodes
1	1,080
2	2,464
3	3,973
4	5,372
5	8,820
6	14,272
7	23,452
8	53,016
9	89,445
10	118,910
11	156,236
12	197,276
13	229,149
14	269,841
15	325,927
16	380,006

Initial conditions were identical for all of the testing and two quantities were tracked, the wall temperature and centerline coolant temperature in the channel. These values were chosen since they are used in determining the

heat transfer that occurs in the heated channel. The convergence study was carried out by taking the results from the finest mesh (case 16) as the reference values. Results from coarser meshes were compared to those of the finest mesh to determine the degree to which mesh resolution affected the results.

For each mesh, wall temperature data was extracted from FLUENT at all wall locations that fell within the z-coordinate ranges of the 15 heated sections. Those values were averaged to get a single value for the wall temperature in that heated section. To obtain the centerline coolant temperatures (and to later compare those to the probe values), another script was written to extract the data from the FLUENT output files with z-coordinates as above and x and y values between -3 and 3 mm (the radius of the probe). These values were averaged to find the average centerline coolant temperature in each of the heated sections. The difference between the wall and centerline temperatures was calculated for each of the 15 heated cell locations across the height of the heated section of the flow channel. Then that difference was compared to the maximum case to determine the separation from the maximum value. The error between the two temperature differences as seen in equation 30 was calculated and graphed in Figure 16. The average column represents the average difference of the temperature differences between the tested number of nodes and maximum number of nodes across the 15 heated cells and the maximum column represents the value of the error at the cell with the highest separation from the maximum nodal value. The error is defined as

$$\%error = \frac{|\Delta T_n - \Delta T_{max}| * 100}{\Delta T_{max}} \quad (30)$$

where ΔT is the difference between the wall and centerline coolant temperatures for the heated cell, the n subscript denotes the index number of the node being compared and the max subscript denotes the run made with 380,006 nodes.

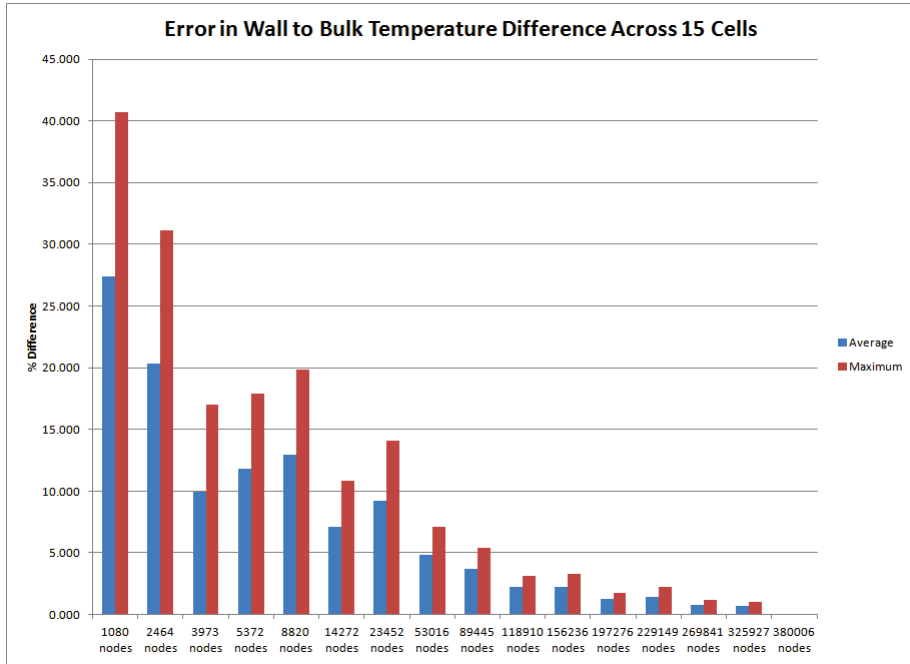


Figure 16: Error in Wall to Bulk Temperature Difference Across 15 Cells

The error between the results of the max and individual nodal mesh was desired to be below 5% for both the average and maximum values to ensure good agreement with the maximum case. The cutoff of 118,910 nodes was therefore determined for the single channel case since nodal meshes above that

number of nodes had error values under the 5% required value. Therefore, the 118,910 node model was selected as the coarsest nodalization that met the criterion of no more than 5% error. Run time on a 10 core blade server with 2 gb ram committed for each is 6 hours for the most finely resolved mesh and 3.5 hours for the 118,910 node mesh. These results were expanded to be used as the base for each channel of the multi-channel model.

4.1.4 Solution

The solution converged after 135 iterations. Included below are the cell outputs graphed using the native FLUENT graphing utility. As in the MATLAB model, the temperature, velocity, pressure and heat transfer coefficient are graphed with respect to location along the z-axis. The FLUENT graphs begin at 0.165 m and run to 0.565 m which show only the heated section of the pipe. The locations from 0 to 0.165 m and 0.565 m to 0.73 m represent the unheated reflector sections of the fuel rod and the turns the water makes around the fins of the fuel rod.

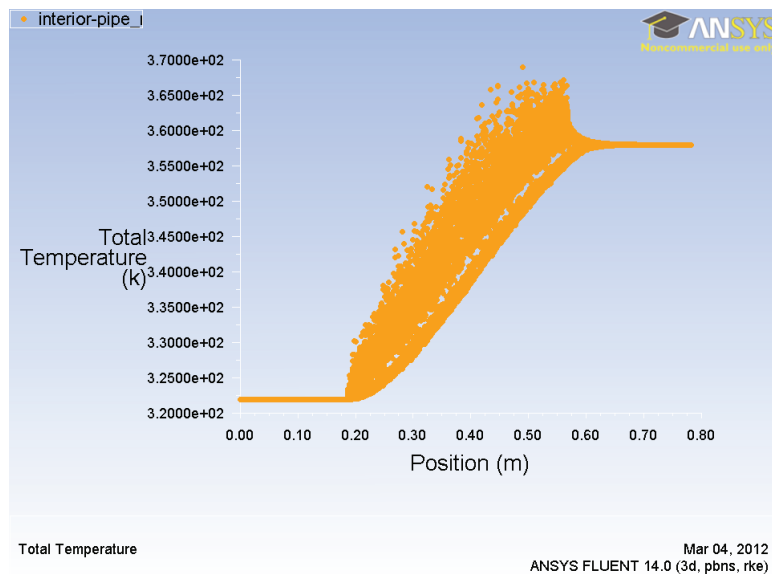


Figure 17: FLUENT Temperature of Water in the channel versus Position

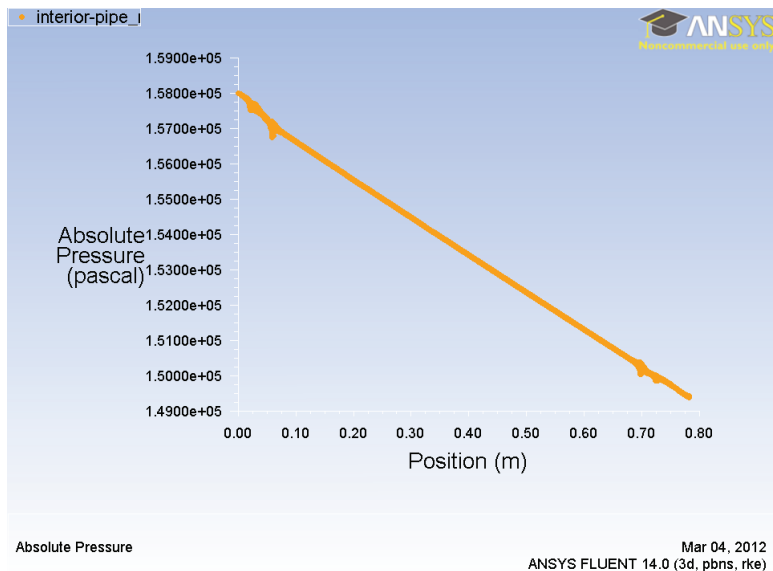


Figure 18: FLUENT Pressure in flow channel versus Position

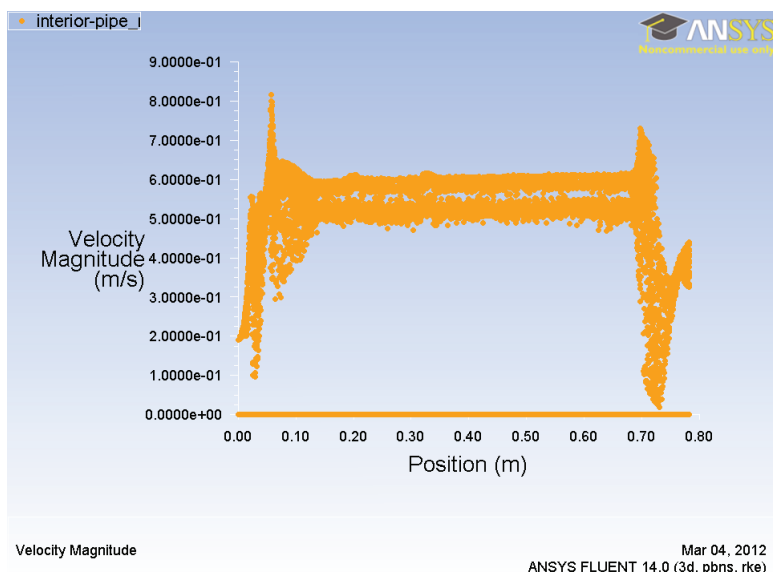
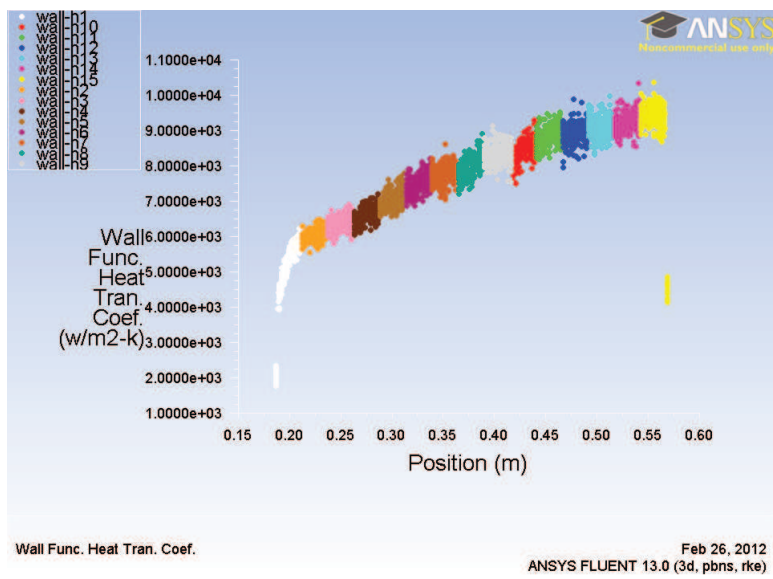


Figure 19: FLUENT Velocity of Water in the channel versus Position



These results show a significant variance of the temperature and velocity and water in the channel at the same z-axis location due to the radial dependency. On average, the temperature's radial maximum difference along the heated channel is 18 K and the velocity's radial maximum difference along the heated channel is 0.14 m/s. These significant differences show the advantage of FLUENT since those radial trends are lost in TRACE and MATLAB. Also, k-factors were not needed to simulate the losses due to turns in the FLUENT model since by including the actual geometry in the model, that source of error was removed from the solution.

4.1.5 Multi Channel FLUENT Model

The single channel FLUENT model was expanded to include the three flow channels surrounding the single channel to investigate the importance of cross-flow between adjacent channels. Depending on the amount of crossflow that occurs and its effect on the significant quantities that the heat transfer coefficient relies on (wall and centerline coolant temperatures) in the multi channel model, the decision will be made to either use the single or multi channel model in the development of the new heat transfer coefficient correlation. If the temperature difference between the single and multi channel models lie within error, that will be taken to signify that the single channel model is adequate. If the results lie outside of the combined error, there is a significant difference between the two models so the multi channel model will be used in future testing.

To construct the multi channel model, its geometry was first built in SolidWorks. Six identical fuel elements were constructed to match the TRIGA geometry. The area inside of this fuel element array was then cut from the model and defined as the flow sections for the four flow channels. 15 equally sized sections were created for the heated section as in the single channel model; however, there were 3 heated areas that encompassed half of the circumference of the fuel element (the ones connected to the center channel) and 3 heated areas that only included a sixth of the fuel element (those connected to the farthest part from the center of the 3 surrounding channels) as shown in Figure 21 .

The heat fluxes assigned to the model were determined from the SCALE/KENO-VI runs done at each of the 5 power levels are included in the SCALE/KENO-VI section 4.2.

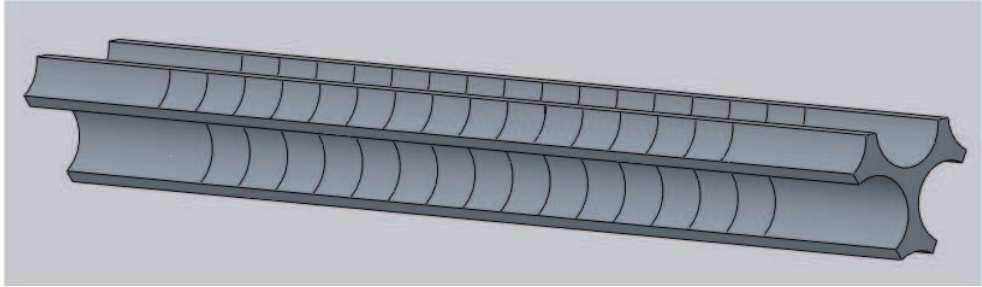


Figure 21: Geometry for the Multi Channel Model

The geometry was imported into the native ANSYS meshing software and the multi channel model was meshed at the resolution indicated by the single channel nodalization study. Since the crossflow boundaries needed to be correctly meshed with a minimum of 5 nodes across the 7 mm gap of the crossflow sections and an aspect ratio no greater than 5, a finer resolution was required in that area and the number of nodes ultimately used was 560,460. All of the faces of the each heated element were individually defined to maximize the accuracy of the heat flux inputs into FLUENT. The heat flux for each fuel element was assumed to be radially symmetric. Therefore, the heat flux entering different flow channels with the same fuel element in contact with them will have the same heat flux emanating from that fuel element (in $\frac{W}{m^2}$).

The inlet flow conditions for the multi channel model were the same for each of the four channels since the model was constructed with a common face for all the flow inputs. The addition of separate faces for each inlet increases

the degrees of freedom in the system and allows for finer adjustments to be made to the model. However, the single face setup decreases the degrees of freedom when attempting to match the probe data so uniform inlet conditions will be assumed unless the measurements cannot be matched. In that case, a multiple inlet face model will be used to attempt to match the probe data.

The model was run at different velocity inlet conditions and the temperature of the coolant was tracked as a function of x,y and z position in the flow channels. The results of the runs were compared to the results from the temperature probe. At 950 kW of overall TRIGA power, the inlet velocity was varied from 0.07 m/s to 0.1 m/s based on an initial estimate obtained from TRACE, to attempt to achieve agreement between FLUENT and the probe data. The data were extracted from FLUENT for x and y values that were at the location of the probe in the flow channel. After agreement between the probe temperature data and the FLUENT model temperature data was achieved by ensuring that the FLUENT temperature values at the probe locations were within the error of the probe, the x and y velocity data were compared to the z velocity in the channel to determine the effect of crossflow on the overall model. The results from the FLUENT runs are shown in Figure 22.

The 0.1 m/s case shows the best agreement with the measured values from the TRIGA probe and the temperature distribution of that case is shown in Figures 23 and 24. Figure 23 shows the temperature distribution of the coolant throughout the four channels. As expected, the lowest temperature is the channel on the upper right of the figure which has least amount of heat

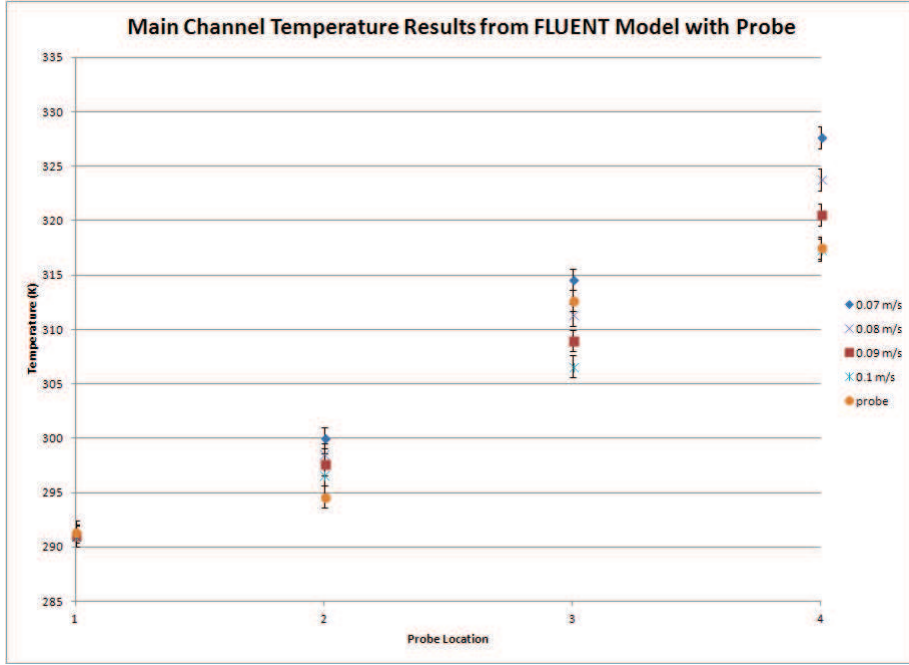


Figure 22: FLUENT Comparison to Probe Data for Multi Channel FLUENT Model

entering the channel due to its location in the TRIGA. The upper left and bottom flow channels have the highest temperatures since they lie slightly closer to the center of the TRIGA and the heated section that only affects their channel has a higher heat flux input into the flow channel than the 3 sections surrounding the center channel. Figure 24 shows a cut along the Z-axis of the center channel results. As expected, the temperature of the coolant increases as the water rises in the channel. This figure also shows that there is significant mixing of the coolant at upper locations in the center channel.

The crossflow for that case was then graphed as a function of x and y position in the fuel channel. The crossflow was determined by using the magnitude of the combination of the x and y vectors for the velocity at the boundary be-

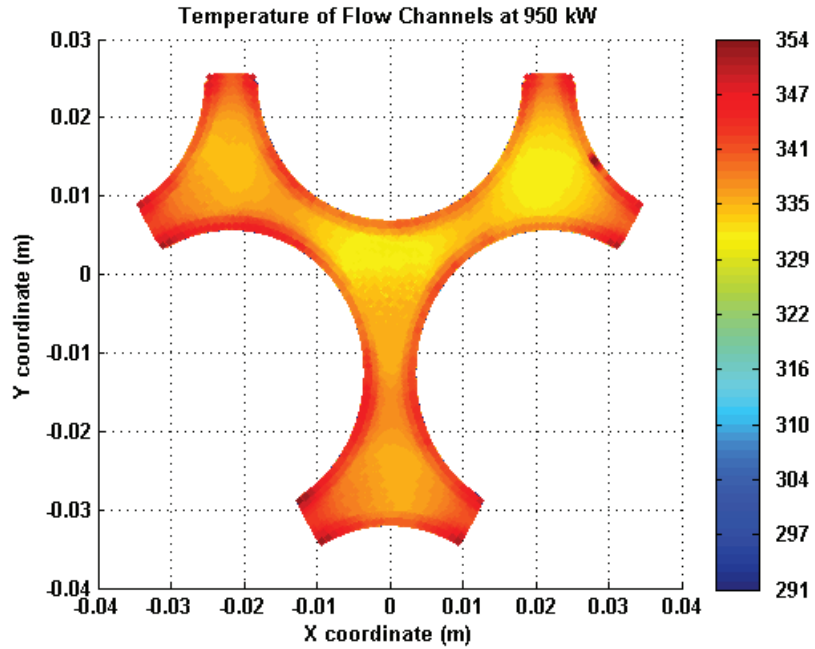


Figure 23: Temperature in K of Multi Channel FLUENT Model at 950 kW - X and Y Axis Cut

tween each of the channel connections. Those values are shown in Figure 25.

The maximum value at a flow channel boundary occurs between the center channel and the neighboring channel that is connected at the bottom of Figure 25. From the output of the MATLAB extractor, the value is 0.037 m/s at the boundary between the center and lower channel in Figure 25, with more than 50 nodal locations reporting above 0.035 m/s (to ensure this isn't an outlier). This value was compared to z velocity of the fluid flow in the channels as seen in Figure 26.

The maximum reported z velocity was 0.21 m/s, however in the two adjoining channels with the highest crossflow, the maximum was 0.19 m/s but to be conservative, the 0.21 m/s will be used as the maximum z velocity. The

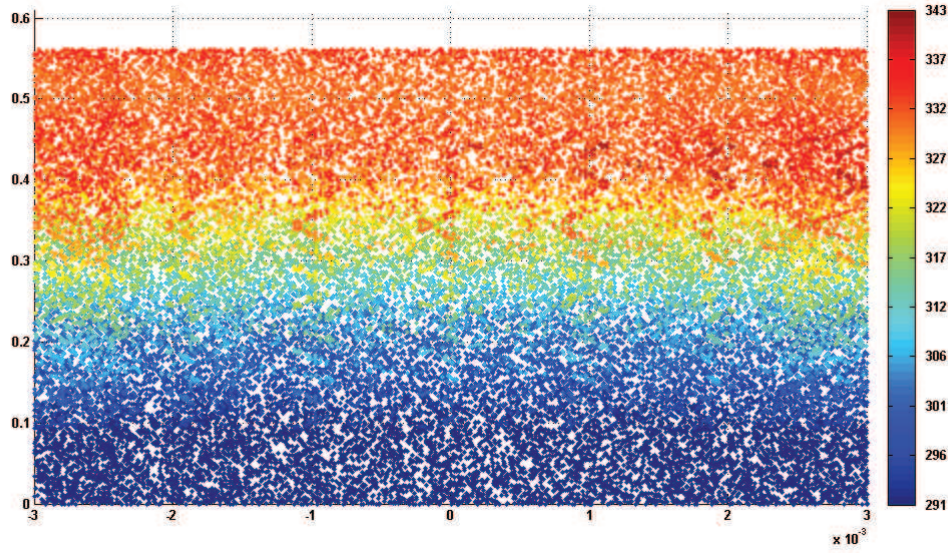


Figure 24: Temperature in K in Center Channel of Multi Channel FLUENT Model at 950 kW - Z Axis Cut

crossflow was still above 0.035 m/s at some points between the channel with the highest z velocity and the center channel so this estimate is valid. The ratio between the maximum crossflow and the maximum z velocity is 17.6 %.

To determine if the crossflow causes a difference in the results in the FLUENT model, the same inlet flow conditions and input heat fluxes were used for the single and multi channel model. Those values were then compared to one another as well as the probe values to determine the effect of the crossflow on the centerline coolant temperatures. This was also tested for the 4 channel model with no probe to determine if including the probe in the models were significant. These results are shown in Figure 27.

These results show that the three models provide significantly different results for the same initial conditions with the last probe location having a 7

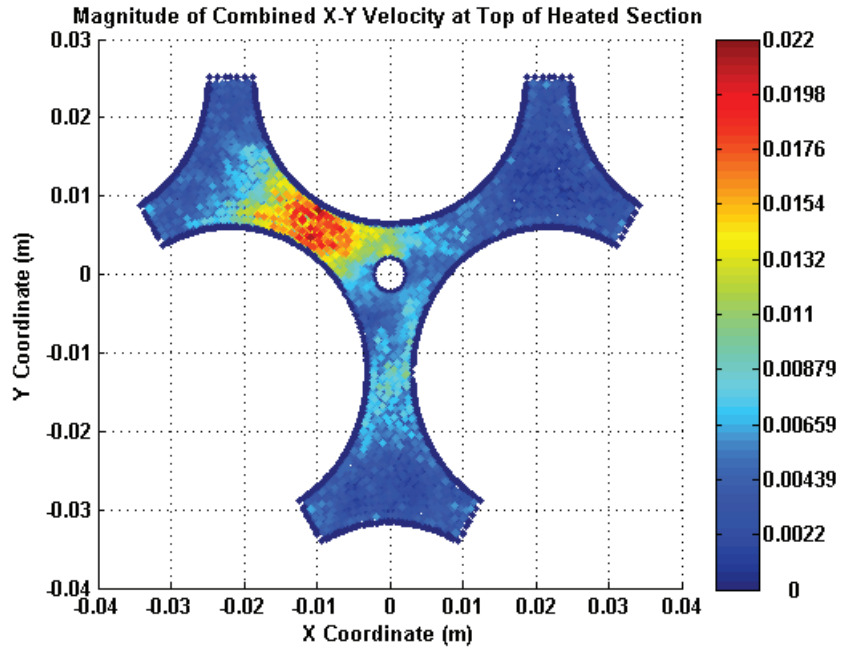


Figure 25: Crossflow in m/s from Multi Channel FLUENT Model at 950 kW

degree separation between the probe and no probe multi-channel models and a 15 degree difference between the single and multi channel models. Therefore, the multi channel model with the probe must be used in further testing.

4.2 Fuel rod power profiles

The KENO-VI package is a computer package that was developed by Oak Ridge National Lab and couples with SCALE, another Oak Ridge National Lab code, to perform criticality calculations on the TRIGA core setup. KENO-VI is a three dimensional Monte Carlo code that specializes in nuclear criticality safety analyses.

The input values for the heat fluxes were determined using SCALE/Keno-

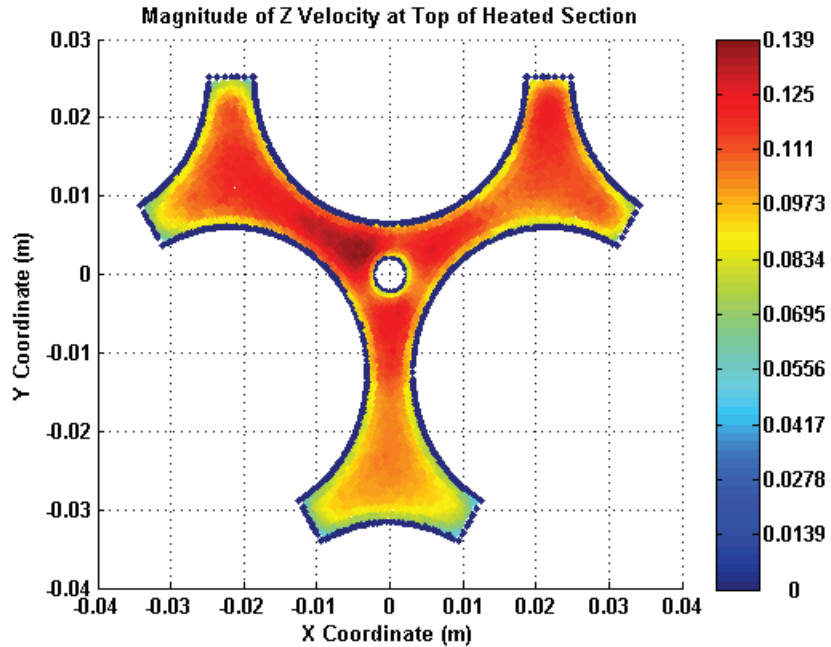


Figure 26: Z Velocity of Flow in m/s from Multi Channel FLUENT Model at 950 kW

VI with the geometry of the current TRIGA core. The setup of the core is shown in Figure 28.

The number 1 denotes a standard fuel rod which SCALE/KENO-VI tracks as one large entity as opposed to rod by rod. The overall power production results are reported in the output file but for individual treatment of the rods, they each need to be a differently defined geometry. To determine the number of fissions in the average rod, the results from the number 1 rod are taken and divided by 107 since there are 110 fuel elements in the core with 3 of them being individually tracked. Those 3 tracked are represented by the 8, 9 and 10 numbers. These rods are further divided into 15 heated sections to allow for an axial breakdown of the fission profile in the rod. Number 3 is used as a water

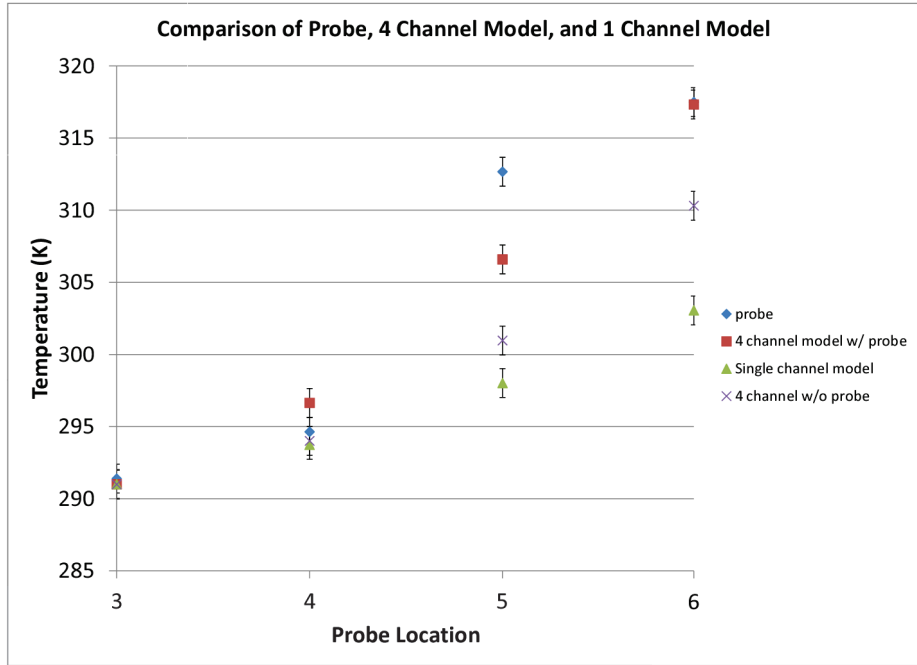


Figure 27: Centerline temperature values for single channel, multi channel with and without probe to determine significance of models

```

6   6   6   6   6   6   6   6   6   6   6   6   6   6   6   6   6   6   6   6
6   6   6   6   6   6   1   1   1   1   1   1   1   1   1   1   1   1   1   1   1   6
6   6   6   6   6   1   1   1   1   1   1   1   1   1   1   1   1   1   1   1   3   6
6   6   6   6   1   1   1   1   1   1   1   1   1   1   1   1   1   1   1   1   1   6
6   6   6   1   1   1   1   1   1   1   1   1   1   1   1   1   1   1   1   1   1   6
6   6   6   1   1   1   1   1   1   1   1   1   1   1   1   1   1   1   1   1   1   6
6   6   6   1   1   1   1   1   1   1   1   1   1   1   1   1   1   1   1   1   1   6
6   6   6   1   1   1   3   1   1   1   1   1   1   1   1   1   1   1   1   1   1   10
6   6   6   1   1   1   3   1   1   1   1   1   1   1   1   1   1   1   1   1   1   1
6   6   6   1   1   3   1   1   1   1   1   1   1   1   1   1   1   1   1   1   1   1
6   6   6   1   1   3   1   1   1   1   1   1   1   1   1   1   1   1   1   1   1   1
6   6   6   6   6   1   1   1   1   1   1   1   1   1   1   1   1   1   1   1   1   6
6   6   6   6   6   6   1   1   1   1   1   1   1   1   1   1   1   1   1   1   1   6
6   6   6   6   6   6   6   6   6   6   6   6   6   6   6   6   6   6   6   6   6   6

```

Figure 28: Configuration for SCALE runs

gap to simulate the 3L and central thimble which are two locations in the TRIGA reactor where there is only water instead of the usual fuel rod. These

locations are used as irradiation locations for neutron activation analysis and other forms of nuclear testing. Number 4 is used to represent a control rod (Shim 1, Shim 2 and the Reg rod). Number 5 is used to denote the transient rod. Finally, 6 is used to model fuel-grid plates at the core boundary.

SCALE/KENO-VI reports the location in the fuel rod, fission density, deviation and the number of fissions that occur in that section of the rod. The regions are defined by the locations in the rod with region 1 denoting the lowest heated section and region 15 the highest heated section. The exact boundaries of each region are included in Table 10 and bottom of the graphite follower which is 9 cm below the beginning of the heated section is defined as $z = 0$ cm. The value for total fissions is normalized by the total number of fissions in the entire reactor.

Table 10: Region Boundaries

Region	Lower Boundary (cm)	Upper Boundary (cm)
1	9.00	11.54
2	11.54	14.08
3	14.08	16.62
4	16.62	19.16
5	19.16	21.70
6	21.70	24.24
7	24.24	26.78
8	26.78	29.32
9	29.32	31.86
10	31.86	34.40
11	34.40	36.94
12	36.94	39.48
13	39.48	42.02
14	42.02	44.56
15	44.56	47.10

The results for number of fissions are given in Tables 11 - 15. It

Table 11: KENO-VI results 200kW (fissions are e-4)

Region	Rod 8 Total Fissions	Rod 9 Total Fissions	Rod 10 Total Fissions
15	3.14	3.21	2.94
14	3.46	3.08	3.57
13	3.51	4.50	4.39
12	4.85	5.79	5.07
11	5.35	6.05	5.55
10	5.55	6.49	5.93
9	5.68	7.41	5.90
8	6.30	6.75	6.45
7	6.41	7.16	6.73
6	6.45	7.25	6.35
5	6.10	6.81	6.37
4	5.78	7.00	6.28
3	4.97	6.70	5.16
2	4.78	5.63	5.41
1	4.23	5.06	5.02
Total	76.6	88.9	81.1

The fission data was summed over the entire heated section denoted by total in the tables and that value was compared to the average normalized number of fissions in the other 107 rods. That ratio of the power in the specific rod versus the average rod in the TRIGA is included in Table 16.

The rod power ratio values were then converted into kW by taking the average rod power of 8.63 kW (corresponding to a ratio of 1) and multiplying by the determined ratio for each rod to get the overall rod power output. The power was spread out along the heated length of the rod based on the results of each of the 15 heated sections measured using KENO-VI. The power of each section, found by using the values in Tables 11 - 15 was divided by the surface

Table 12: KENO-VI results 400kW (fissions are e-4)

Region	Rod 8 Total Fissions	Rod 9 Total Fissions	Rod 10 Total Fissions
15	2.37	3.18	2.73
14	3.29	3.52	3.22
13	3.17	4.53	3.96
12	4.24	5.40	4.61
11	4.37	5.68	5.31
10	4.84	6.62	5.69
9	5.40	7.27	6.70
8	5.70	7.35	7.22
7	6.37	7.71	6.69
6	5.96	7.82	6.22
5	5.68	7.83	6.76
4	4.86	7.66	6.42
3	5.07	6.26	7.04
2	4.79	5.42	5.30
1	4.22	5.58	4.34
Total	70.3	91.8	82.2

area of the section (all had a surface area of 0.002996 m^2) to have the heat flux for each section in units of $\frac{W}{m^2}$. Those values were input into FLUENT as the heat flux values for the 3 rods that make the center channel of the four channel model. The rods in the four channel model were labeled as in Figure 29.

The power distributions at 950kW for the 6 rods tracked differ slightly in their shape and are shown in Figure 30 .

The difference in shape is due to two main factors. The different control rod positions change the flux profile of the reactor which cause a change in the location where the fissions are at a maximum in the fuel rods. The increase in heating of the coolant at higher power levels also changes the moderation of

Table 13: KENO-VI results 600kW (fissions are e-4)

Region	Rod 8 Total Fissions	Rod 9 Total Fissions	Rod 10 Total Fissions
15	2.07	3.47	3.15
14	3.19	3.80	3.41
13	3.67	4.14	4.66
12	4.29	5.23	5.13
11	4.82	5.86	5.51
10	4.95	6.53	6.11
9	5.29	8.38	6.95
8	6.05	8.24	6.77
7	5.72	7.66	6.50
6	5.65	7.20	6.67
5	6.12	7.40	6.47
4	5.21	6.87	6.13
3	4.33	6.38	5.31
2	3.97	5.77	4.51
1	3.62	4.98	4.49
Total	68.9	91.9	81.8

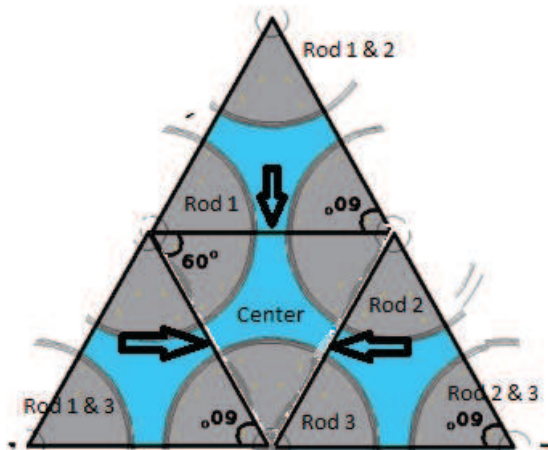


Figure 29: 6 rods involved in the four channel model

Table 14: KENO-VI results 800kW (fissions are e-4)

Region	Rod 8 Total Fissions	Rod 9 Total Fissions	Rod 10 Total Fissions
15	2.77	3.35	2.86
14	2.89	4.09	3.29
13	3.06	5.02	3.86
12	4.02	5.62	4.12
11	4.69	5.78	4.79
10	4.86	6.47	6.09
9	6.22	7.61	6.38
8	5.71	7.58	6.90
7	5.85	7.88	6.98
6	5.84	7.27	6.09
5	5.89	6.99	6.70
4	5.04	6.83	6.47
3	4.71	5.92	5.14
2	4.20	4.91	4.77
1	4.33	4.88	4.23
Total	70.1	90.2	78.7

the neutrons in the water which also can affect the amount of fissions occurring in the fuel rod.

Because of the differing shapes of the power distributions as well as the different relative ratio of the fissions occurring in each rod, the FLUENT model must be run using each of these individual rod values as opposed to assuming the rods have the same relative power output at all of the 5 power levels and each of the 3 main fuel rods.

Table 15: KENO-VI results 950kW (fissions are e-4)

Region	Rod 8 Total Fissions	Rod 9 Total Fissions	Rod 10 Total Fissions
15	3.19	3.74	3.38
14	3.43	4.53	3.66
13	3.63	4.80	4.12
12	4.08	5.44	5.02
11	4.70	6.42	5.50
10	4.76	7.07	6.02
9	6.44	7.28	5.86
8	5.96	7.81	5.79
7	5.98	7.14	6.94
6	5.50	7.27	6.97
5	5.45	7.18	6.36
4	4.77	6.52	6.34
3	5.05	5.77	5.78
2	4.09	5.33	4.51
1	3.61	4.72	4.55
Total	70.6	91.0	80.8

Table 16: KENO-VI Power Ratios

Power Level	Rod 8 Ratio	Rod 9 Ratio	Rod 10 Ratio
200 kW	0.846	0.983	0.897
400 kW	0.775	1.012	0.906
600 kW	0.756	1.007	0.896
800 kW	0.767	0.987	0.861
950 kW	0.769	0.991	0.880

4.3 Comparison of all 3 models

4.3.1 Convergence Test

The number of cells/nodes in each model was determined using the convergence of the relative error. The models were run at 1 cell (TRACE and MATLAB) or

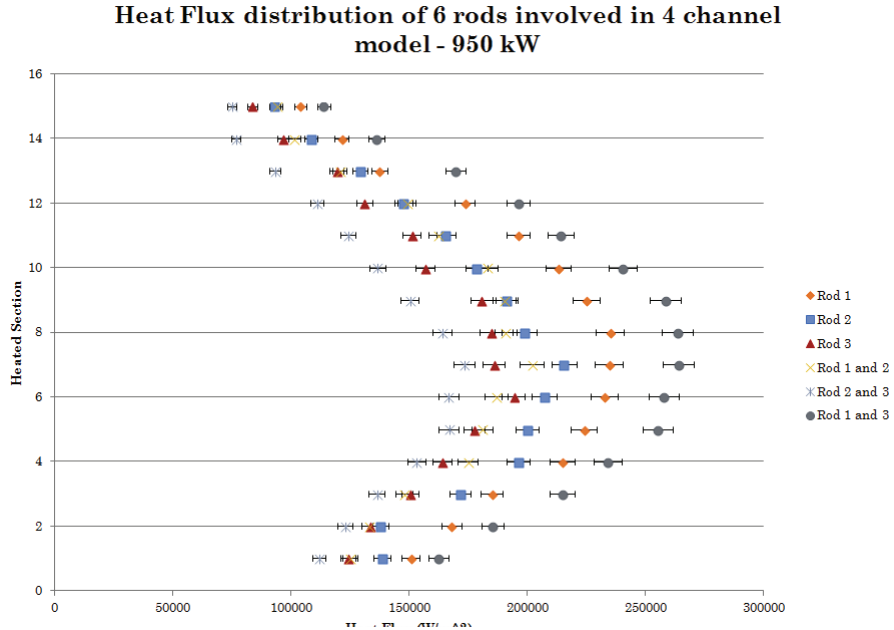


Figure 30: Heat flux distribution in the 6 rods associated with the multi channel model

1000 node (FLUENT) intervals and the relative error between that run and the run preceding it were calculated for three variables, the velocity, temperature and pressure at the end of the heated section. A constant heat profile was used for the TRACE and MATLAB solvers (no reshaping of the heat flux from cell to cell was done) and the sinusoidal heat profile was used for the FLUENT testing since the heat applied to the pipe did not change when the mesh was changed. Three errors were measured:

- Error due to the difference in temperature
- Error due to the difference in velocity
- Error due to the difference in pressure

When each error was less than 1%, it was assumed that there were enough cells/nodes to achieve reasonable results. However, more cells may have been used to achieve a better heat flux profile over the heated section.

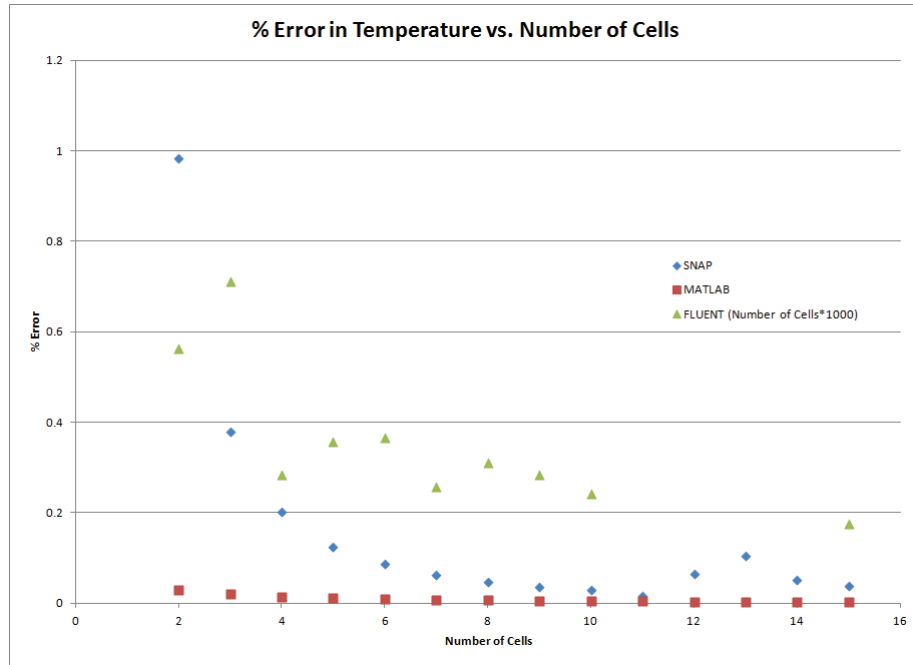


Figure 31: Relative Error in Temperature vs. Number of Cells

For the TRACE model, only 5 cells were needed to achieve a 1% relative error however, 15 cells were used since it allowed for the best heat flux profile with the minimal number of cells. The MATLAB solver used 15 cells as well since it was used as a check of the TRACE model and the MATLAB convergence tests showed that 15 cells would have a very low relative error. For FLUENT, 15000+ was used since it provided an almost 1% error.

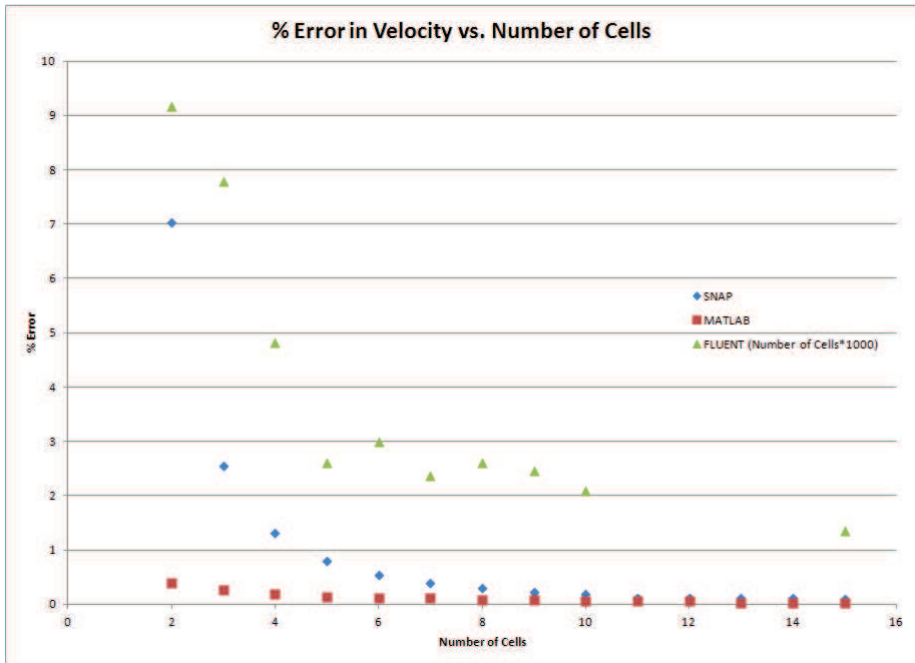


Figure 32: Relative Error in Velocity vs. Number of Cells

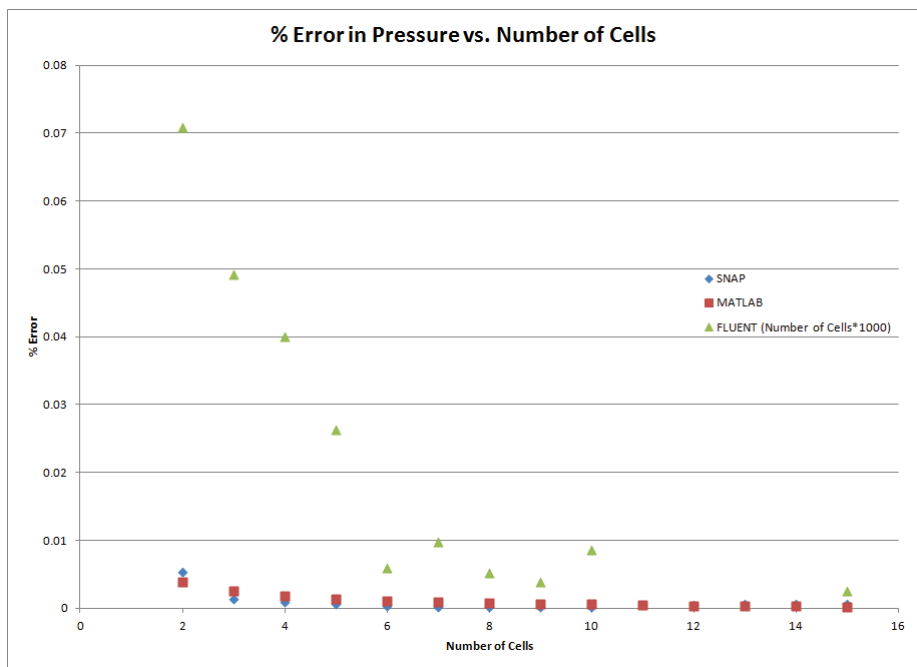


Figure 33: Relative Error in Pressure vs. Number of Cells

4.3.2 TRACE and MATLAB

Using 15 cells for the heated section of the two models, both solvers were executed until a stable solution was achieved. The MATLAB solver had the advantage of solving much quicker than the TRACE solver however, the MATLAB solver required a starting inlet velocity that the TRACE model calculated through iterations. Run times for the TRACE and MATLAB solver were 288 seconds and less than one second respectively. The three main properties (bulk temperature, velocity and pressure) were reported from both of the models and they are compared below.

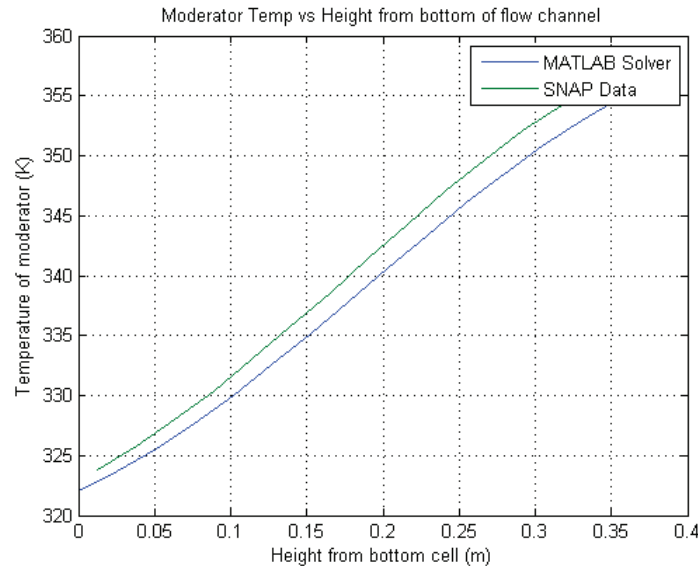


Figure 34: Absolute Temperature (K) vs. Z-location in the pipe (m)

There is strong agreement (less than 1%) across all three variables therefore, the MATLAB model closely models the TRACE output.

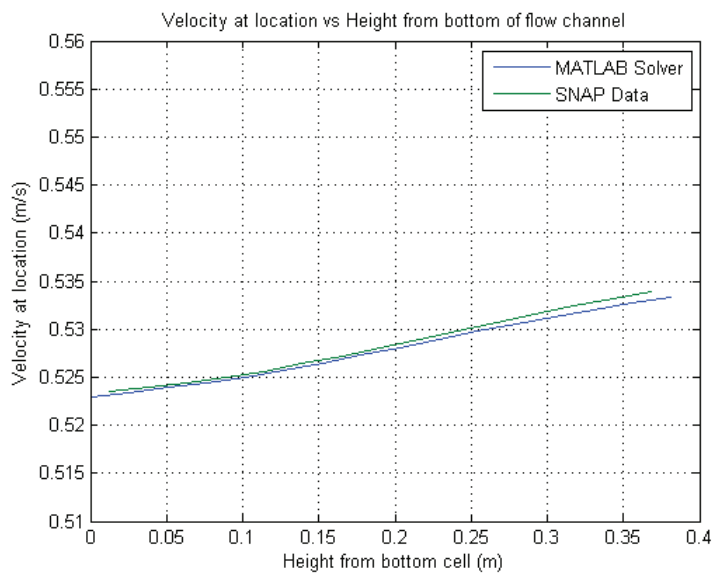


Figure 35: Velocity of fluid (m/s) vs. Z-location in the pipe (m)

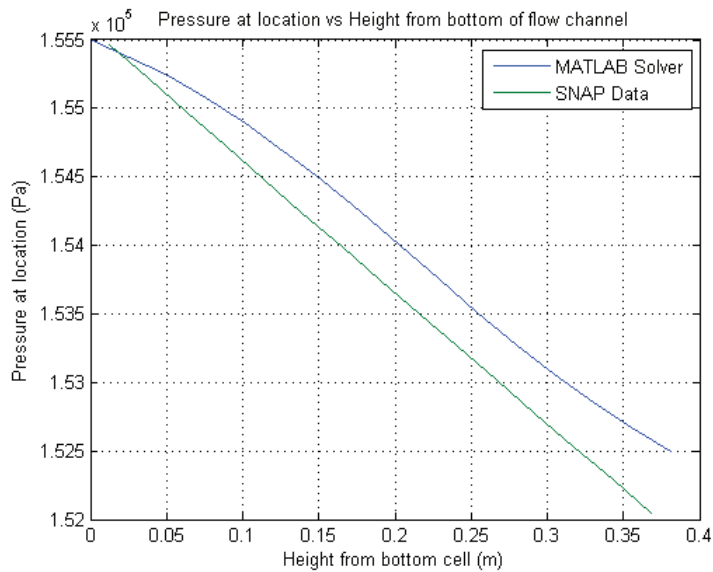


Figure 36: Absolute Pressure (Pa) vs. Z-location in the pipe (m)

4.3.3 All 3 Models

The FLUENT model was compared to the existing data from the TRACE and MATLAB solvers. All 3 exhibit the same geometry (the turns that exist in the FLUENT model were approximated in TRACE and MATLAB models using loss factors) and the same initial conditions of the flow channel were used in all 3 models.

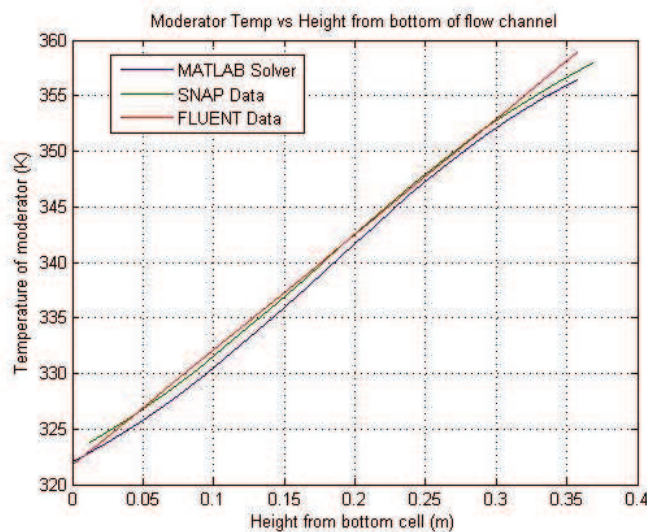


Figure 37: FLUENT Temperature of Water in the channel versus Position

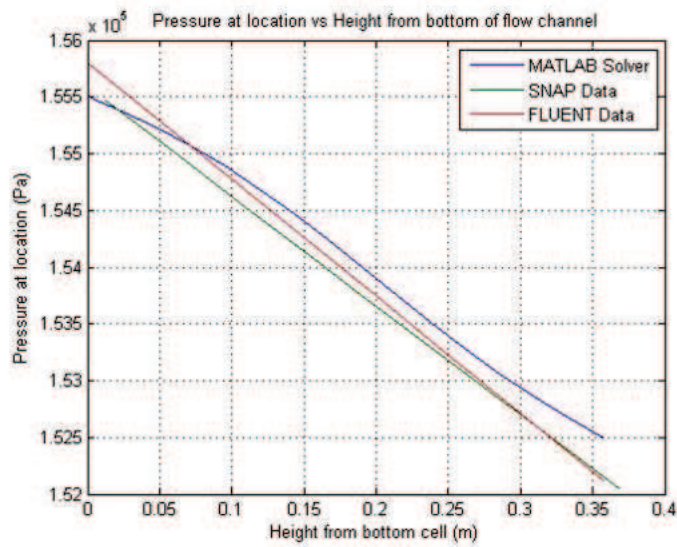


Figure 38: FLUENT Pressure in flow channel versus Position

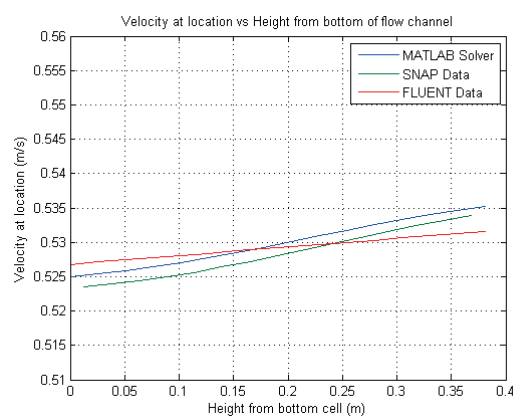


Figure 39: FLUENT Velocity of Water in the channel versus Position

All 3 sets of results agree very well with each other implying that the MATLAB and FLUENT codes are doing an adequate job replicating the results from the TRACE solver. The calculated heat transfer coefficients for the MATLAB and FLUENT solver were within 20% of one another which shows that the MATLAB solver does a decent job approximating the HTC. However, the TRACE model's HTC was half of the HTC of the FLUENT model which rises suspicion on the HTC reported from TRACE. The next step is to change the geometry of the pipe in FLUENT from the cylindrical one used in the TRACE and MATLAB models and instead using the actual non-circular flow area cross section of the flow channel.

5 TRIGA Data Collection and Scale Modeling

5.1 Data Collection and Simulation

To improve the TRACE model, two data sets will be used to encompass the range of operating conditions of the TRIGA used in the models. Those data sets will be acquired from measurements in the TRIGA hot channel and surrounding channels and high fidelity computer simulations.

In addition to the TRIGA measurements and FLUENT model, a proposed scaled model would also provide additional data that could be used to improve the TRACE model. This model includes the hot channel and neighboring channels and the section describing the scaled model will touch on what data would be collected from the model if it were in operation.

5.1.1 TRIGA Reactor

Specific measurements will be taken in the TRIGA reactor to encompass most operating conditions where the models must be valid. The full core power output will be varied for the system to ensure the data set covers the entire range of possible TRIGA power levels.

Limits must be imposed on the full core power output based on maximum allowed operating conditions. The maximum allowed full core power output is 950 kW (corresponding to approximately 21.5 kW for the hot channel power). The range of allowed operating conditions is shown in Table 17.

The full core power will be adjusted independently to determine the effect of the individual parameters on the overall core operating conditions. The

Table 17: Allowed operating conditions for the TRIGA core

Parameter	Range of allowed values	Unit
Main pool temperature	293 - 323	K
Hot channel temperature outlet	293 - 385	K
Wall temperature for hot channel	293 - 430	K

values that will be tested are given in Table 18.

Table 18: Testing conditions for TRIGA core

Parameter	Starting value	Rate of change	End value
Full core power	0 kW	Every 200 kW	950 kW

The quantity of measured values in the TRIGA core will be less than those measured in the FLUENT model since regulations prohibit a significant change to the flow dynamics of a coolant channel. The flow inside of the coolant channels cannot be directly measured due to the flow aberrations caused by any probe. The fuel temperature is measurable only in the hot channel at location B2 as shown in Figure 40 where the thermocouples are already installed on the inside of the fuel element. The location in the fuel element is at the axial center point of the rod and is at a 45 degree angle in the positive axial direction with the axial height in the rod. The wall temperature is not directly measurable since no thermocouples are along the wall of the element. The coolant temperature will be measured using the thermocouple probe as seen in Figure 41. Those coolant measurements will be made for both the hot and surrounding coolant channels.

The probe is 71 centimeters long, has a diameter of $\frac{3}{16}$ inches and reaches to the same depth as the bottom of the fuel elements when fully inserted.

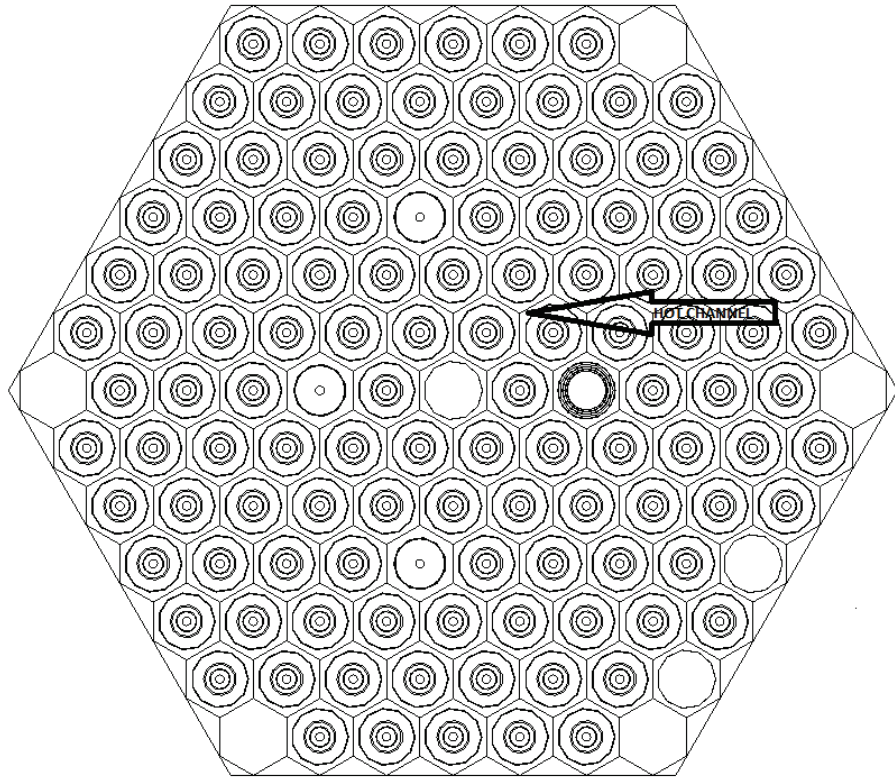


Figure 40: Location of hot channel in the TRIGA core

The sheath of the probe is made of 316 stainless steel which will not allow for removal of the probe from the TRIGA pool immediately after testing due to the activation in the stainless steel. There are six type E thermocouples in the probe which are equally spaced at 9 centimeter intervals with the first thermocouple lying at the bottom of the probe. These locations correspond with most of the length of the fuel element (Thermocouples 1-4), the beginning of the graphite reflector at the bottom of the rod (Thermocouple 5) and the bottom of the entire fuel rod (Thermocouple 6) to provide an inlet temperature. The probe will lie in the center of the flow channel.

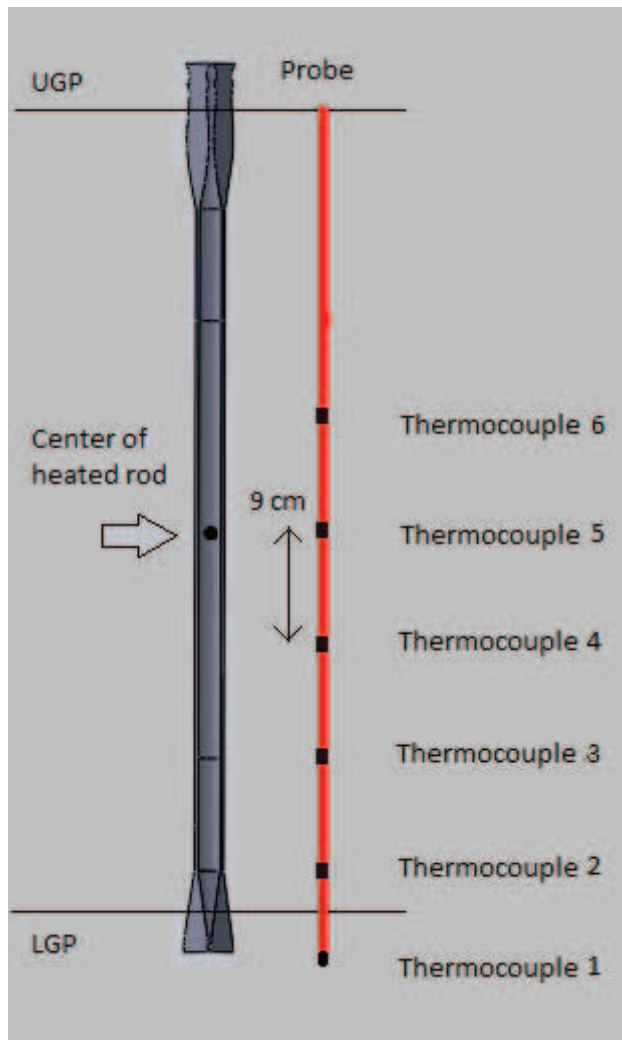


Figure 41: Probe length and thermocouple locations along fuel element

The data set that will result from these tests will be a set of 6 temperatures at 5 different TRIGA power levels, yielding a data set of 30 points for FLUENT model calibration.

5.1.2 FLUENT Testing and Adjustment

An expansive data set can be created from the results of the FLUENT model but it must be calibrated to match the measured data from the TRIGA to the greatest extent possible. The flow rates for the FLUENT model will be adjusted to obtain the same results as the actual measurements taken in the TRIGA with the initial starting point for the flow rate in the FLUENT simulations coming from the original TRACE model. This will be done by finding the centerline water temperature through FLUENT at the thermocouple locations shown in Figure 41 and comparing those to the measured values from the TRIGA. The FLUENT model will include the probe in the flow channel to match the actual system.

Depending on the results of the comparison between the FLUENT and actual systems, the FLUENT model may undergo small calibrations to match the results of the actual system as closely as possible. These changes will include:

- Changes in inlet temperature
 - The exact inlet temperature will not be measurable in the TRIGA system since the first thermocouple is located in line with the graphite reflector in the fuel rod. Since the exact location of the thermocouple in the channel is known, the modified "inlet" temperature will be used in calibrating the model as opposed to the temperature at the actual inlet to the hot channel. The inlet temperature to the FLUENT model will be adjusted until the temperature at the

first thermocouple location in the TRIGA is achieved at the same location in the FLUENT model.

- Changes in flow rate
 - The flow rate will be adjusted to match the temperature readings in the TRIGA with the priority on matching the exit coolant temperature, followed by the inlet coolant temperature and then the remaining four thermocouples are equal in importance. This is order was chosen based on the goal of the model where the overall exit temperature is most important since it bounds the change in coolant temperature from inlet to exit as well as determining the void fraction in the coolant. The inlet temperature is second in importance since it helps determine the overall change in coolant temperature. The remaining four thermocouples are of equal importance since it is desirable to correctly characterize the coolant at all locations but none of the four locations hold any significant importance for model performance. There will be no way to directly compare the flow rates with the TRIGA flow rates since the TRIGA values are not measurable.
- Changes in material properties
 - The property that will be adjusted here will be the heat transfer through the cladding based on the material composition of the cladding as well as the thermal conductivity through the cladding to achieve the correct wall to water heat transfer. This will be

done by matching the single temperature reading at the wall of the cladding in the instrumented fuel rod to the with the corresponding location in the FLUENT model. This value will be third in importance behind matching the inlet and outlet coolant temperatures in the overall adjustment of the model. It has the priority since the correct wall temperature is pivotal in modeling the heat transfer from the wall of the fuel rod into the coolant. This is because the wall temperature as well as bulk coolant temperature are needed to determine the heat transfer from the fuel rod into the coolant.

The priority list of measurements to match are:

1. Outlet coolant temperature at thermocouple 1 location
2. Inlet coolant temperature at thermocouple 6 location
3. Wall temperature at instrumented fuel rod thermocouple location
4. Remaining thermocouples in temperature probe

5.1.3 Using Measured Data to Determine Heat Transfer Coefficient and Minor Loss Coefficient

Once the results from the real time measurements and FLUENT models are obtained, the Nusselt number and heat transfer coefficient correlations will be determined for the system. To do this, Newton's Law of Cooling (31) will be used based on the values determined in the three systems.

$$h = \frac{Q''}{A\Delta T} \quad (31)$$

Q'' will be exactly known for both the scaled model and FLUENT models and the Q'' for the real TRIGA measurements will have to be approximated based on total core output and power profiles in the reactor. A will be known for all of the systems. ΔT will be exactly known for the scaled model based on its design and it will be known for FLUENT as well. ΔT will be known for the actual TRIGA at one location since the bulk temperature will be known and temperature near the wall will be known at one location. The location of that thermocouple is halfway up in the axial direction along the fuel. The FLUENT model will be benchmarked against the location of the thermocouple near the wall to help validate the model.

To derive a correlation for the Nusselt number, a fit will have to be made based on the results from the three systems. The initial trial will be of the standard form in equation (33) which originates from the Dittus-Boelter equation.

$$Nu = ARe^BPr^C \quad (32)$$

Where:

- Re is the Reynolds Number [dimless],
- Pr is the Prandtl Number [dimless]

- A, B and C are all constants [dimless]

This fit is similar in form to the fit used in the TRISTAN-IJS code whose purpose is to simulate heat transfer and fluid flow through a isolated, single channel. The fit from TRISTAN-IJS is:

$$h = \frac{0.023Re^{0.8}Pr^{0.4}k}{d_h} \quad (33)$$

or in terms of the Nusselt number:

$$Nu = 0.023Re^{0.8}Pr^{0.4} \quad (34)$$

Where:

- Re is the Reynolds Number [dimless],
- Pr is the Prandtl Number [dimless],
- k is the thermal water conductivity [W/cm deg C],
- d_h is the hydraulic diameter of the coolant channel [cm]

The Reynolds number through the channels as well as the Prandtl number can be found exactly using the scaled and FLUENT models since all of the values are available but the actual TRIGA system is lacking the velocity of the fluid through the channels. The fit will be adjusted based on the results of the original fit and may begin to more closely resemble other correlations.

This will be done over the entire range of operating conditions tested to ensure that this fit is accurate for all reactor conditions.

If this fit is not of the right form, other common forms in reactors will be tried to best represent the Nusselt number in the TRIGA hot channel such as the Gnielinski correlation and the Sieder-Tate correlation.

The correlation that will be decided upon will be the one which best matches the heat transfer data from the FLUENT model across the range of operating conditions. This will be measured by fitting regression lines to the multiple correlation results against the calculated values based on the TRIGA and FLUENT data sets. The R^2 value for the regression line needs to be at least 0.95 to achieve an adequate fit of the data. The model must be valid from 0 - 30 kW of hot channel power to ensure accuracy when measuring the DNB ratio in the hot channel when determining the safety of the system.

The loss coefficient due to the turns around the end fittings is not calculable for the actual system since the pressure drop must be known as shown in equation (35). Any measurement device lowered into the actual flow channel will perturb the flow enough to cause feedback in the system that will yield an inaccurate result for the loss in the turns. However, the loss coefficients can be calculated in the FLUENT models after being calibrated to the actual measurements since the pressure drop data is available.

$$\Delta p = \rho g h_f \quad (35)$$

Where:

- Δp is the pressure drop across the turn minus the contribution due to elevation change [Pa]
- ρ is the density of the water [kg/m^3]
- g is acceleration due to gravity [m/s^2]
- h_f is the head loss which needs to be found [m]

Once the head loss is found, it can be put into equation (36)

$$h_f = \frac{Kv^2}{2g} \quad (36)$$

- K is the minor loss coefficient due to the turn [dimless]
- v is the averaged fluid velocity [m/s]
- g is acceleration due to gravity [m/s^2]
- h_f is the head loss which needs to be found [m]

Using those two equations, the minor loss due to the turn can be calculated and used in the final TRACE model. The minor loss coefficients can be adjusted to match the correct flow rates and outlet temperatures as provided from the scaled model and FLUENT model. The effect of these changes in K on the overall result of the TRACE model are given in table 6. The loss coefficients will be the final step in adjusting the TRACE model to best represent the actual system and might require multiple iterations on their adjustment to optimally match the TRIGA hot channel.

5.1.4 Scaled Model

The scaled model would have a unique advantage by making measurements determinable that are not possible in the TRIGA since:

- It will operate at safer conditions (lower temperatures)
- It will be absent of nuclear material
- It will be fully instrumented including wall thermocouples and flow meters in addition to the measurement devices available in the TRIGA
- It will allow for the operating conditions to be more carefully controlled than the TRIGA

The measurements that will be taken in the model are:

- Coolant temperature above and below core
- Coolant temperature in the hot and surrounding flow channels at 5 axial locations (a scaled probe with the same relative spacing as the one used in the actual TRIGA)
- Flow rate leaving each individual flow channel
- Flow rate entering the main water tank
- Wall temperature of the stainless steel cladding of the heated rods in the hot and surrounding channels

This will be done for multiple power outputs from the heated rods and multiple pool temperatures due to the heating of the main pool with the integrated heater and cooler. This will yield different flow rates and temperature profiles in the system. The flow rate in the hot channel will be solved for using the similitude approach discussed in section 5.3.6 and the pump will drive the flow to achieve the desired flow rate.

These data will be scaled to be comparable to the full size TRIGA reactor. Then the results from the full size TRIGA testing will be compared to the results from the scaled model and used to calibrate the FLUENT model over the entire range of operating conditions. The scaled flow rate will be taken from the model system and used as the input parameter for the FLUENT system. The temperatures measured in the flow channel as well as the wall temperatures will also be used to check the results from FLUENT. The range of operating conditions based on the safety of the system for the scaled model are shown in Table 19 and are analogous to the values for the TRIGA included in Table 18. The errors in the temperature measurements will be the same as those in the actual TRIGA. The calorimetric flow meters have a measurement error of less than 3% in the range of conditions they will be operating in for the scaled model.

Table 19: Allowed operating conditions for the scaled TRIGA core

Parameter	Range of allowed values	Unit
Main tank temperature	293 - 303	K
Hot channel temperature outlet	293 - 323	K
Flow velocity through hot channel	0 - 8	m/s
Wall temperature for hot channel	293 - 350	K

The values that will be tested will range over the entire allowed operating conditions and will be varied by the scheme shown in Table 20. The rate of changes were selected based on trying to get a training set for the FLUENT model that adequately covered the entire range of the TRIGA.

Table 20: Testing conditions for scaled TRIGA core

Parameter	Starting value	Rate of change	End value
Main pool temperature	293 K	Every 2 K	303 K
Hot channel power	0 kW	Every 200 W	1 kW

5.2 Measurement of coolant temperature in a TRIGA flow channel

Actual measurement of the water temperature in the TRIGA flow channels was required to validate results obtained from the developed computer models. This was done using the stainless steel probe discussed in section 5.1.1.

5.2.1 Design of apparatus to lower probe into the core

The OMEGA manufactured temperature probe (PP6-36-E-G-18) could not be lowered into the core due to the fact that the wires leaving the sheath were not insulated from the water as seen in Figure 42, which would cause incorrect readings to be sent to the thermocouple measurement device due to the electrical conductivity in the water.

The thermocouple measurement device, the USB-TC, was manufactured by Measurement Computing and is shown in Figure 43.

It is an eight channel thermocouple input device that reads the voltage across the two different wire types (chromel and constantan) connected to the thermocouple and uses the thermocouple tables to output a temperature to the user. These temperatures are updated twice a second and can be recorded using the software provided with the device. The device also has a built in ambient temperature sensor so that it self calibrates to its surroundings.

To rectify the bare wire issue, aluminum pipe was purchased along with fittings to join the sections of pipe together until the wires exited the pool. The outer diameter of the pipe was 1 inch with an inner diameter of 0.875 inches. The requirements of the design were:



Figure 42: Bare thermocouple probe for water measurements in TRIGA flow channels

- Water tight
- No radiation streaming through the pipe system
- Avoids drive assembly at top of pool
- Must be disassembled to a point where the wires are still dry but the system can be lowered under the deck plates for reactor lockdown
- Must exit the pool high enough to allow for the pipe to be secured during reactor operation due to buoyancy in the pipe.

The water tight requirement was satisfied using Swagelok fittings to bind the pipes together. The wall thickness of 0.0625 inches was enough to allow



Figure 43: 8 channel thermocouple input device

the fittings to swage to the pipe without compromising the integrity of the pipe.

The radiation streaming issue and the drive assembly requirement were both satisfied by incorporating a turn in the pipe close to the entrance point in the grid plate (1 meter above the upper grid plate) that allowed the longer, vertical section of pipe to be located outside of the core diameter. The turn was a 2 foot long, 90 degree turn connected to the vertical sections of pipe using two 90 elbow Swagelok fittings as seen in Figure 44.

The disassembly requirement was satisfied by using a system with 8 foot long aluminum pipes joined by Swagelok unions to allow for the top pipe to be disconnected and stored while not in use. This allowed for the deck plates to be closed above it and the excess wire to lie on the edge of the pool. The full pipe assembly is shown in Figure 45.

To satisfy the final requirement, the wires that connected to the female thermocouple connections leaving the probe were 50 feet long to ensure they could easily reach the USB-TC device that lied on the edge of the pool. An

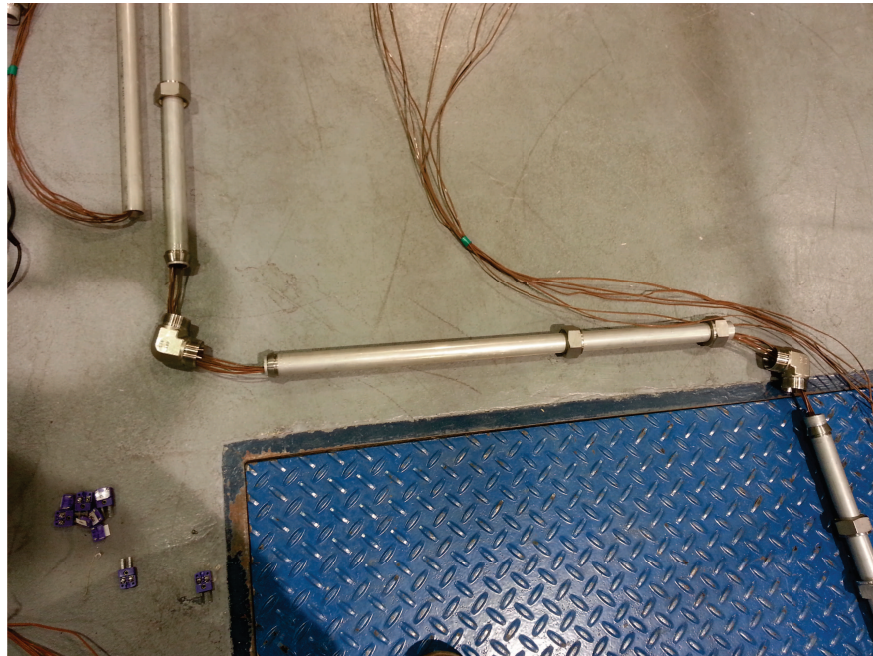


Figure 44: 90 degree turn in aluminum pipe system to protect thermocouple wires

extra 8 foot length of pipe was added to the top of the pipe system to have the wire exit above the water level. The connections between the probe and extra lengths of wire are shown in Figure 46.

The connections were staggered in the aluminum pipe to allow for the pipe to fit snugly over the connections while still allowing for a tight seal to occur within the Swagelok fittings since the connection widths were 0.75 inches.

5.2.2 Procedure of probe use during reactor operation

To insert the probe into the flow channel, the probe was assembled at all of the Swagelok fitting points besides the last connection because a fully assembled probe would be too challenging to get into the core during reactor shutdown

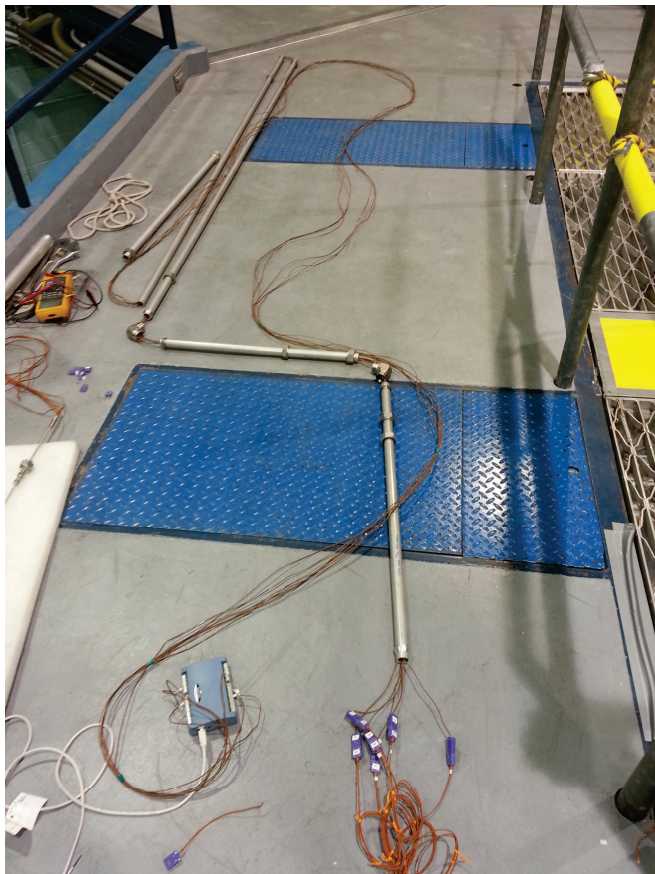


Figure 45: Full pipe system with fittings disconnected

due to its length. The probe was lowered into the water until the top of the first 8 foot section was close to the water level. Then wire was threaded through the other 8 foot segment of pipe and the pipe segment was tightened onto the first 8 foot section. Then the probe was fully lowered into the water until the probe reached the upper grid plate as shown in Figure 47.

The probe was carefully inserted into the core to ensure that the probe tip wouldn't be damaged during installation. To check if the probe was fully inserted, an underwater camera was lowered into the pool and focused on the

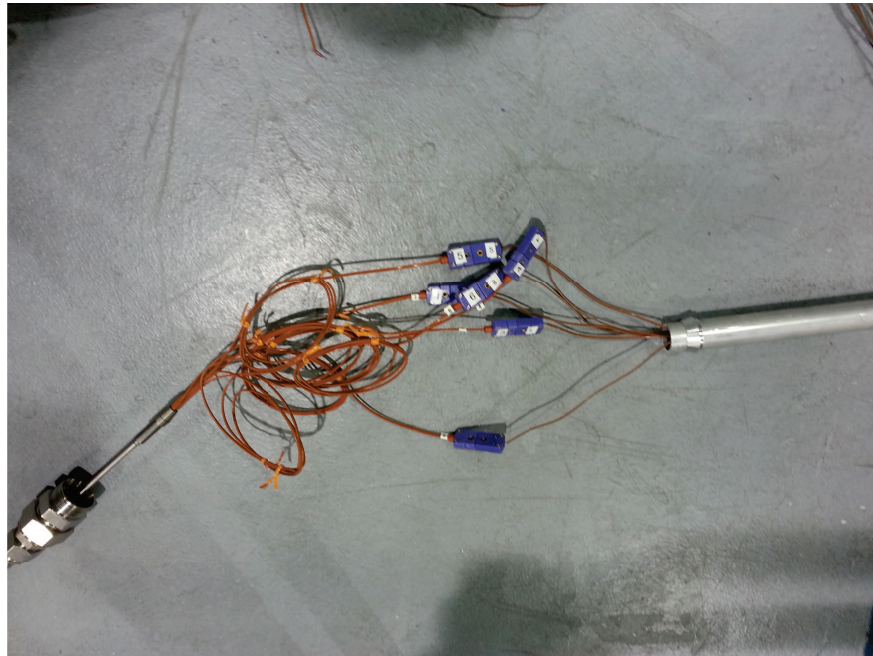


Figure 46: Connections between thermocouple probe and lengths of wire

upper grid plate to determine if the probe was fully down. The output from the camera is shown in Figure 48.

The probe was confirmed as being fully inserted and the turn caused the main section of pipe to be outside of the diameter of the core as required and shown in Figure 49.

Before reactor startup, the pipe exiting the core needed to be secured so that buoyancy due to the pipe being filled with air would not cause the pipe to shift during reactor operation. This was done using a clamp that went around the top of the pipe exiting the water connected to a pivotable gate on the edge of the reactor pool as shown in Figure 50.

After the probe was locked down, the reactor staff did startup checks and

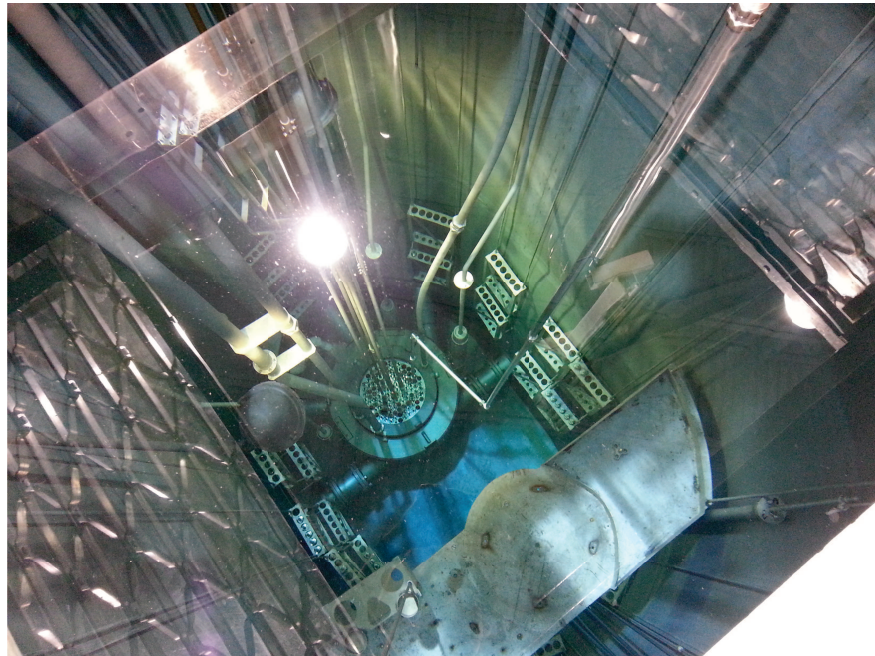


Figure 47: Probe just above reactor core with pipe system attached

confirmed that the addition of the probe in the reactor core did not cause a greater than 5 cent change in the reactivity of the core during startup to 50 watts. Then the following procedure was done to measure each set of coolant temperatures at each reactor setting.

1. Connect USB-TC to computer and start up TracerDAQ software supplied by Measurement Computing
2. Setup data logging software to collect for 20 minutes, all 6 channels, with a half second refresh rate, and record them in a text file
3. Notify the reactor operator that the system is ready to move to the next power level



Figure 48: Camera output to check if probe fully inserted in flow channel

4. Reactor operator announces the change over the loudspeaker and moves to the new power level
5. After the power level is achieved, wait enough time to where the reactivity and pool temperature have a less than 1% change over 5 minutes to ensure a stable power level
6. Begin data collection for 20 minutes
7. Once software is finished collecting data, export to excel and check deviation in data to ensure stability in the flow channel
8. Notify reactor operator if the data is acceptable and move to next power level and repeat

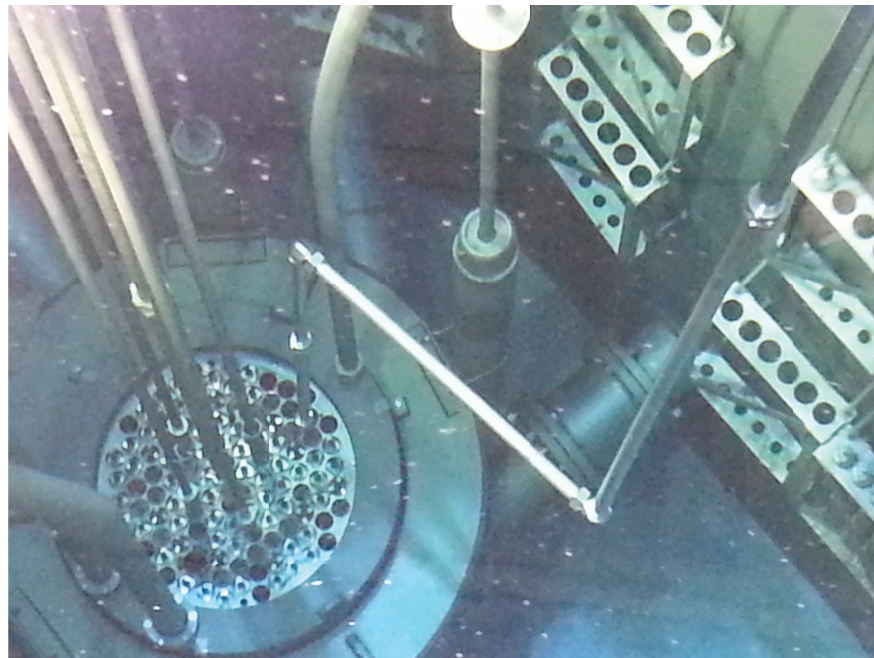


Figure 49: Turn in pipe after full insertion in flow channel

After measurements are done for the day, the reactor was shutdown with the probe still inserted to minimize reactivity change and then the probe was removed until the first Swagelok connection was out of the water. The connection was disconnected and the 8 foot pipe segment was threaded off the remaining wire and checked for radioactivity. If it was not contaminated, the pipe was stored outside the reactor. If it happened to be too active for standard storage, the pipe would be left in the pool until it had reached low enough of a level to be removed from the pool and stored safely. The 3 foot extra piece was then connected where the 8 foot one was to allow for storage in the water so that the pipe still exited the water but below the deck plates. The pipe was clamped down to the side of the pool and the wire was left on the edge of the

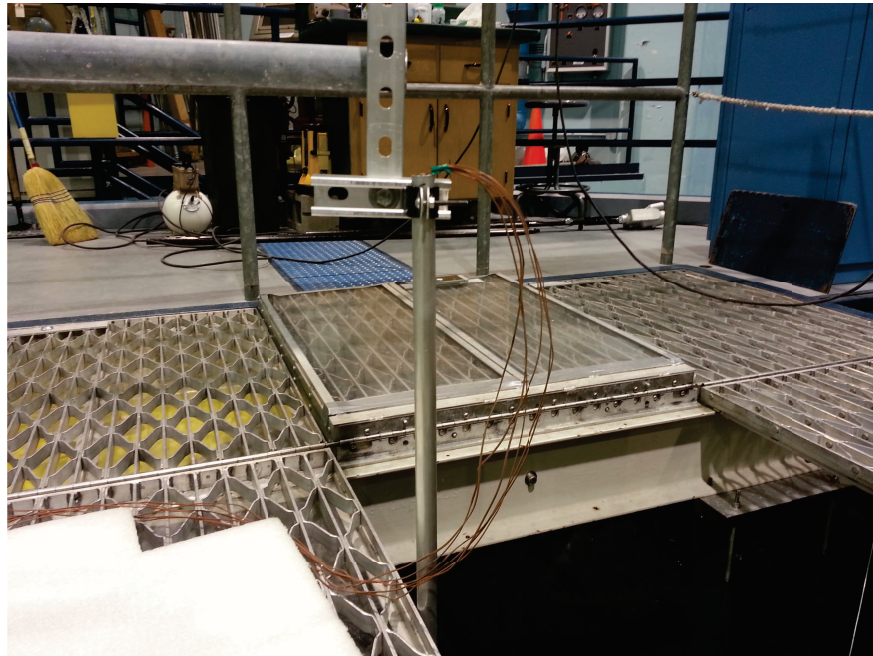


Figure 50: Pipe secured above water during TRIGA operation

pool for later use.

5.2.3 Results from probe measurements

The coolant temperatures were measured at 5 reactor power levels: 200, 400, 600, 800 and 950 kW. The data taken over the 20 minute span was averaged and plotted with respect to the thermocouple location and temperature detected. The one degree plus or minus error bar was due to the inherent error due to the type E thermocouple. The results are given in Figure 51.

As expected, the temperatures in the channel increase at higher vertical locations in the channel. Each of the heated sections follow a generally linear trend except for the 950 kW level which is non linear due to thermocouple 5

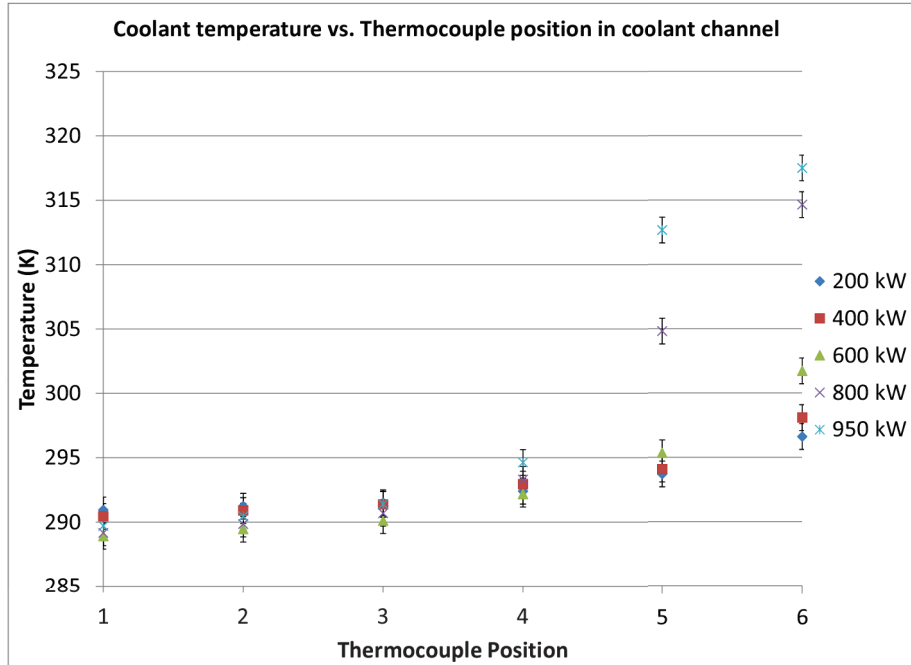


Figure 51: Results of initial probe measurements at 5 reactor power levels

or 6. This is most likely due to the changing of the axial heat profile in the fuel rods due to the change in control rod depth. There is also an increase in the deviation seen in the measurements for 950 kW as compared to lower power levels. They can be seen in Figure 52.

The range of these values over the measurement time is 4.5 degrees which is larger than the 2 degree error range. This implies that a significant effect is occurring in the channel at this height to cause these deviations, most likely turbulence.

Further measurements will be made at different inlet temperatures and pump levels to increase the data set for model adjustment.

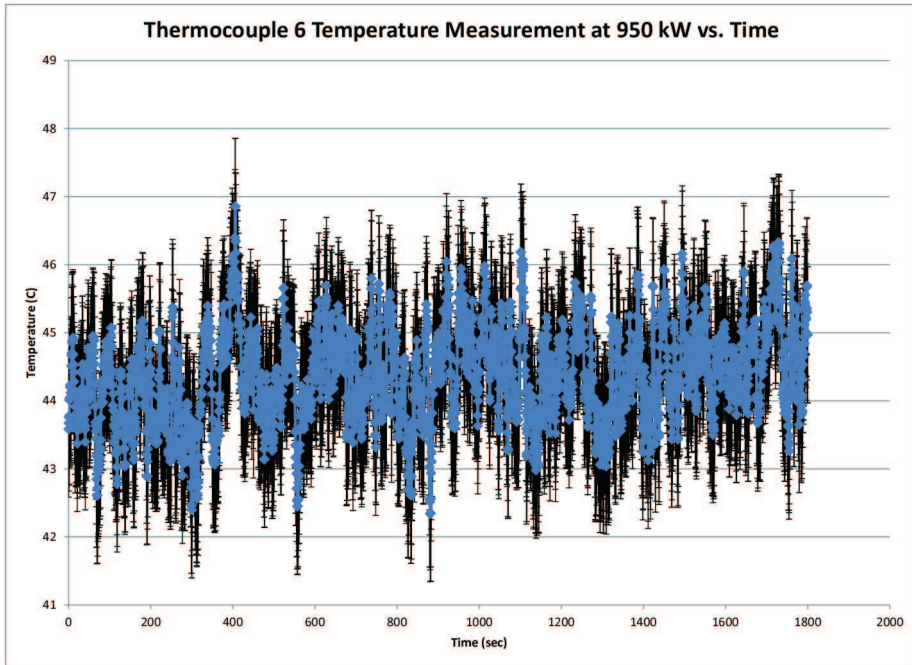


Figure 52: Results from thermocouple probe during 30 minute run at 950 kW

5.2.4 Proposed new probe

The current probe lacks in two key areas, sensitivity in the z direction measurements (too large of a separation between thermocouples) and the thermocouples not encompassing the entire heated section. OMEGA allows for probe designs to be submitted to them that are not one of the offered models for production to handle the exact needs of user. The proposed new probe will be of the same length and diameter but the number of thermocouples will increase to 12 where 2 thermocouples will be located at locations 1 and 2 from

the old thermocouple probe, 8 will be equally spaced along the 37.1 cm of heated section of the channel and 2 more above the channel at 9 cm intervals to measure the outlet temperature before the water reaches the plate. This will help to remove the dependence on an individual thermocouple for model calibration.

5.2.5 FLUENT Model Adjustment Based on TRIGA Probe Measurements

The single channel FLUENT model with the probe inserted was used to best represent the actual probe measurement in the TRIGA. The model was run based on the heat into the flow channel by using the overall reactor power and axial and rod peaking factors. The flow rate was adjusted to attempt to match the temperature at thermocouple 3 and 6 locations as close as possible with the overall rule of each thermocouple had to be within 1% of the measured value. The FLUENT coolant temperatures used were an average of three nodes at the location of the probe in the channel to best parallel the actual testing system. The results are given in Table 21, all probe temperature measurements have an uncertainty of $\pm 1^{\circ}\text{K}$ and the FLUENT measurements have an uncertainty that range from 0 to 0.7%.

All of the errors are below 1% except for the 2 highlighted in red. This might be due to turbulence in the channel, insufficient data points to calibrate the model, or natural deviation. The proposed new probe will help to increase the sensitivity of the model validation and clarify the source of the errors.

Table 21: FLUENT Adjustment based on TRIGA Probe Results

Power Level (kW)	Thermo couple Location	FLUENT Temp (K)	Probe Temp (K)	% Error	Mass Flow Rate (kg/s)
200	3	291.5	291.5	0.006	0.0625
200	4	292.8	292.4	0.126	0.0625
200	5	294.4	293.7	0.248	0.0625
200	6	296.5	296.6	0.024	0.0625
400	3	291.4	291.4	0.013	0.09
400	4	293.1	292.9	0.057	0.09
400	5	295.3	294.1	0.422	0.09
400	6	298.3	298.1	0.065	0.09
600	3	290.1	290.1	0.009	0.08
600	4	293.0	292.2	0.288	0.08
600	5	296.8	295.3	0.487	0.08
600	6	301.8	301.7	0.012	0.08
800	3	290.6	290.7	0.039	0.0525
800	4	296.7	293.3	1.154	0.0525
800	5	304.8	304.8	0.011	0.0525
800	6	314.7	314.7	0.026	0.0525
950	3	290.1	291.4	0.450	0.055
950	4	297.0	294.6	0.790	0.055
950	5	306.1	312.7	2.105	0.055
950	6	317.4	317.5	0.047	0.055

5.3 Development of a scaled hot channel model

A scaled model of the hot channel in the TRIGA core as well as the ring surrounding the hot channel was designed to measure values such as flow rates and water temperatures that are not measurable in the actual TRIGA due to safety constraints. This setup allows for other configurations such as unheated rods or control rods to be inserted into the assembly to mimic other sections of the core. The amount of power applied to each fuel rod is customizable to

increase the flexibility of this model.

To develop a feasible model with regards to cost and size, the proposed model is smaller than the actual size of the TRIGA fuel rods. This allows for three significant advantages:

- Less power is needed to achieve the same amount of heating in the flow channel
- The size allows for better portability and requires less area for operation and storage
- The cost is reduced due to the smaller heat flux required as well as less materials needed for construction
 - However, smaller instrumentation to measure the needed quantities may increase the cost with a net reduction in the overall cost of the model.

The development of the model will be described in three parts:

1. Scaling factors and similitude
2. Parts required to build the model
3. Measurements of flow and temperature profiles

5.3.1 Scaling factors and similitude

A full scale model would not be feasible for this project since it would be too expensive and too large. A 30 kW heating element, normally found in

dishwashers, has a large power draw which would only be exacerbated due to the need of 12, 30 kW heated elements. Together, they would require over 300 Amps to operate all 12 at once. The smaller model will allow for easy transport in a small vehicle and operation in a classroom.

Since this model needs to reflect the same flow patterns and heat distributions as the TRIGA core, similitude was used to ensure that these values are conserved. Dimensionless variables such as the Reynolds number and Nusselt number are two key indicators of the flow that need to be the same in both the actual system and model to allow for the results of the model to be scaled to the TRIGA flow channels. The heating of the flow channel is equated by having the same wall temperature to coolant temperature difference to achieve the same heat transfer coefficient at the wall.

Therefore, since the scaled model has less water in the flow channel, the heat applied needs to be less to achieve the same temperature distribution.

The flow parameters are equaled using two dimensionless parameters, the Reynolds and Nusselt numbers (equations (37) and (38)).

$$Re = \frac{\rho V D}{\mu} \quad (37)$$

Where ρ is the density of the water, V is the velocity of the water, D is the diameter of the flow channel, and μ is the dynamic viscosity of the water.

$$Nu = \frac{\frac{f}{8}(Re - 1000)Pr}{1 + (12.7(\frac{f}{8})^{0.5}(Pr^{\frac{2}{3}} - 1))} \quad (38)$$

Where Pr is the Prandtl number and f is the Darcy friction factor.

Many of these variables are intrinsic to the system. The known quantities for the scaled model are in table 22.

Table 22: Variables for scaled model

Variable	Known?
Hydraulic diameter	Yes (depends on scaling factor)
Heat Power Applied	No
Heated Surface Area	Yes
Water Average Velocity	No
Density	Yes
Expansion Coefficient	Yes
Dynamic Viscosity	Yes
Rod length	Yes (depends on scaling factor)
Pressure	Yes
Wall Temperature	Yes (set to same as actual)
Prandtl Number	Yes
Wall Roughness	No

Therefore, there are three unknowns and three equations that must be conserved. To solve this system, the Reynolds number equation is solved first to match the outlet Reynolds number of the actual system. The velocity of the model system is varied until the Reynolds numbers of the two systems are the same. This is possible since the dynamic viscosity and density are dependent upon the pressure and temperature which are already known for the two systems. The velocity is achieved in the scaled model by using the pump installed at the inlet of the heated element water tank.

To determine the wall roughness, the Nusselt number equation is used to equate the flow in the two systems. The Prandtl number depends on temperature and the Reynolds number is known from the previous equation solution. The friction factor depends on three variables, the Reynolds number, the wall roughness and the diameter of the flow channel. Then the Moody diagram (Figure 53) can be used to determine the friction factor of the system. Since the Reynolds numbers of the two systems are the same but the diameters are different, the wall roughness will need to be decreased to obtain the same overall friction factor. However, for this system, the Reynolds number is in the range between 10000 and 30000 which the lines on the Moody diagram converge for values of the wall roughness between 5e-7 and 1e-3 in meters. Therefore, the boundary layer at the wall is not strongly dependent on the wall roughness so any wall roughness in this range is valid for our experiments.

The final unknown variable is the power applied to the channel. To determine the correct value, the temperature inside of the fuel rod is measured using a finite element solution to the two-dimensional heat equation inside of the stainless steel rod. The wall fluxes for the actual and model system are matched to achieve the same heat transfer into the water.

This was done solving the two dimensional heat transfer equation for conduction in a solid. The original equation has the form:

$$\frac{d^2T}{dr^2} + \frac{1}{r} \frac{dT}{dr} + \frac{d^2T}{dz^2} + \frac{1}{k} g(r, z) = 0 \quad (39)$$

Where T is the temperature in the solid in K, r is the radial distance

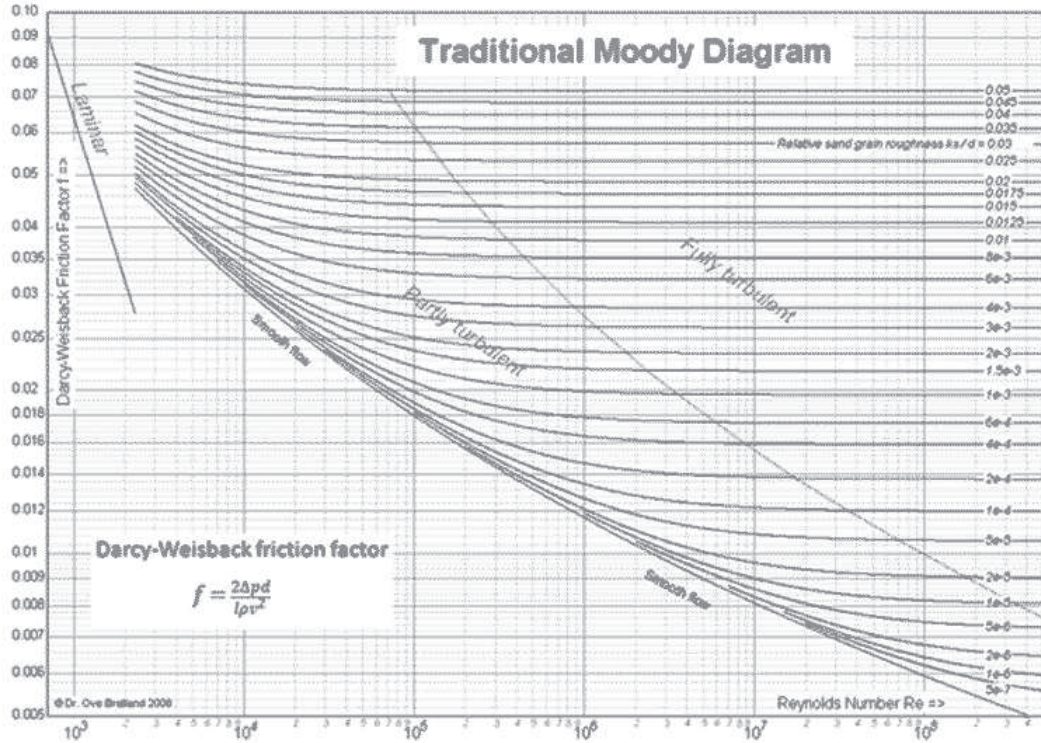


Figure 53: Moody diagram for the Darcy friction factor

component in m, z is the axial distance component in m, k is the thermal conductivity in W/m²K, and g is the energy generation rate in W/m³

An analytical solution to this PDE is not feasible for this system so finite differencing will be employed to determine a numerical solution. The first and second order differentials can be replaced in the following manner. The index i is used to denote a cell at location i in the radial direction and the index j is used to denote a cell at location j in the axial direction. 15 cells in each direction were chosen to balance between computational time and desired accuracy.

$$\frac{d^2T}{dr^2} = \frac{T_{i-1,j} - 2T_{i,j} + T_{i+1,j}}{\delta^2} \quad (40)$$

Where δ is the mesh size in meters

$$\frac{1}{r} \frac{dT}{dr} = \frac{1}{i\delta} \frac{T_{i+1,j} - T_{i-1,j}}{2\delta} \quad (41)$$

$$\frac{d^2T}{dz^2} = \frac{T_{i,j-1} - 2T_{i,j} + T_{i,j+1}}{\delta^2} \quad (42)$$

After substituting in these equivalences, four boundary conditions need to be used to arrive at a final equation. They are:

$$\frac{dT}{dr} = 0 \quad (43)$$

$$k \frac{dT}{dr} + h_b T_b = h_b T_{\text{inf}} \quad (44)$$

$$-k \frac{dT}{dz} + h_o T_o = h_o T_{\text{inf}} \quad (45)$$

$$k \frac{dT}{dz} + h_L T_L = h_L T_{\text{inf}} \quad (46)$$

Where h is the heat transfer coefficient in $\text{W}/\text{m}^2\text{K}$ and T_{inf} is the temperature of the fluid far from the heated element.

The first boundary condition implies that the temperature at the radial center of the rod is finite and should be evaluated at $r=0$. The second is valid as long as the wall temperature is known at the radial boundary and should be evaluated at $r=R$. The third (evaluated at $z=0$) and fourth (evaluated at $z=L$) are valid as long as the temperature of the rod is known at the top and bottom with regards to the z -direction.

By substituting these boundary conditions in to the main equation, four equations can be found to determine the temperature in the rod at different locations. This system will be solved by starting with a known wall temperature profile and solving the system radially inward to find the temperature profile. This was done using MATLAB to solve and visualize the results. The power profile and dimensions of the TRIGA fuel element were fed into the script and the temperature profile that resulted can be seen in figure 54.

The power for the scaled system will be lower than the actual system to achieve the same profile, wall temperature and power per area as the TRIGA case.

Based on the requirements for the Reynolds number and power per area applied to the system to be the same for both the model and actual system, the scaling factors between the two models are in equations (47) and (48).

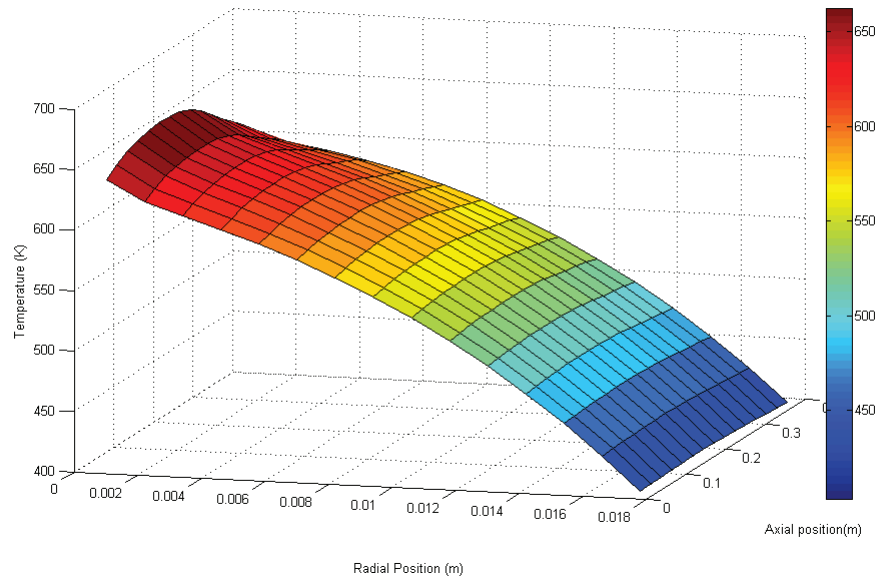


Figure 54: Temperature profile in fuel rod using two dimensional heat transfer equation

$$V_a = (SF)V_s \quad (47)$$

Where a denotes the actual system, s denotes the scaled system and SF denotes the scaling factor.

$$Q_a = \frac{Q_s}{(SF)^2} \quad (48)$$

Therefore, there is a relation between the two systems if all of the variables are known for the model system as well as the scaling factor. The one-fifth

model was decided on to balance two main characteristics, power needed to have the correct heating profile and size of the entire system in relation to the size of the measuring devices (flow meters and thermocouples). The one-fifth model is still large enough to accommodate the thermocouples which are in the 0.1-0.25 mm diameter range for the measurement of the wall and coolant temperatures. The flow rate will not be able to be measured in-line but instead at the outlet to the flow channel since of its small size. Cross-flow measurements will be quite tough considering the space between channels only has a width of 1.2 mm.

5.3.2 Parts required to build the model

The parts required are:

- Heating elements which have a range of 0 - 1 kW
- Stainless steel piping to achieve the same wall roughness as the fuel rods in the TRIGA as well as similar thermal conductivity
- Tap water
- Stainless steel upper and lower grid plates the achieve the correct flow patterns
- Compressor/pump to drive flow since the velocity in the channel will not be high enough to have the correct Reynolds number
- Large tank with built in heater/cooler to allow for multiple pool conditions and be large enough to make the inlet water temperature essentially

constant.

- Narrow channel above the tank to set atmospheric pressure level

A sketch of the proposed system is shown in figure 55.

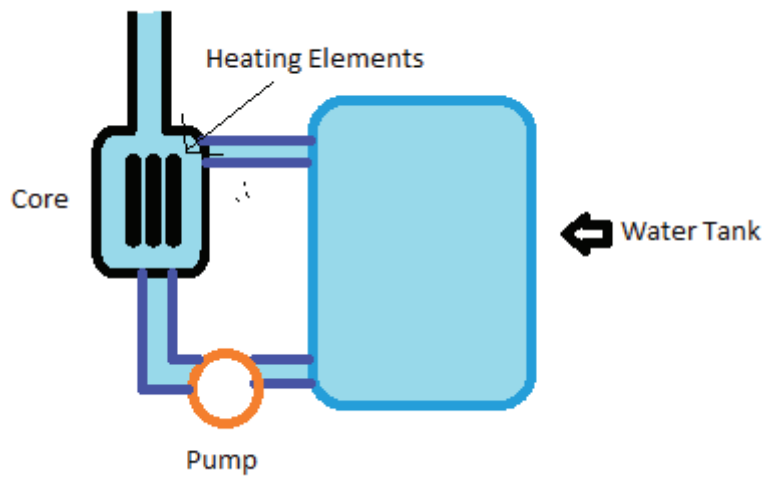


Figure 55: Overall Setup

The TRIGA reactors are certified based on a scenario where the only system driving the flow is the natural circulation that exists due to the heating of the water in the flow channels. There will still be natural circulation in the scaled system but the flow induced will not scale to that seen in the full scale system. Since a greater flow velocity is required in the scaled model to simulate the same flow characteristics that exist in the actual system, a pump is needed to achieve the correct flow rate.

The water tank surrounding the heated elements will be made of a clear plastic to allow for the system to be visible during operation. The top of

this tank will be removable to allow for the easy shuffling of the fuel rods so different core setups can be quickly created. The main water tank material is not required to be translucent but it would be preferable to ensure the water level is constant throughout the experiment.

The heating elements will be heating wires that lie in the center of each fuel rod. However, the entire length of the rod is not heated, only the center section where the erbium-zirconium-hydride 8.5 wt% uranium fuel is as shown in figure 56.

The pipes will be made of stainless steel since it has a wall roughness close to the TRIGA fuel rods, and has a thermal conductivity very close to the ZrH(1.6) fuel. Sea-cure stainless steel has the ideal thermal conductivity of 18.3 W/m-K, so that the heat transfer is quite similar to that between the actual fuel rods and water coolant. A clear material for the rods is not feasible since most clear acrylic has a thermal conductivity of 1 W/m-K and silicone has a thermal conductivity of 147 W/m-K.

The radial layout for the system is seen in figure 57 with each rod having a radius of 3.754 mm and the main tank having a radius of 2.5 cm.

To ensure all of the dimensions of the scaled fuel elements are correct, the technical drawings from General Atomics can be used to scale down each part of the fuel elements including the end fittings and fins that are important to correctly mimicing the TRIGA.[?]

Tap water can be used as opposed to deionized water since corrosion and water properties are not significantly different than those for deionized water for this system. The water tank for the heated section will be a 0.5 liter tank

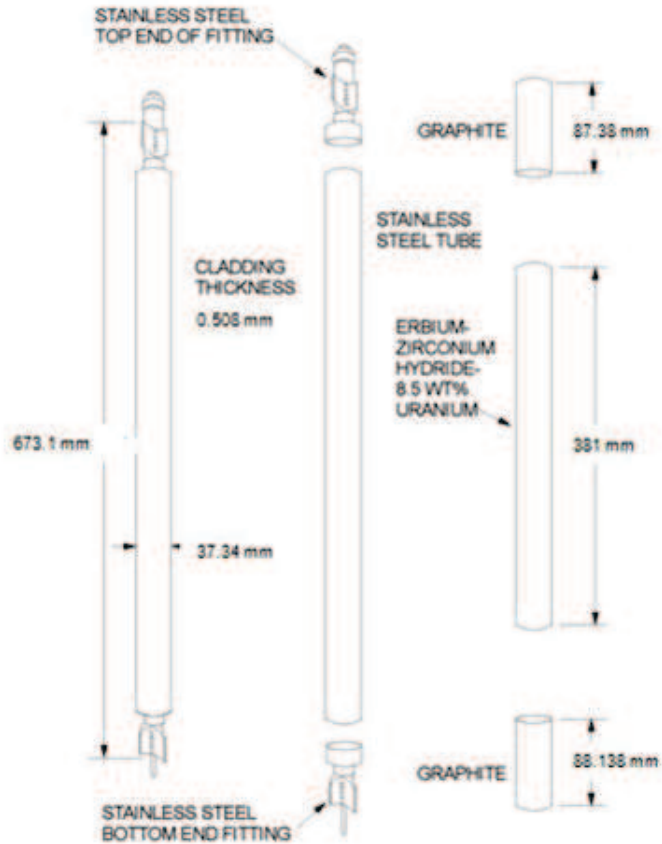


Figure 56: Dimensions of fuel rod

that has a height of 25 cm diameter to give adequate room on all sides of the core. The main, temperature controlled, water tank will have a size of 100 liters to ensure that the pressure of the system is maintained without reaching critical levels. With no cooling of the main tank, the temperature of the tank will increase based on assuming that the tank is at 293 K at the start and perfectly insulated (a conservative estimate). The expected max channel flow rate of 0.047 kg/s is multiplied by 13 because of the 13 flow channels to get

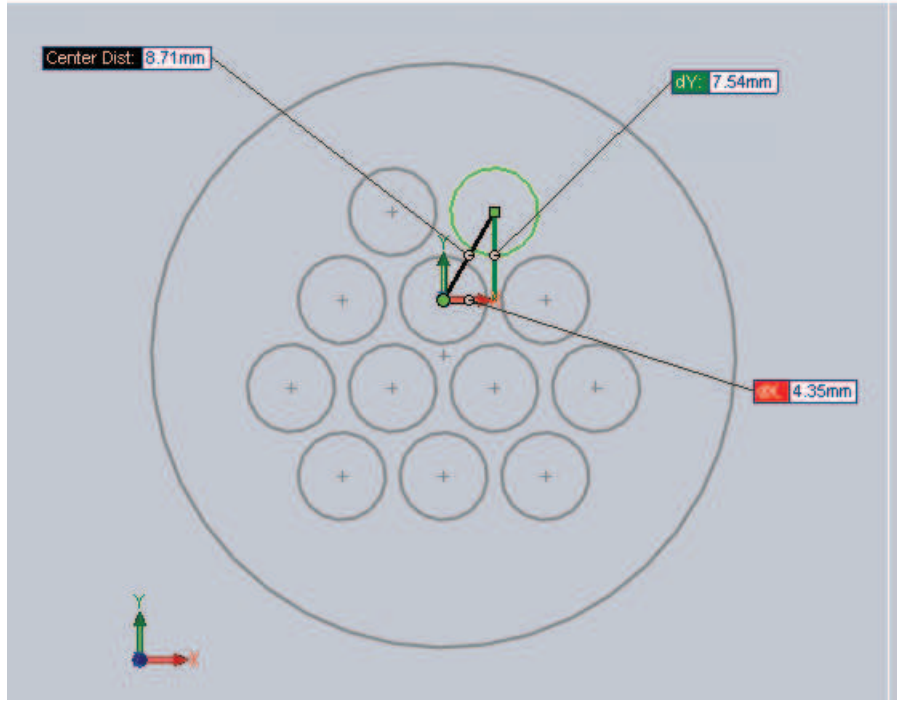


Figure 57: Radial view of model design

a total flow of 0.611 kg/s (a conservative estimate since it assumes all the channels are the hot channel). The main tank has a total mass of water of 93.358 kg. Since the exiting temperature for the water exits at just over 299 K due to equation (49), the following algebraic equation results:

$$\Delta T = \frac{Q}{c_p \dot{m}} \quad (49)$$

Where ΔT is the change in temperature in K from the inlet to the outlet, and \dot{m} is the mass flow rate in kg/s.

$$Total\ temperature\ in\ tank = \frac{299.016 * 0.611 * t + ((93.358 - 0.611 * t) * 293)}{93.358} \quad (50)$$

This results in a t of 25.4 sec for a total temperature of 294 K. If the main tank size were increased, the amount of time it would take increase the temperature in the tank would increase linearly. The water surrounding the fuel rods will be exposed to heat from the outside ring of fuel rods. While this will slightly increase the flow rate entering the main tank, the temperature of that water is less than the water exiting the coolant channels. Therefore, that flow will be assumed to not contribute a significant change to the water temperature entering the tank. A flow meter at the exit to each channel will be used to ensure the flow rate through each respective flow channel is adequate.

The pump needs to have enough power to drive the needed flow velocity since the natural circulation due to the heating is not significant enough to drive the flow at the required flow velocity (at least 2 liters per second).

Another desired attribute of the model is that it can be easily transported for demonstrations. Therefore, the main water tank needs to be separable from the testing tank which will be done by using compression fittings to connect the pipes running from the pump and main water tank to the testing tank. This will allow for transport of the system in a van or truck bed and allow for quick setup and takedown.

The upper and lower grid plates will also be scaled accordingly and will include openings for an additional ring in case the model is expanded at a later

date.

5.3.3 Measurements of flow and temperature profiles

Three main measurements of the model system need to be made to correctly scale the results up to the actual TRIGA system.

1. Temperature of water in the flow channel (radially and axially)
2. Velocity of water in the flow channel (z-direction)
3. Wall temperature to determine heat applied to the water

The overall goal of this model is to determine key quantities (wall temperatures, water temperatures and flow rates) in the hot channel of the system. Those values can then be scaled to the actual TRIGA system where the values can be used for the validation of the computer models. Ideally, this model will not only allow for hot channel measurement but also for the neighboring channels.

Type E thermocouples will be used to determine the temperature of the water in the channels. One temperature probe will be quite similar to the one used in the TRIGA to get an axial cut at multiple locations in the channel simultaneously. However, this will disturb the flow in the center of the channel. A single thermocouple will be lowered to the bottom of the flow channel and drawn up slowly through the channel to get a full profile of the temperature in the channel while minimizing flow aberrations.

To find the temperature of the wall of the fuel rod, thermocouples will be installed along the inside of the rods. A minimum of 5 thermocouples will be

required along the wall of each fuel rod that is in a flow channel. They will be at locations at the top, bottom and center of the heated section of the rod with the two remaining thermocouples being placed equally between the end of the rod and the center. This will allow for the heat transfer coefficient to be determined for the system at multiple locations on the fuel rod.

To allow for quick removal and insertion into the system, the probes will be along the outsides and top of the water vessel on hooks that can be grabbed by a "fishing pole" like apparatus to lower into any flow channel. That will allow for easier switching of probes as well as minimal interaction when they are not in the flow channel.

A calorimetric flow probe will be used to determine the flow rate due to its small size and accuracy at low flow rates (below 5 m/s). The calorimetric probe is preferred over a turbine flow meter since the turbine flow meter has a greater effect on the flow through the channel. Regardless, the flow meter should be removable from each flow channel. There will not be much axial and radial profiling of the flow since it is almost constant over the course of the flow channel with the exception of the turns at the top and bottom fins and grid plates. An overall flow rate for the system will also need to be determined by measuring the total flow leaving the tank. Additionally, temporary probes should be added to the crossflow connections between the neighboring flow channels to determine the amount and direction of crossflow if the scale is large enough to accommodate a flow meter but can be removed when less perturbations to the flow are desired.

5.3.4 Extra additions/Values for Scaled System

For the case of a 0.2 scaled system, the dimensions and target properties are in table 23:

Table 23: Values for 0.2 scaled model

Variable	Value
Hydraulic diameter	0.003705 m
Heat Power Applied	1200 W
Heated Surface Area	0.000887 m ²
Water Average Velocity	4.54 m/s
Density	933.56 $\frac{kg}{m^3}$
Expansion Coefficient	0.000731 (dimless)
Dynamic Viscosity	0.00028 Pa-s
Rod length	0.1346 m
Pressure	103187 Pa
Outlet Temperature	299.1 K
Wall Roughness	2.1e-6 m
Reynolds Number	32150
Friction Factor	0.026
Mass of water in heated section	0.000801 kg
Change in temperature due to heat	6.016 K

The flow rate in the hottest channel will be approximately 0.047 kg/s to achieve the required conditions to mimic the actual TRIGA core.

These numbers were determined using a similitude calculator developed to be a dynamic tool where the size of the scaled channel could be adjusted and the heat applied and velocity needed to achieve scaled results from the actual TRIGA would be output to the user. This was written in MATLAB where the user would be prompted for the amount of scaling desired and the dimensions and conditions of the scaled system were output.

5.3.5 Safety Analysis Report

To increase the safety of this system, the maximum temperature of the water will be limited to 323 K. Therefore, the maximum power applied to hot flow channel is 3000 W given by the equation 49. The location of the highest water temperature will be the exit to the hot channel and will be the location that the model is benchmarked by.

The model will operate at 1200 W to correctly scale from the actual TRIGA core while staying within safety limits. The pressure of the system is near atmosphere so no danger arises from the pressurized system.

5.3.6 Scaled Model Validation using FLUENT

To help validate the model before construction, the calculations for the design of the scaled model were compared to a FLUENT model with the proposed dimensions. The fifth size model was built identically to the one in chapter 5 with the dimensions scaled down. The data that was compared between the proposed model and FLUENT model were the net change in water temperature entering and exiting the hot channel as well as the flow velocity through the channel. Their values are included in table 24.

The water temperature differed by less than 3% and the velocity differed by less than 1% between the two models which strengthened the model design for the scaled model.

Table 24: Data taken from both scaled models

Variable	Scaled Model Value	FLUENT Model Value
Heat Applied to Channel	1200 W	1200 W
Average Water Velocity	4.54 m/s	4.51 m/s
Difference in Water Temperature	6.016 K	6.182 K

6 Results

6.1 Fitting FLUENT Results to HTC Correlations

The main goal of using FLUENT in this research is to develop a new heat transfer coefficient correlation for the system that better represents the heat transfer than the model used in SNAP. To obtain this new correlation, data from the FLUENT runs were extracted using a script written in MATLAB to remove the appropriate data values. The Reynolds and Prandtl numbers were calculated from this data. Then the heat flux, wall temperature, and bulk temperature were used to find the heat transfer coefficient of the system which was converted to the Nusselt number. The Reynolds and Prandtl numbers were then used along with the new calculated Nusselt number to derive a HTC correlation given the data. Then each of the functional forms were used as a basis for fitting the FLUENT results and the coefficients and exponents of each form were replaced by variables and the values of these variables were adjusted until the best fit from the form was obtained based on the r^2 value. This method was then repeated for all power levels and a fit was made across

the entire scope of available data from the temperature probe to make the recommended fit as accurate as possible.

The data extracted from the FLUENT runs depended on the equations used to find the Reynolds, Prandtl, and Nusselt numbers as well as the HTC (eqs. 51 - 54).

$$Re = \frac{\rho V D}{\mu} \quad (51)$$

$$Pr = \frac{c_p \mu}{k} \quad (52)$$

$$h = \frac{k N u}{D} \quad (53)$$

$$h = \frac{Q}{A \Delta T} \quad (54)$$

The density (ρ), specific heat (c_p), viscosity (μ), thermal conductivity (k), and heat flux (Q/A) were all directly taken from the FLUENT data output and averaged over each of the 15 heated cells. The total velocity (V) was extracted from the FLUENT data and then averaged over the cell, weighting for the area of each nodal surface, to obtain the average velocity in each of the 15 heated

sections that were used in the SNAP model. The cell volumes were output from the FLUENT data and the velocities extracted were weighted based on the volume of the cell. This would account for the fact that the cells are all not the same size in the model. The temperature difference between the wall and average temperature of the fluid (ΔT) was found by isolating the wall data and finding the average temperature over the wall surface area of the heated cell. The bulk temperature was found by averaging the temperature over the entire cell. This method was chosen over using a centerline water temperature since SNAP uses the average water temperature when it calculates the heat transfer in the cell. The diameter (D) of the flow channel was the hydraulic diameter of the flow channel used in previous chapters. The MATLAB code for this extractor is included in Appendix B.

The results of the data extraction from the 830,000 node model are included in Table 25.

The Nusselt numbers obtained for each of the 15 heated sections using equations 53 and 54 were then compared to the Nusselt numbers using 4 different base HTC correlations: Dittus-Boelter, Gnielinski, Shah, and SmoothCyl.

The results of those fits are included in Table 26.

6.1.1 Validity of the 4 Fitting Equations

The 4 equations used for fitting were based on the equations of the 4 HTC correlations: Dittus-Boelter, Gnielinski, Shah, and SmoothCyl. However, these equations are not valid for all Reynolds and Prandtl numbers. The range of Reynolds numbers that describe the flow in the center heated channel are in

Table 25: Results from 830,000 node, 4 channel model run, 950 kW

Section	Re	Pr	HTC ($\frac{W}{m^2 K}$)	Nu
1	1317.786	8.805	2557.503	66.814
2	1308.823	8.471	2187.402	57.506
3	1325.996	8.172	2129.394	55.724
4	1353.792	7.757	2164.873	56.274
5	1418.669	7.279	2126.034	55.067
6	1501.208	6.772	2185.447	56.224
7	1598.879	6.306	2201.337	55.954
8	1738.156	5.946	2174.395	54.028
9	1906.030	5.395	2175.049	54.698
10	2052.225	5.085	2165.369	53.652
11	2269.853	4.758	2133.742	52.826
12	2468.254	4.436	2122.507	53.016
13	2645.850	4.236	2047.431	50.966
14	2766.480	4.133	2003.311	49.241
15	2899.912	3.976	1910.010	47.191

the transitional range (1800-3700) for the maximum power and have an overall range of (1450-3200) for the entire range of powers the fit is valid over. The Prandtl numbers range from 8.9 to 3.6. The ranges of valid Re and Pr numbers for each of the 4 HTC correlations are given in Table 27:

While the Shah correlation appears to be in the right range for both of the Reynolds and Prandtl numbers, it also requires that the velocity be > 3 m/s. Therefore, the Gnielinski correlation is the only correlation that has ranges which cover at least some of the Reynolds and Prandtl numbers measured.

Therefore, a new heat transfer correlation will be created since none of the current heat transfer correlations encompass the range of conditions of the TRIGA flow channels. The new correlation will be accurate for the specific TRIGA geometry as well as the flow conditions which are based on the FLU-

Table 26: Nusselt number determined from 4 different HTC correlation fits from 830,000 node, 4 channel model run, 950 kW

Section	Dit-Bolt	Gniel	Shah	Smooth
1	19.153	10.253	38.534	24.966
2	18.893	10.052	38.182	24.665
3	18.632	9.886	37.793	24.381
4	18.609	10.069	37.561	24.456
5	18.624	10.330	37.334	24.601
6	18.731	10.735	37.157	24.895
7	19.012	11.370	37.115	25.446
8	19.499	12.278	37.226	26.306
9	20.035	13.254	37.361	27.251
10	20.656	14.323	37.567	28.320
11	21.365	15.482	37.851	29.516
12	22.125	16.677	38.187	30.777
13	22.714	17.617	38.426	31.771
14	23.155	18.330	38.589	32.525
15	23.531	18.924	38.738	33.161

Table 27: Valid ranges for Heat Transfer Coefficent Correlations

Fit	Reynolds Number Range	Prandtl Number Range
Dittus-Boelter	$Re > 10,000$	$0.6 < Pr < 160$
Gnielinski	$3000 < Re < 500,000$	$0.5 < Pr < 2000$
Shah	$Re > 360$	$1 < Pr < 1000$
SmoothCyl	$50,000 < Re < 1,000,000$	$0.6 < Pr < 2000$

ENT data that was experimentally validated using the probe experiments.

Since the Nusselt numbers calculated from the four methods do not exactly agree with the validated FLUENT data, a variable fit was done using each of the four original functional forms to adjust those forms to better represent the FLUENT results. The 4 equations used for the fits are included in equations 55 - 58.

$$Nu = ARe^BPr^C \quad (55)$$

$$Nu = \frac{(\frac{f}{8})^A(Re - 1000)^BPr^C}{1 + (D(\frac{f}{8})^E(Pr^F - 1))} \quad (56)$$

$$Nu = A\left(\frac{RePrD}{L}\right)^B; \quad (57)$$

$$Nu = \frac{ARe^BPr^C}{1 + 2.443Re^D}(Pr^E - 1) \quad (58)$$

A MATLAB script was written to use the Nusselt numbers obtained from the FLUENT data as the desired result from the fits. The variables were adjusted to obtain the norm between the Nusselt number calculated from the fitting function and the result from the FLUENT run. The coefficients were adjusted until the norm was below a level required by the script. Then the r^2 was determined for the resultant data and reported along with the new coefficients. The starting values for the coefficients were the same values as the established 4 fits. The starting and ending values for the coefficients are included in Table 28 along with the r^2 values. The error in these coefficients are due to the combination of the error due to the probe measurements since

they were used in calibrating the FLUENT model as well as the error due to number of nodes in the FLUENT model. The probe measurements caused between a 5-10% difference in the inlet velocity based on the power level for the FLUENT model which changed the range of possible Reynolds numbers by the same percentage. The error due to the FLUENT nodalization was found to be 2% as compared to the maximum number of nodes so they were combined to yield the overall error for the fits.

Table 28: Coefficients for the 4 functional forms used for Nusselt number fitting, 950 kW

Term	Start Dit- Bolt	End Dit- Bolt	Start Gniel	End Gniel	Start Shah	End Shah	Start Smooth- Cyl	End Smooth- Cyl
A	0.023 \pm 0.00148	0.0185 \pm 0.00148	1 \pm 0.0306	0.3832 \pm 0.0306	1.953 \pm 8152.8	101910 \pm 0	0.037 \pm 0	0.0445 \pm 0.00356
B	0.8 \pm 0.06614	0.8268 \pm 0.06614	1 \pm 0.0403	0.5048 \pm 0.0403	0.333 \pm 0	0 \pm 0 \pm 0	0.8 \pm 0	0.6866 \pm 0.05492
C	0.4 \pm 0.08030	1.0038 \pm 0.08030	1 \pm 0.1265	1.5820 \pm 0.1265	N/A \pm 0	N/A \pm 0	1 \pm 0	1.1580 \pm 0.0926
D	N/A \pm 0	N/A \pm 0	12.7 \pm 1.2254	15.318 \pm 1.2254	N/A \pm 0	N/A \pm 0	-0.1 \pm 0	-0.159 \pm 0.01270
E	N/A \pm 0	N/A \pm 0	0.5 \pm 0.0912	1.1406 \pm 0.0912	N/A \pm 0	N/A \pm 0	0.667 \pm 0	0.7567 \pm 0.06053
F	N/A \pm 0	N/A \pm 0	0.667 \pm 0.0778	0.9726 \pm 0.0778	N/A \pm 0	N/A \pm 0	N/A \pm 0	N/A \pm 0
R ²	N/A \pm 0	0.3211 \pm 0	N/A \pm 0	0.4356 \pm 0	N/A \pm 0	0.1227 \pm 0	N/A \pm 0	0.3255 \pm 0

The functional form that has the largest r² value is the Gnielinski form. The

Gnielinski fit showed the best initial r^2 value across all power levels. Therefore, it will be used as the basis for the fit over the entire spectrum of heat fluxes measured by the temperature probe in the TRIGA. The graph of the that fit is shown in Figure 58.

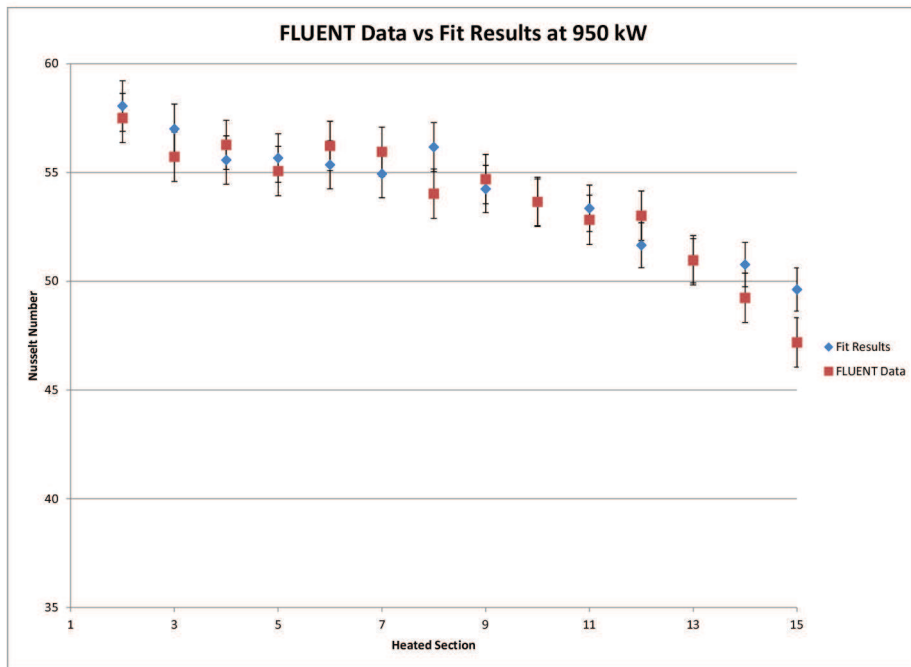


Figure 58: HTC Fit for 950kW FLUENT Data

The results from the 5 different power levels are given in Tables 29 - 32. The results for each individual power level were taken and fit to equation 56. The coefficients for the 5 power levels were then averaged to find the coefficients that would be reported as the final fit. The results from the individual fits and averages of those coefficients are shown in Figures 59 - 62 and Table 33.

Table 29: Results from 830,000 node, 4 channel model run, 200 kW

Section	Re	Pr	HTC ($\frac{W}{m^2 K}$)	Nu
1	1467.335	8.904	2081.329	56.524
2	1450.199	8.756	1780.633	50.237
3	1438.317	8.691	1740.804	49.681
4	1407.187	8.598	1743.234	50.182
5	1405.926	8.466	1650.324	47.845
6	1408.170	8.334	1702.084	49.722
7	1413.279	8.206	1712.243	49.941
8	1454.598	8.147	1634.060	46.598
9	1493.266	7.784	1601.944	46.751
10	1510.036	7.662	1594.070	46.208
11	1570.108	7.440	1524.054	44.358
12	1604.484	7.154	1511.190	44.638
13	1638.070	6.994	1427.858	42.208
14	1660.826	6.931	1418.746	41.543
15	1707.403	6.759	1279.478	37.352

Based on the results of the fits of the five different power levels, the Gnielinski functional form with the coefficients given in Table 33 is the equation recommended for improved heat transfer in the SNAP model. The errors were obtained by combining the individual errors for each coefficient with the standard deviation from each of the five measurements. The final equation is given in equation 59.

$$Nu = \frac{\left(\frac{f}{8}\right)^{0.308 \pm 0.185} (Re - 1000)^{0.395 \pm 0.180} Pr^{1.928 \pm 0.515}}{1 + ((13.734 \pm 3.514) \left(\frac{f}{8}\right)^{0.768 \pm 0.253} (Pr^{0.811 \pm 0.427} - 1))} \quad (59)$$

Table 30: Results from 830,000 node, 4 channel model run, 400 kW

Section	Re	Pr	HTC ($\frac{W}{m^2 K}$)	Nu
1	1758.319	8.887	2344.496	61.312
2	1745.266	8.709	1996.261	52.643
3	1750.071	8.617	1917.590	50.468
4	1739.120	8.491	1908.181	50.073
5	1756.334	8.332	1829.995	48.056
6	1763.921	8.168	1868.968	48.990
7	1758.538	8.022	1824.216	47.474
8	1787.120	7.965	1741.510	44.509
9	1824.854	7.581	1706.130	44.325
10	1839.831	7.434	1689.539	43.403
11	1928.585	7.163	1632.103	42.005
12	1995.751	6.829	1608.667	41.857
13	2058.644	6.613	1545.182	40.124
14	2106.588	6.488	1523.310	39.082
15	2197.649	6.237	1436.095	37.036

Table 31: Results from 830,000 node, 4 channel model run, 600 kW

Section	Re	Pr	HTC ($\frac{W}{m^2 K}$)	Nu
1	1534.844	8.856	2465.355	64.448
2	1521.288	8.618	2110.475	55.591
3	1528.294	8.452	2026.049	53.211
4	1531.064	8.224	2009.254	52.546
5	1564.613	7.952	1963.678	51.317
6	1598.456	7.658	2001.551	52.122
7	1630.385	7.382	1984.478	51.216
8	1694.237	7.187	1936.871	49.003
9	1773.802	6.698	1922.290	49.343
10	1830.405	6.450	1908.860	48.370
11	1959.565	6.122	1846.753	46.821
12	2076.528	5.751	1831.582	46.887
13	2190.397	5.501	1787.905	45.626
14	2285.345	5.350	1740.694	43.855
15	2423.229	5.116	1637.050	41.439

Table 32: Results from 830,000 node, 4 channel model run, 800 kW

Section	Re	Pr	HTC ($\frac{W}{m^2 K}$)	Nu
1	1316.837	8.823	2517.962	65.796
2	1305.566	8.519	2160.486	56.837
3	1318.350	8.256	2107.940	55.225
4	1338.239	7.891	2104.184	54.796
5	1392.658	7.465	2093.853	54.374
6	1461.006	7.010	2128.052	54.938
7	1540.242	6.595	2129.067	54.354
8	1653.147	6.288	2097.277	52.391
9	1782.057	5.767	2093.035	52.971
10	1885.407	5.479	2107.150	52.581
11	2055.863	5.149	2029.366	50.621
12	2210.473	4.812	2045.375	51.488
13	2357.647	4.592	1969.722	49.417
14	2480.127	4.463	1896.721	46.973
15	2635.739	4.276	1802.691	44.860

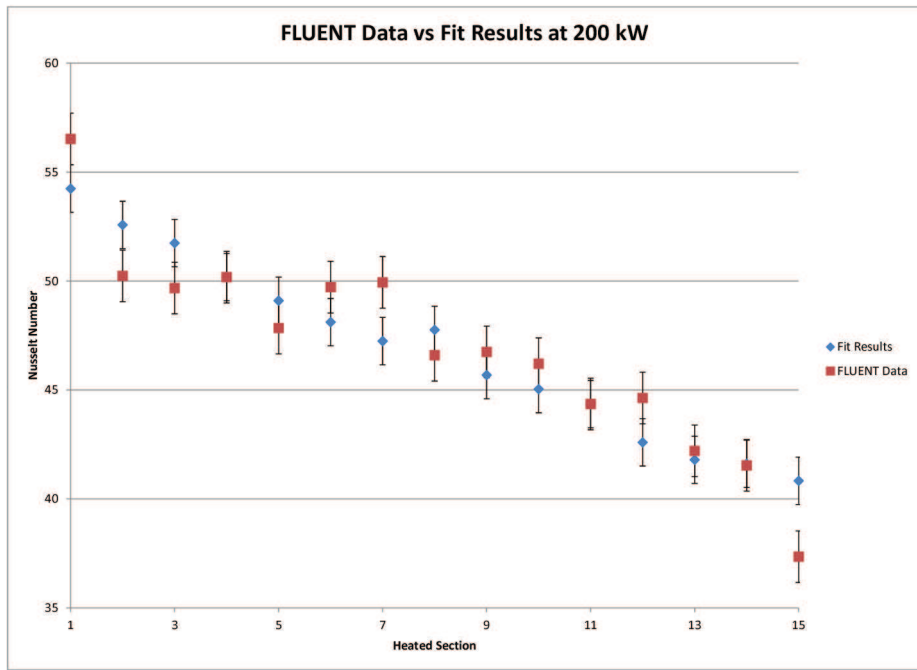


Figure 59: HTC Fit for 200kW FLUENT Data

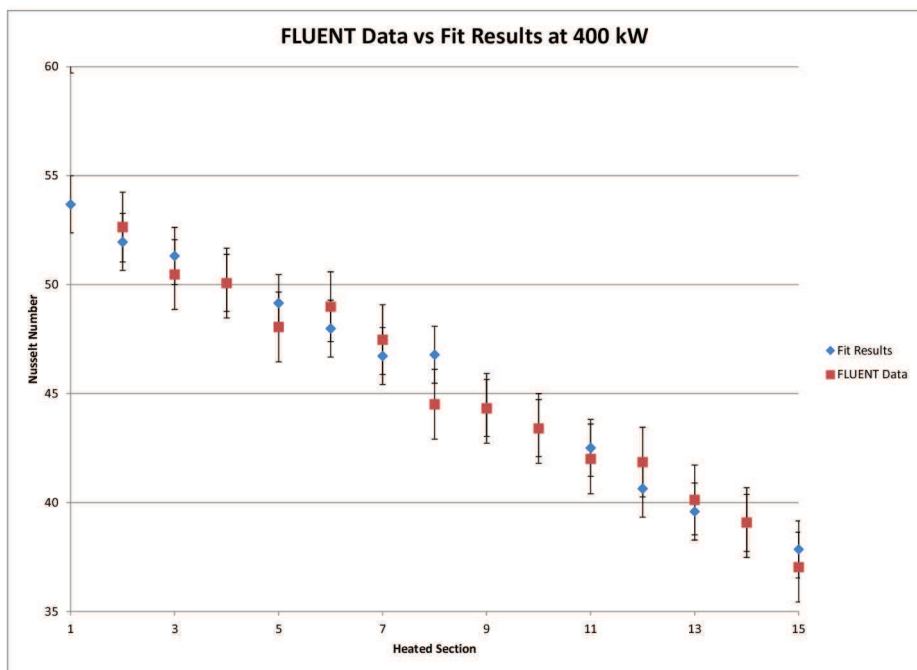


Figure 60: HTC Fit for 400kW FLUENT Data

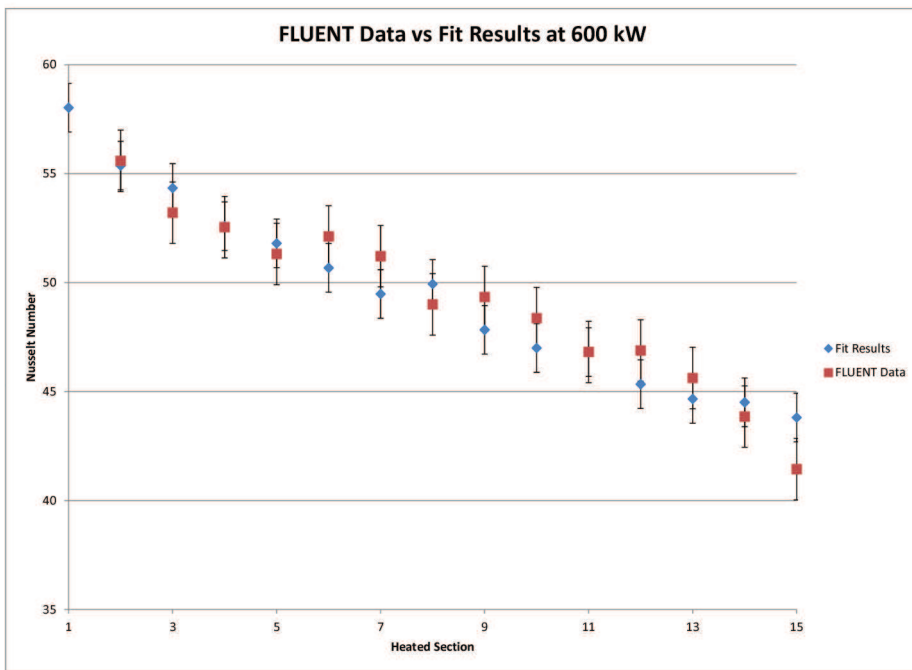


Figure 61: HTC Fit for 600kW FLUENT Data

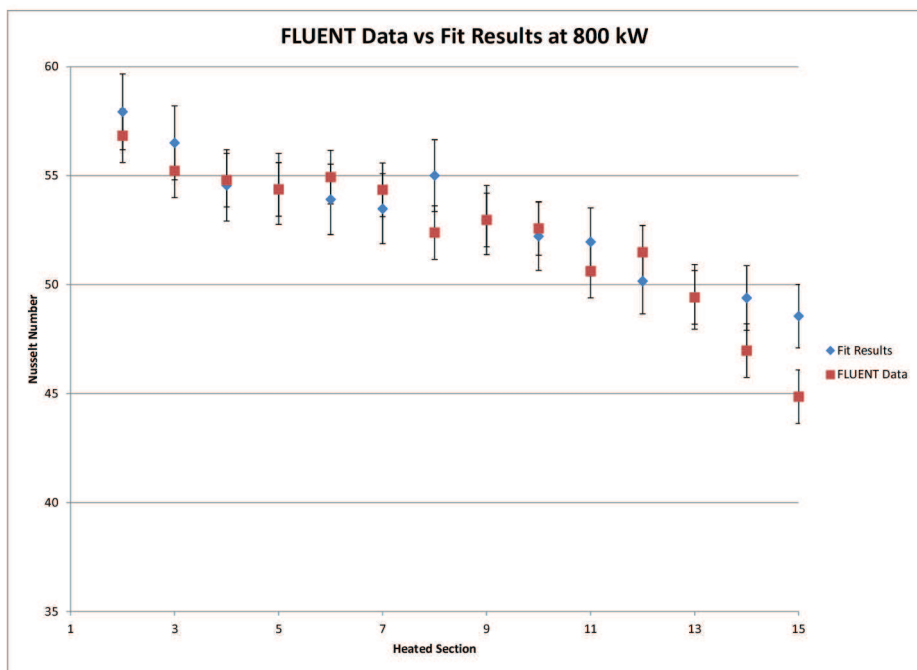


Figure 62: HTC Fit for 800kW FLUENT Data

Table 33: Heat Transfer Coefficient Fits for All Power Levels

Power Level	Coef A	Coef B	Coef C	Coef D	Coef E	Coef F
200 kW	0.077 ± 0.0061	0.171 ± 0.0137	2.755 ± 0.2204	8.332 ± 0.6665	0.522 ± 0.0418	1.428 ± 0.1143
400 kW	0.196 ± 0.0156	0.271 ± 0.0216	1.817 ± 0.1454	14.478 ± 1.1582	0.706 ± 0.0565	0.621 ± 0.0497
600 kW	0.379 ± 0.0303	0.467 ± 0.0373	1.630 ± 0.1304	16.912 ± 1.3530	0.826 ± 0.0660	0.586 ± 0.0469
800 kW	0.508 ± 0.0406	0.563 ± 0.0450	1.854 ± 0.1483	13.632 ± 1.0905	0.648 ± 0.0519	0.448 ± 0.0359
950 kW	0.383 ± 0.0307	0.505 ± 0.0404	1.582 ± 0.1266	15.318 ± 1.2254	1.141 ± 0.0912	0.973 ± 0.0778
Average	0.308 ± 0.185	0.395 ± 0.180	1.928 ± 0.515	13.734 ± 3.514	0.768 ± 0.253	0.811 ± 0.427

6.2 Loss Factor Determination for Non-Heated Sections

The term loss factor (minor loss factor or K factor) refers to the pressure drop that occurs due to a change in the geometry of a flow channel. These factors are unitless and are experimentally determined for bends, expansions, and contractions that occur in the channel. In practice, the expected head loss is proportional to the kinetic energy of the flow and is estimated based on the experimentally determined, geometry dependent, K factor tabulations. Loss factors for 45 and 90 degree bends, and a range of contraction ratios and expansion ratios have been well documented. However, other geometries such as the one that is relevant here, are much more complex and do not have an analogous documented case. In the TRIGA, the unique geometry is due to the fins on the end fittings that cause mixing of the flow throughout the end segments. Through these sections, some of the water travels around the fins, experiencing between a 45 to 90 degree turn with some of the water passing the fins with no aberration. Therefore, the unheated section above and below the graphite followers were individually modeled to determine the loss factor in each of these sections. The method used to find these factors was similar to the same method done experimentally for the documented cases.

In the documented experiments to determine the loss factors due to various fittings, pressure taps were installed upstream and downstream of the change in the geometry of the channel. The pressure difference was measured and then used to find the K factor using a combination of both equations 60 and

61.

$$\frac{P_1}{\rho_1} + \frac{V_1^2}{2} + gz_1 - h_L = \frac{P_2}{\rho_2} + \frac{V_2^2}{2} + gz_2 \quad (60)$$

$$h_L = K \left(\frac{V^2}{2g} \right) \quad (61)$$

These equations can be combined to yield equation 62.

$$K = \frac{2\Delta P}{\rho V} \quad (62)$$

Where K is the loss factor (unitless) due to the pipe geometry, ΔP is the change in pressure between the beginning and end of the segment with the pressure change due to the change in pressure due to the increase in elevation removed, ρ is the density of the water and V is the average velocity of the water in the pipe section.

Since all of these values are available to be output in the FLUENT models, the determination of the K factor was performed using those results. However, equation 62 is based on both the density and velocity of the liquid which is significantly different for different input power levels of the heated section. The density of the water is constant for the lower heated section since there has been no heating of the water until after the water exits the lower section.

In the upper section case, depending on the outlet water temperature from the heated section, both the density and velocity change causing two degrees of freedom in the K factor equation.

The upper and lower section models were built using SolidWorks and their geometry is shown in Figures 63 and 64. They were nodalized to achieve a minimum orthogonality ratio of 0.1 and a skewness factor no greater than 0.75 to ensure proper sizing of the cells. The upper section had 450,039 tetrahedral cells and the lower section had 421,514 cells based on these criteria. The mesh density was greatest around the 3 fin segments since their geometry is more intricate than the rest of the channel.

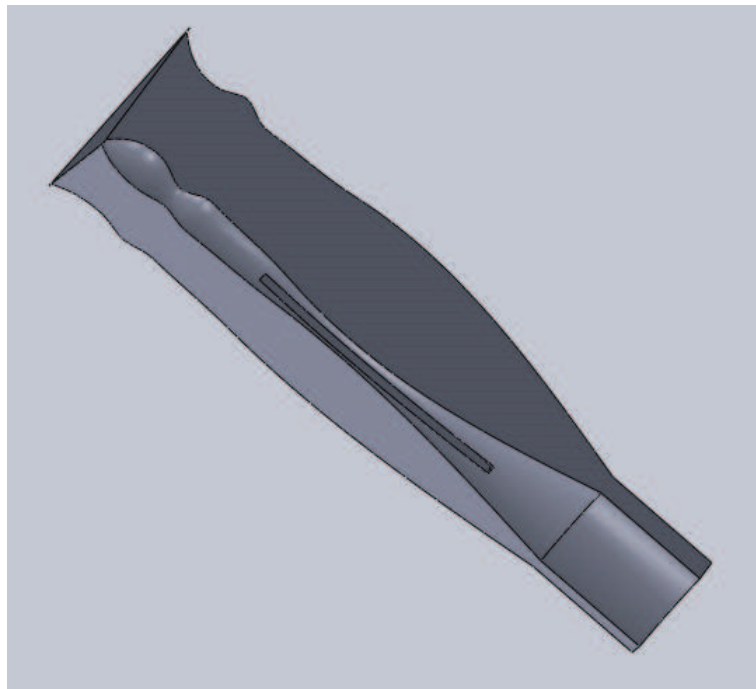


Figure 63: Geometry of upper unheated section

The inputs for the lower unheated section were the same as the ones used

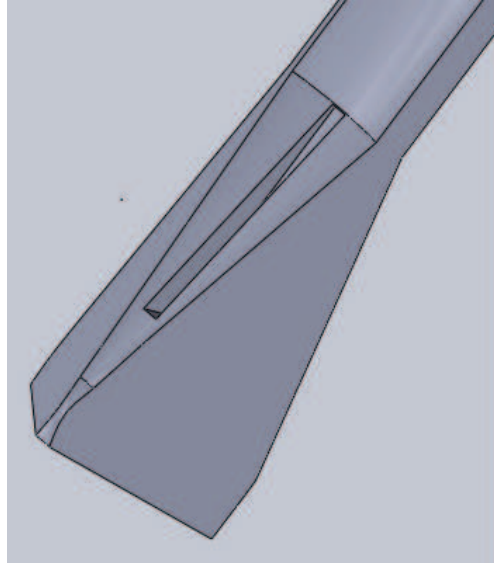


Figure 64: Geometry of lower unheated section

for the full FLUENT model. Those inputs are in Table 34.

Table 34: Input values for K factor determination of lower unheated section

Power Level (kW)	Inlet Temperature (K)	Mass Flow Rate (kg/s)
200	291	0.025
400	291	0.032
600	291	0.038
800	291	0.042
950	291	0.047

The inputs for the upper unheated section have the velocity and temperature conditions of the exit from the FLUENT heated section model. Those values are in Table 35.

The K factor was calculated for each of the 5 power levels. The pressure of the inlet to each of the models was set based on the heated FLUENT model. The pressure at the outlet of each of the unheated models was averaged and

Table 35: Input values for K factor determination of upper unheated section

Power Level (kW)	Inlet Temperature (K)	Mass Flow Rate (kg/s)
200	305	0.025
400	313	0.032
600	319	0.038
800	324.5	0.042
950	329	0.047

then subtracted from the inlet pressure to find the change in pressure. This value was then subtracted from the pressure decrease due to the change in the height of the channel to find the pressure difference only due to the minor losses caused by the geometry of the segment. The density and velocity were also averaged across the outlet and used in equation 62 to find the K factor. A slight change in the K factor was observed across the 5 power levels and can be seen in Tables 36 and 37.

Table 36: K factors for Lower Section from FLUENT Testing

Power Level	K Factor
200 kW	1.61
400 kW	1.62
600 kW	1.63
800 kW	1.65
950 kW	1.67

The estimated K factors that were used for the turns by using the method in section 3.1.1 were 1.244 and 0.844 for the lower and upper sections respectively. There is a 31% difference between the 950 kW case and previously calculated K factor for the lower section and a 30% difference between the 950 kW case and previously calculated K factor for the upper section. Therefore, the K

Table 37: K factors for Upper Section from FLUENT Testing

Power Level	K Factor
200 kW	1.10
400 kW	1.11
600 kW	1.12
800 kW	1.14
950 kW	1.15

factor used in the TRACE model will be the one determined by FLUENT. The K factor implemented is the average of these factors since the value does not change much over the range of the power levels. 1.63 will be used for the lower section and 1.12 will be used for the upper section.

6.3 TRACE Results Based on New Correlations

6.3.1 K Factor Implementation

The two changes to the loss factors were implemented into the TRACE model separately to determine their individual effect. Then both were included in the model to determine the overall change due to the new K factors. The results from these runs at 950 kW are given in Table 38. The temperature difference corresponds to the difference in temperature between the inlet temperature and the outlet temperature of the heated section.

Table 38: Results from K Factor Implementation into TRACE Model

Power Level	Original ΔT (C)	Upper Adj ΔT (C)	Lower Adj ΔT (C)	Both Adj ΔT (C)	Diff btw Org. and Both
200 kW	13.94	14.47	14.69	15.16	8.8%
400 kW	21.28	22.04	22.36	23.07	8.4%
600 kW	27.12	28.02	28.42	29.31	8.1%
800 kW	32.17	33.21	33.68	34.73	8.0%
950 kW	36.69	38.15	38.56	39.74	8.3%

There is an average of a 8.3% difference in the temperature between the original K factors and the new K factors. Therefore, the K factor adjustment is a significant change to the original TRACE model and will be utilized in any further testing hereafter.

6.3.2 Results from HTC Correlation Implementation into TRACE model

The HTC correlation was implemented by using the pipe wall option in TRACE to define the wall HTC of the hot leg as a user defined function that matched the new HTC correlation. The results from these runs at 950 kW are given in Table 39. The temperature difference corresponds to the difference in temperature between the inlet temperature and the outlet temperature of the heated section.

Table 39: Results from HTC Correlation Implementation into TRACE Model

Power Level	Original Temp Difference (C)	Adjusted Temp Difference (C)	Difference btw Original and Adjusted
200 kW	13.94	13.16	5.6%
400 kW	21.28	20.26	4.8%
600 kW	27.12	25.94	4.4%
800 kW	32.17	30.78	4.3%
950 kW	36.69	35.11	4.5%

There was an average of a 4.7% difference in the temperature between the original and adjusted TRACE model. Therefore, the HTC correlation adjustment is a significant change to the original TRACE model and will be utilized in any further testing hereafter.

6.4 Sources of Error and Uncertainties

6.4.1 Error due to TRIGA and Scaled Model Measurements

There are a few intrinsic measurement errors with the meters and devices used in the TRIGA and scaled model measurements. They are included in table 40.

Table 40: Sources of error

Source	Value
Thermocouples in probe	max ± 1 °C [17]
Pool temperature measurement	max ± 0.1 °C [20]
Thermocouples in instrumented fuel element	max ± 1.1 °C [18]
Power fluctuation at steady state	within 2% of reported value [19]
Location of probe	± 2 mm radially, insignificant axially
Flow meter in scaled model	$\leq 3\%$ [16]
Thermocouples in scaled probe	max ± 1 °C [17]

6.4.2 Thermocouples and RTDs

The maximum error in the thermocouples vary by type of thermocouple. The probe uses special type E thermocouples which have an absolute temperature error of ± 1 °C [17] while the instrumented fuel element uses type K thermo-

couples which have an absolute temperature error of ± 1.1 °C [18]. The same thermocouple type as used in the actual probe will be used in the scaled probe. The probe will be calibrated in a volume of water with a known temperature to determine the difference in temperature reading between each thermocouple in the probe. The pool temperature measurement is done by using a resistive thermal device where the change in resistance of the device indicates the change in temperature of the water. This is done only using one metal type as opposed to the dual metal thermocouples which reduces the overall error in the measurement. The resistive thermal device is made of platinum and measures the bulk water temperature 30 cm from the surface of the pool. This pool temperature is slightly elevated as compared to the water underneath it since a layer of warmer water lies near the surface due to buoyancy effects. This layer helps to reduce N-16 dose at the pool surface. Since the temperature difference is known, an adjustment is made to get the actual bulk temperature in the pool.

6.4.3 Power Fluctuations

The power calibration for the reactor is done by turning off the pumps driving flow in the reactor pool and increasing the power of the reactor while measuring the water temperature with a 9 thermocouple element array. This is compared to the pool temperature at full shutdown to determine the power level observed by calculating the ratio between the temperatures. The data is then fit to a linear function to describe the behavior of the power change relative to the change in water temperature. This is done by taking 50 readings at

10 millisecond intervals and averaging those temperatures to achieve a water temperature over that time step. The multimeter used in reading the thermocouple outputs has a sensitivity of 0.1 microvolts. The power calibration and errors are included in Appendix ??.

6.4.4 Error due to FLUENT Measurements

Errors in the FLUENT measurements can be attributed to the errors associated with averaging the values at the same vertical height to get the average coolant temperature during post processing. Intrinsic errors in FLUENT result from the mesh size being too coarse but the error was reduced to 1% by using the minimal number of cells to minimize runtime as seen in figure 65.

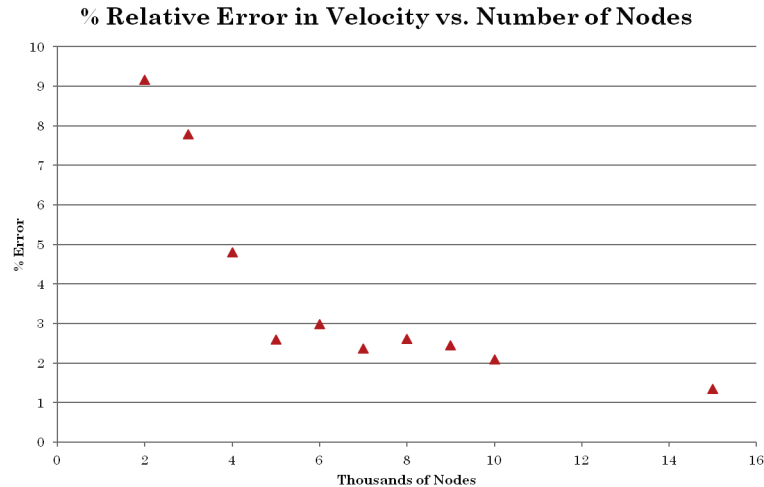


Figure 65: Error due to mesh size in FLUENT for single channel model

7 Conclusion

This document has outlined the creation of an improved thermal hydraulic model describing the flow channels in the TRIGA reactor. By measuring the temperatures in the TRIGA during operation at multiple power levels and utilizing a computational fluid dynamic solver, more accurate data was obtained for the flow channel. This entirely different approach from previous methods created a data set that was used to find TRIGA specific correlations for implementation into the nodal solvers. This data set was used to create a new heat transfer correlation that better reflected the flow and temperature characteristics of the actual flow channel. This correlation was then added to improve the accuracy of the model when handling the heat transfer in the representative flow channel within the nodal finite difference model. The computational fluid dynamic simulations were also used to determine more accurate loss factors due to the end fittings on the TRIGA fuel rods. Instead of estimating the loss using tabular data, the pressure drop measured in these sections was transformed into the loss factors associated with these drops and implemented into the nodal model.

These improvements enable higher fidelity modeling of the University of Texas TRIGA reactor in support of a potential maximum power increase. These correlations apply to TRIGA reactors depending on their individual geometries and operating conditions. While the use of these correlations has been demonstrated in TRACE, these correlations are broadly acceptable and

their validation against additional high-fidelity simulation data as well as measurements collected at similar TRIGA facilities can be an area of future work. Other future work would include building the physical scaled channel model, developing a larger model in the computational fluid dynamics code to have recirculating flow, and creating a full core model to fully encompass the effects due to crossflow and end effects.

A scaled channel model would allow for additional data to be collected for the flow channel and scaled to the actual TRIGA flow channels using similitude. This would allow for the FLUENT model to be validated further and improve the calculated correlations based on the new data. It would also allow for quantities such as the flow rate through the channel to be measured which are not allowed for the TRIGA due to current safety regulations. A FLUENT model with recirculating flow would remove the variable of the flow input velocity because the system would naturally develop its own flow due to buoyancy and other effects. This would simplify the model by decreasing the degrees of freedom. The full core model would increase the fidelity of the results because the crossflow and end effects would be modeled more accurately with all of the flow channels included in the model.

A MATLAB Solver code

```

clear all;
%Constants
g=9.81;
Diameter=0.0205;
L=0.3711;
qdot=21500;
f=0.0215;
MassFlow=0.145;
%Variables
for i=0:L/10:L
    Heights((i/(L/10))+1)=i;
end
Tsurf=[0,0,0,0,0,0,0,0,0,0];
Temps=[322,0,0,0,0,0,0,0,0,0];
Pressures=[156000,0,0,0,0,0,0,0,0,0];
Velocities=[0.25,0,0,0,0,0,0,0,0,0];
FlowAreas=[0.00053,0.00053,0.00053,0.00053,0.00053,0.00053,0.00053,
0.00053,0.00053,0.00053];
MajorLoss=[0.02155,0.02155,0.02155,0.02155,0.02155,0.02155,0.02155,
0.02155,0.02155,0.02155];
MinorLoss=[0,0,0,0,0,0,0,0,0,0];
Heat=[qdot/11,qdot/11,qdot/11,qdot/11,qdot/11,qdot/11,
qdot/11,qdot/11,qdot/11,qdot/11];
HTC=[0,0,0,0,0,0,0,0,0,0];
csubp=[0,0,0,0,0,0,0,0,0,0];
k=[0,0,0,0,0,0,0,0,0,0];
Nu=[0,0,0,0,0,0,0,0,0,0];
Pr=[0,0,0,0,0,0,0,0,0,0];
Q=[0,0,0,0,0,0,0,0,0,0];
B=[0,0,0,0,0,0,0,0,0,0];
Re=[0,0,0,0,0,0,0,0,0,0];
mu=[0,0,0,0,0,0,0,0,0,0];
mdot=[0,0,0,0,0,0,0,0,0,0];
Densities=[0,0,0,0,0,0,0,0,0,0];
Densities(1)=988.1;
mdot(1)=Densities(1)*Velocities(1)*FlowAreas(1);
for i=2:1:11
    mdot(i)=mdot(1);
end
csubp(1)=0.0109*(Temps(1)^2)-6.8945*Temps(1)+5270.8;
Pr(1)=(0.0002685*(Temps(1)^2))-0.2225*Temps(1)+47.354;
k(1)=(-0.00000628*(Temps(1)^2))+0.00511*Temps(1)-0.3529;
Beta(1)=(0.000005621*Temps(1))-0.001348;
mu(1)=(0.0000003695*(Temps(1)^2))-0.00003097*Temps(1)+0.006687;
Re(1)=Densities(1)*mdot(1)*Diameter/mu(1);
% Nu(1)=(f/8)*(Re(1)-1000)*(Pr(1))/(1+(12.7*((f/8)^0.5)
*((Pr(1))^(2/3))-1));

```

```

Nu(1)=((f/8)^0.308)*((Re(1)-1000)^0.395)*((Pr(1))^1.928)
/(1+(13.7*((f/8)^0.768)*(((Pr(1))^(0.811))-1)));
HTC(1)=k(1)*Nu(1)/Diameter;
Tsurf(1)=(Heat(1)/(pi*(L/10)*Diameter*HTC(1)))+Temps(1);
Q(1)=mdot(1)/Densities(1);
%Calculations
for i=1:1:10
    Temps(i+1)=(Heat(i)/(csubp(i)*mdot(i)))+Temps(i);
    Pr(i+1)=(0.0002685*(Temps(i+1)^2))-0.2225*Temps(i+1)+47.354;
    k(i+1)=(-0.00000628*(Temps(i+1)^2))+0.00511*Temps(i+1)-0.3529;
    Beta(i+1)=(0.000005621*Temps(i+1))-0.001348;
    mu(i+1)=(0.00000003695*(Temps(i+1)^2))-0.00003097
        *Temps(i+1)+0.006687;
    Densities(i+1)=((Densities(i))/(1+(Beta(i+1)
        *(Temps(i+1)-Temps(i))))));
    Re(i+1)=(Densities(i+1)*mdot(i+1)*Diameter)/(mu(i+1));
    % Nu(i+1)=(f/8)*(Re(i+1)-1000)*(Pr(i+1))
    /(1+(12.7*((f/8)^0.5)*(((Pr(i+1))^(2/3))-1)));% Gnielinski
    Nu(i+1)=((f/8)^0.308)*((Re(i+1)-1000)^0.395)*((Pr(i+1))^1.928)
        /(1+(13.7*((f/8)^0.768)*(((Pr(i+1))^(0.811))-1)));%From FLUENT
    HTC(i+1)=k(i+1)*Nu(i+1)/Diameter;
    csubp(i+1)=0.0109*(Temps(i+1)^2)-6.8945*Temps(i+1)+5270.8;
    Tsurf(i+1)=(Heat(i+1)/(pi*(L)*Diameter*HTC(i+1)))+Temps(i+1);
    Velocities(i+1)=Densities(i)*FlowAreas(i)*Velocities(i)
        /(Densities(i+1)*FlowAreas(i+1));
    Q(i+1)=mdot(i+1)/Densities(i+1);

    A=Pressures(i)/(Densities(i)*g);
    B=(0.5*Velocities(i)*Velocities(i)/g)*(1-((Densities(i)^2)
        *(FlowAreas(i)^2)/((Densities(i+1)^2)*(FlowAreas(i+1)^2))));
    C=Heights(i);
    D=1/(Densities(i+1)*g);
    E=Heights(i+1);
    F=MajorLoss(i+1)*(Heights(i+1)-Heights(i))*Q(i)*Q(i)
        /(2*g*D*FlowAreas(i));
    G=Heat(i)/(Densities(i)*g*Q(i));
    H=csubp(i)*(Temps(i+1)-Temps(i))/g;
    Pressures(i+1)=(A+B+C-E-F+G-H)/D;

end
Locations=[0.0127,0.0381,0.0635,0.0889,0.114,0.139,0.165,0.19,
0.216,0.241,0.2667,0.292,0.3175,0.343,0.368];
SNAPTemps=[323.53,325.18,327.05,329.19,331.64,334.31,337.21
,340.33,343.48,346.63,349.74,352.69,355.45,358.05,360.47];
SNAPPPressures=[155260,155016,154772,154285,154041,153799,153556
,153314,153071,152830,152588,152348,152106,151865,151521];
SNAPVelocities=[0.2493,0.24955,0.2498,0.2501,0.250417,0.25079
,0.25118,0.2516,0.252,0.2525,0.2534,0.2541,0.2545,0.2547,0.2548];
plot(Heights,Temps,Locations,SNAPTemps)

```

```

legend( 'MATLAB Solver' , 'SNAP Data' );
grid on;
xlabel( 'Height from bottom cell (m)' );
ylabel( 'Temperature of moderator (K)' );
title( 'Moderator Temp vs Height from bottom of flow channel' );
axis([0 0.4 320 360])
figure(2);
plot(Heights , Pressures , Locations , SNAPPPressures )
legend( 'MATLAB Solver' , 'SNAP Data' );
grid on;
xlabel( 'Height from bottom cell (m)' );
ylabel( 'Pressure at location (Pa)' );
title( 'Pressure at location vs Height from bottom of flow channel' );
%axis([0 0.4 152000 156000])
figure(3);
plot(Heights ,HTC)
grid on;
xlabel( 'Height from bottom cell (m)' );
ylabel( 'HTC at location (W/(m^2 K))' );
title( 'HTC at location vs Height from bottom of flow channel' );
axis([0 0.4 500 1000])
figure(4);
plot(Heights , Velocities , Locations , SNAPVelocities )
legend( 'MATLAB Solver' , 'SNAP Data' );
grid on;
xlabel( 'Height from bottom cell (m)' );
ylabel( 'Velocity at location (m/s)' );
title( 'Velocity at location vs Height from bottom of flow channel' );
axis([0 0.4 0.24 0.27])
figure(5);
plot(Heights ,Re)
grid on;
xlabel( 'Height from bottom cell (m)' );
ylabel( 'Reynolds number at location' );
title( 'Reynolds number at location vs Height from bottom of flow channel' );
%axis([0 0.4 8000 20000])

```

References

- [1] Rao et al. *THERMAL HYDRAULICS MODEL FOR SANDIA'S ANNU-LAR CORE RESEARCH REACTOR* 1988.
- [2] Oak Ridge National Lab <http://www-rsicc.ornl.gov/> 2012.
- [3] Nuclear Regulatory Commission *Symbolic Nuclear Analysis Package User's Manual* 2009.
- [4] Nuclear Regulatory Commission <http://www.nrc.gov/reading-rm/doc-collections/nuregs/contract/cr6974/> 2011.
- [5] Marcum, Wade R. *Thermal Hydraulic Analysis of the Oregon State TRIGA Reactor Using RELAP5-3D* 2008
- [6] Azzoune et al. *NUR research reactor safety analysis study for long time natural convection operation mode* Nuclear Engineering and Design. Elsevier. Vol. 240 (2010), 823-831.
- [7] Merroun et al. *Analytical benchmarks for verification of thermal-hydraulic codes based on sub-channel approach* Nuclear Engineering and Design. Elsevier. Vol. 239 (2009), 735-748.
- [8] Umar et al. *An experimental study of natural convection in the hottest channel of TRIGA 2000 kW Pacific Basin Nuclear Conference Preceedings.* 2006.

- [9] Fiantini and Umar *Fluid flow characteristic simulation of the original TRIGA 2000 reactor design using computational fluid dynamics code* 2nd International Conference on the Advances in Nuclear Science and Engineering. 2009.
- [10] Mesquita et al. *EXPERIMENTAL INVESTIGATION OF TEMPERATURE PATTERNS IN THE IPR-R1 TRIGA NUCLEAR REACTOR* 3rd World TRIGA Users Conference. 2006.
- [11] Buke and Yavuz *CALCULATION OF THE FLOW PARAMETERS IN TRIGA CORE COOLANT CHANNEL* iaea.org 2000.
- [12] Paul Whaley *Safety Analysis Report of the University of Texas at Austin TRIGA Reactor* University of Texas at Austin 2012.
- [13] Fox, McDonald. *Introduction to Fluid Mechanics*. Wiley, 3rd Edition, 1985.
- [14] Incropera, DeWitt. *Fundamentals of Heat and Mass Transfer* Wiley, 6th Edition, 2006.
- [15] ANSYS FLUENT 13.0 *User's Guide* ANSYS, 2011.
- [16] FLO-CORP *Data Sheet for VFlo CFVF1* 2012.
- [17] OMEGA *Revised Thermocouple Reference Tables for Type E Thermocouples* 2012.
- [18] OMEGA *Revised Thermocouple Reference Tables for Type K Thermocouples* 2012.

[19] University of Texas Nuclear Engineering Teaching Lab *Power Calibration using 9 Thermocouple Array for Yearly Calibration* 2012.

[20] ASTM *ASTM Standards E 1137 for Industrial Platinum Resistance Thermometers* 2012.

Vita

Alexander Douglas Brand was born in Webster, Texas. After completing his work at Clear Lake High School in Houston, Texas, he entered the University of Texas at Austin. He received the degree of Bachelor of Science in Physics from the University of Texas at Austin in May, 2008. In June 2008, he entered the Graduate School at the University of Texas at Austin. He received the degree of Master's of Science in Engineering in May 2010.